3-3-2017

Structural strength evaluation and retrofitting of Hangar Q At Millville Airport

Harshdutta Indradutta Pandya
Rowan University

STRUCTURAL STRENGTH EVALUATION AND RETROFITTING OF HANGAR Q AT MILLVILLE AIPORT

by
Harshdutta I. Pandya

A Thesis

Submitted to the
Department of Civil and Environmental Engineering
Henry M. Rowan College of Engineering
In partial fulfillment of the requirement
For the degree of
Master of Science in Civil Engineering
at
Rowan University
December 9, 2016

Thesis Chair: Ralph Dusseau, Ph.D., P.E.

Dedications

I would like to dedicate this manuscript to my family, friends and professors.

Acknowledgements

I would like to express my sincere gratitude to my research supervisor Dr. Ralph Dusseau for the continuous support of my MS study and related research, for his patience, motivation, and immense knowledge. His guidance helped me in all the time of research and writing of this thesis. I could not have imagined having a better advisor and mentor for my MS study. Besides my advisor, I would like to thank the rest of my thesis committee: Dr. Douglas Cleary, for his insightful comments and encouragement, but also for the hard questions which motivated me to widen my research from various perspectives. My sincere thanks also goes to Mr. Aaron Nolan and Mr. Eric Dubois who provided me with an opportunity to join their team as laboratory assistant and who gave access to the laboratory and research facilities. Without their precious support it would not be possible to conduct this research.

Last but not the least, I would like to thank my family: my parents and to my sister for supporting me spiritually throughout writing this thesis and my life in general.

Abstract

Harshdutta Pandya
STRUCTURAL STRENGTH EVALUATION AND RETROFITTNG OF HANGAR Q AT MILLVILLE AIPORT
2016-2017
Ralph Dusseau, Ph.D., P.E.
Master of Science in Civil Engineering

Hangar Q was built in Millville, New Jersey as a part of the Home Defense Program of World War II. The airport is now owned and operated by the Delaware River and Bay Authority (DRBA) as the Millville Airport. Hangar Q was a historic nine-bow truss hangar when it was first constructed, standing at 30 feet high, 130 feet wide, and 160 feet deep. It was originally constructed with no side walls and no back wall or front sliding doors. It was later updated from a completely open design to a closed design. The objective of this study was to evaluate the structural strength and stability of Hangar Q against dead, snow, and wind loads in an open condition and recommend improvements as needed. RISA-3D was used to model the hangar as an open eight truss hangar. In the analysis, strength deficiencies at locations in top chord, bottom chord and bracing members were observed. Suggested modifications to strengthen the deficient members are presented. Additional work included design and detailing of concrete elements including the foundation of the piers, the piers and the cross beams on top of piers.

Table of Contents

Table of Contents (Continued)

Table of Contents (Continued)

List of Figures

List of Figures (Continued)

Figure Page

List of Figures (Continued)

Figure Page

List of Tables

Table Page

Chapter 1

Introduction

Millville Army Airforce Base started construction of Hangar Q (130 feet wide by 160 feet long by 30 feet high and 20,800 square foot) in February 1941 as a part of the "Home Defence Program." Construction was completed in 1943 during World War II. Millville Airport was dedicated as "America's First Defence Airport" in 1941 and nowadays is owned and operated by the Delaware River and Bay Authority (DRBA). During the war, Millville Airport was a residence to more than 10,000 personnel and trained 1500 pilots. After the end of the war, some buildings were demolished and the remainder were turned over for civilian use. Millville Airport is presently a hub for industry and aviation in the Southern New Jersey region.

The Hangar Q was originally designed and constructed as an open nine-truss hangar with standard bow truss construction. It is considered as a highly significant historic building due to the limited number of bow truss hangars remaining in the United States. In the time span of 30 years after construction of these bow trusses, the Hangar Q was no longer in usable condition and it began to steadily decline which resulted in distress and deformation of concrete elements and steel section members respectively. Reconstruction attempts have been done to try and improve the condition of Hangar Q.

As a result, Hangar Q was converted from an open, nine-truss hangar to a closed, eight-truss hangar. Modifications to Hangar Q in 1966 included installation of two sets of twin 25 feet x 25 feet coiling doors, creating two 50 feet x 25 feet openings; construction of front and back steel walls; construction of cinder-block

walls between piers and construction of a concrete masonry unit wall down the center of the hangar, dividing it into two separate bays.

As part of the installation of the coiling doors, the last truss was modified and is no longer considered to be historic, which is why it is now considered an eight-truss hangar. Hangar Q is now recognized as a significant historic structure and is in need of reconstruction.

The main focus of work was to carry out structural strength evaluation of Hangar Q and to determine which deficient (overstressed) truss members should be upgraded (or retrofitted) using steel cover plates to satisfy limiting criteria of flexural strength and axial strength of doubly and singly symmetric steel members of the truss. Eventually, the reconstruction of Hangar Q would be carried out. After meeting with the DRBA, it was clear that the option they wanted to move forward with was to disassemble and store the trusses. After storing the trusses, the Hangar Q will then be reconstructed within a period of 10 years as an open 8-truss hangar (130 feet wide by 140 feet long by 30 feet high and 18,200 square foot). The areas of research consisted of an updated structural analysis of the rebuilt steel truss structure (including the eight historic trusses) per contemporary loading conditions and design codes including dead, wind, and snow loads and load combinations, and analysis and design of new concrete foundations, piers, and cross beams.

Chapter 2

Literature Search and Review

A major component of this study consisted of an in-depth literature search. The purpose of this search was to collect, catalogue, and summarize information related to truss hangar structural evaluation, rehabilitation, retrofitting and proposed reconstruction. This database of literature was intended to serve as a resource to DRBA regarding the bow string trusses used in Hangar Q and technical issues pertinent to older truss hangars.

Strengthening Requirements of Old Timber Warren Trusses

The aim of the investigation by H. C. Foo and G. Akhras (1996) [22] was to study the load reversal behavior and strengthening requirements of single and two span continuous truss systems adopting a parametric analysis approach. The Department of National Defence (DND) of Canada owned and operated old timber Warren truss hangars. These two-span Warren-truss buildings were constructed in the 1940s and were originally designed as two independent single span trusses. Both truss systems were subjected to various combinations of loads in accordance with National Building Code of Canada [13] (National Research Council of Canada 1985) and Construction Engineering Technical Order (CETO) [14] requirements. Load-reversal behavior of a two-span double-parallel chord Warren truss system was investigated. It was found that, under specific loads as provided by CETO [14] and combined loading as specified in the National Building Code of Canada (1985) [13], a double Warren truss showed load-reversal characteristics, specifically at and near the interior support. The resulting redistribution of loads had both a positive and adverse impact on member behavior. Truss members that were overstressed under actual and realistic loading conditions were determined. Member behavior of each truss system under

individual load conditions was examined with respect to their compressive and tensile strengths. Truss members that required reinforcement as a result of the reversal loading were determined and compared with CETO specifications to ensure that existing timber Warren-truss buildings met the latest Building Code requirements. An earlier study (Foo et al. 1993 [24]) investigated the effects of the proportion of dead weights i.e., uniformly distributed self-weight of truss members and non-uniformly distributed roof load on the structural behavior of the truss. These effects were accounted for by examining and comparing analytic results of trusses with a truss self-weight of 0.3 kN/m^2 with that of a truss self-weight of 0.4 kN/m^2. Results of the study suggested that the effects were insignificant. A truss self-weight of 0.3 kN/m^2 was used for this study.

Five different truss configurations (*Figure. 1*) were evaluated. Truss 1 was a single span truss, truss 2 was a two span continuous truss with unbalanced loading, truss 3 had the same structural configuration as truss 2 but with balanced loading. Truss 4 had a similar configuration to truss 2 but with the continuity members (top chord at central column) and unbalanced loading. Lastly, truss 5 was the same as truss 4 but with balanced loading. Column supports were assumed to be fixed for all five structural configurations.

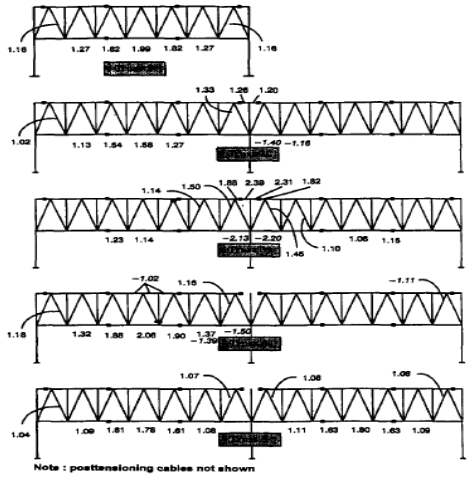

Figure 1. Overstressed Members [22]

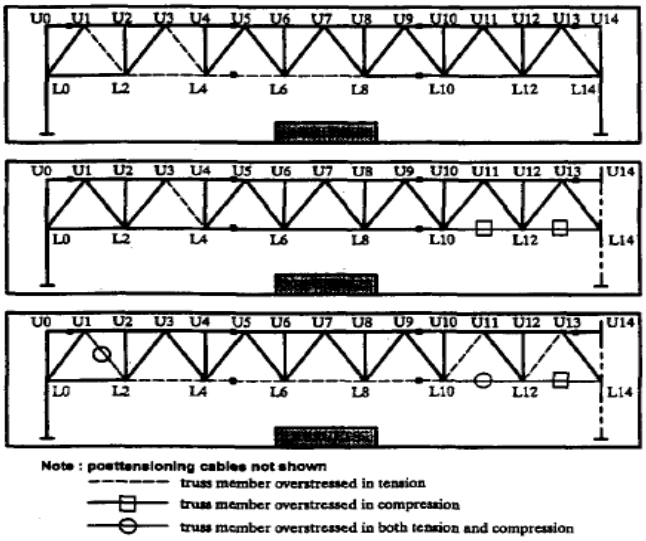

Figure 2. Members Needing Reinforcement [22]

In addition to the five members that needed reinforcement (*Figure 2*) against load reversal, as specified in CETO, results of this [22] study suggested that three bottom chord members near the interior support also needed to be reinforced against overstressing. Reinforcement of these three bottom chord members can be made similar to existing reinforcement details for other bottom chord members. Review of this paper provided insights regarding the load combinations that were used which

gave us knowledge about the types of load combinations that should be used to analyze the strength requirements of aircraft Hangar Q.

Structural Evaluation of Steel Truss Aircraft Hangars at Corpus Christi Army Depot

The objective of the evaluation by Ghassan K. Al-Chaar, Jason Ericksen, and Pramod Desai (1999) [7] was to conduct case studies of steel truss aircraft hangars at Corpus Christi Army Depot (CCAD) in Texas to determine the structural adequacy of four steel truss aircraft hangars by conducting structural analyses using the code guidelines in place at the time of the study. As noted [7], these structures were analyzed, designed and built compatible to flexible building codes and standards, and over the period of time many of these codes and standards were modified which indicated increases in loads in their fundamental design guidelines. Besides this, environmental parameters over the years had reduced the load bearing capacities of some structural members. Contemporary hurricanes had indicated the vulnerabilities of these structures to hurricane-level wind loads. Some out of date aircraft hangars and other structures built with steel-truss-type roofs had been damaged or destroyed in recent hurricanes. Wind-coupled damage observed in hangars had included overstressed structural members, hangar door systems blown out of their frames (*Figure 3),* and obsolete structural member connections.

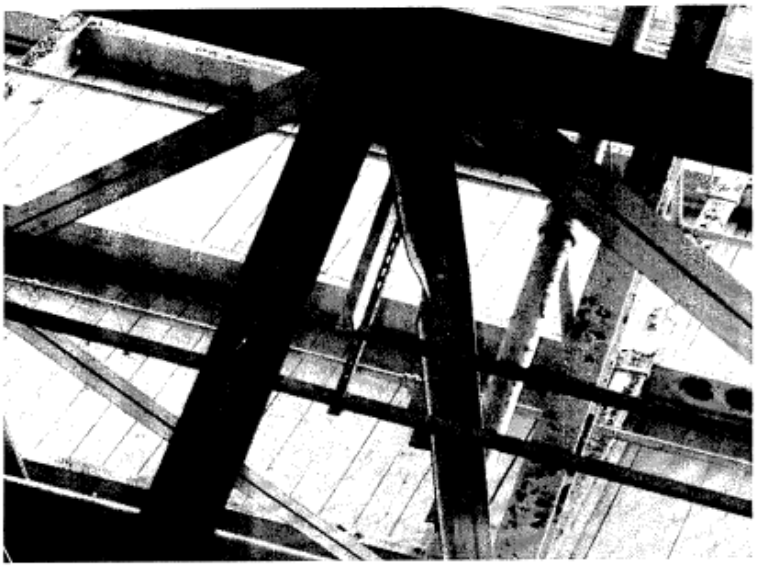

Figure 3. Bent Vertical Member of Hangar 43 [7]

In several instances, failure of a structure originated with a failure in hangar doors or windows, accompanied by high variations between internal and external wind pressures that caused total collapse. Similar door deterioration was observed in Hangar Q.

Many of the steel truss aircraft hangars at Corpus Christi Army Depot (CCAD) were similar to those that had performed poorly during hurricanes in other parts of the country. Engineering analysis of these kinds of structures can recognize structural vulnerabilities, and retrofit schemes might be developed to reduce these vulnerabilities to intense wind loads.

The existing conditions of CCAD aircraft hangars numbers 43, 44, 45, and 47 were evaluated. Structural deficiencies and overstressed members and joints were identified, and retrofit methods to meet the requirements of current codes were developed.

The Allowable Strength Design (ASD) [12] was considered to calculate interaction stress ratios for each member of the trusses in the SAP90 SAPSTL steel

design post-processor. In every run of the analysis, all the wind loads were applied as separate loading combinations and SAPSTL calculated the maximum compressive and tensile stress ratios for each member of all load combinations incorporated. The steel was assumed to be 36 ksi, conforming to American Institute of Steel Construction (AISC) [12] specifications. The stress ratios were calculated by ASD requirements.

Structural analyses [7] were carried out for the most influential loading combinations. Comparing the actual stresses with allowable stresses reduced the list of deficient members notably. A similar comparison was adopted for the analysis of Hangar Q.

The evaluation of allowable stresses [7] was defined as the design allowable stresses with the factors of safety equal to 1.0. Consideration of knee braces in trusses to enhance the structural performance was a prevalent practice in modern structures. As a commentary of this paper, this evaluation provided know-how regarding structural behavior of aircraft hangars under the most common loading combinations and also indicated potential retrofit schemes against damage due to hurricane and high wind loads.

Condition Assessment and Rehabilitation Plan, Hangar One

The intent of RISA 3D analysis of Hangar One [4] was to conduct condition assessment and rehabilitation of Hangar One by NASA Headquarters and Ames Research Centre, California (2011).The main objective of the assessment was to evaluate the stability of the existing structural system for gravity, seismic, and wind load strengthening options for the following scenarios to be considered for rehabilitation: basic re-skinning; re-skinning and use as storage; re-skinning and use as a hangar; and reskinning with historic and high inhabitancy considerations. Hangar

One was built in 1932 to accommodate the USS Macon and constructed with free standing interior structures inside of the hangar. Reframing of interior structures was carried out to support the hangar internally. This condition assessment provided analysis of the existing conditions and various alternatives for the rehabilitation plan of Hangar One. Hangar One is a historic structure, like Hangar Q. The analysis of Hangar One includes the removal of contaminated materials, primarily leaving a steel structure. It was designated as a California historic civil engineering landmark in 1977 and a naval historic site in 1966.

A condition assessment and rehabilitation plan was required to evaluate the condition of the facility and to assess potential re-use alternatives, identify requirements, and potential costs. The condition assessment utilized and mentioned many of the former reports, studies and photographs accumulated to date by NASA.

Structurally, the hangar building was located in a seismic zone. A rigorous geotechnical analysis was carried out as a part of this study to provide structural engineering parameters for design and analysis. This analysis concluded that the site contained liquefiable soils. To complete an analysis of the structural frame of the building in accordance with contemporary codes, the soils were assumed to be strengthened and the cost associated with strengthening was included in this report. The structural analysis determined that, while there were deficiencies within the structural frame, there were no immediate requirements to repair and retrofit most of structural components. Structural members which needed reinforcing were identified.

The rehabilitation plan discussed structural improvements, material replacement alternatives, and specialized construction issues to meet the relevant historic requirements. Hangar One's structural frame system is a union of structural steel arched trusses and braced frames. These arches and frames are supported by A-

shaped frames which transferred loads into the pile foundation system following structural load distribution paths.

Fourteen trusses were placed at 72 feet centre to centre spacing advancing in the direction of the length of the hangar building *(Figure 4)* as well as 2 gable arches that were placed at 40 feet measured from the main arches at each end of hangar. Two 4 inch expansion joints were put between the arches labeled 4th and 5th and 10th and 11th, respectively, which divided the building structurally into three separate sections. Overall, the structure was in moderate condition. Hangar One did not have apparent indications of structural distress, and also did not have explicit evidence of preceding building damage due to either wind or seismic load occurrences.

The main arches resisted the lateral loads and then they transferred those loads to the A-shaped frames which were supported by pile foundations. The trusses, comprised of V-braces and H-braces between the arches, provided the means by which the lateral loads were transferred to the main arches. Several pile foundations were damaged and distressed. The horizontal reaction of the building was taken by internal concrete tie beams which were provided below the slab on grade for bracing up and to erect both sides of the building.

Figure 4. A - Frames NASA Hangar One [4]

The east side of the hangar wall had a new opening that was built after the construction of the hangar. The new opening did not impact the structural strength and stability of the hangar. Over time, 11 new doors had been put into the hangar walls. At these particular locations, the concrete perimeter wall was cleared away to incorporate the door placement. In the construction of Hangar One, the typical structural steel was A7 Grade 30.

Wind load analysis was performed according to American Society of Civil Engineers (ASCE) 7-10 [10] as required by NASA. The 3-second gust basic wind speed of 85 miles per hour with exposure C and applicable importance factors was employed for calculating the wind loads. An importance factor of 1.15 was considered for the high occupancy option given in [10].Wind loading and seismic loading were modified to 75% of the applied loads allowed by California Historic Building Code (CHBC) 2010 [15] for Historic Buildings in determining the adequacy of the structure. For the selected purpose of the analysis, per ASCE 41-06 [16], a linear elastic procedure was followed for the structural analysis. To incorporate this analysis, a 3D model of the hangar was developed using a commercially available structural analysis software, RISA 3D. Hangar One, with two expansion joints and two geometrically symmetrical end sections, i.e., the north and south sections, needed two separate computer models to develop one model for the end sections i.e. gable arch to arch 4 and arch 11 to gable arch of other side and another RISA 3D model for the middle section i.e. arch 5 through arch 10. A discrete model for the door rib was also developed to check the loading and evaluate the door structure stability under applied loading.

The ribs of the doors transferred the lateral load to the end sections from one end to another end using pin connections at the top of the door on arches 1 and 14,

i.e., the first and last arches. The loading due to arches included the gable arch on both ends of the hangar because they were not a contributing part of the lateral load resisting system so that they were not included in the model.

As-built documents and drawings were used to model the geometry of the arches and the structural member sizes. Since there were a number of built-up sections in addition to the standard steel sections used in the hangar, custom section sets were created in the RISA database to derive a better geometrical model. The RISA 3D model incorporated all of the steel structural elements including the lateral load resisting elements, the arches, all the trusses and cross members between the arches, A-frames, and the trusses connecting the A frames. The pile foundations were modeled as springs to consider the effect of deep foundations. The structural stability and strength performance of the hangar was evaluated based on the criteria of ASCE 41- 06 [16]. The load combinations were listed for the failure mode of the elements and also the applicable reduction factor (0.75) allowed per CHBC [15] to get the Demand Capacity Ratio (DCR) values (unity checks) from running the model on RISA 3D (*Figure 5*). Stated structural software was also used to evaluate the seismic performance of the building. The load combinations input in RISA 3D were regulated to simplify the analysis and computation of the DCR values to get satisfactory output of the analysis.

The DCR values remained intact by reducing the demand in proportion to the increase in capacity allowed per ASCE 7-10 [10]. The analysis was performed for all considered load cases - gravity, wind, and seismic. The results were obtained using the envelope solution, which included all load combinations and reports the highest unity value from all load combinations for each member.

It was important to note that the single angle members experienced a number of deficiencies. Due to high slenderness ratios (l/d) of small single angles and longer length members, the structural strength of the member was reduced thus resulting in an increase of the DCR values. In the structural analysis, the slenderness ratios recommended by AISC [12] were not limited. The actual slenderness ratios (l/d) were used to calculate the capacities of the members.

The single angles may have been originally designed as tension members only. In this evaluation of Hangar One, NASA had considered the smaller angles above the A-Frames (secondary bracing elements) as tension members only. The single angle braces between the A-frames were primarily lateral force resisting elements and to be consistent with Federal Emergency Management Agency (FEMA) 274 (National Earthquake Hazard Reduction Program (NEHRP) commentary on the guidelines for the seismic rehabilitation of buildings) [17] section C10.5.4.2 B they were considered as tension/compression elements. A number of these primary single angles were among the overstressed members, i.e. the members did not fulfil limiting stress criteria.

It was important to note that most of the deficiencies were caused by seismic loads and very few were caused by wind. There were separate and individual graphs for seismic and for wind for the two different categories. The structural analysis and evaluation of the hangar building was based on soil site class D forces and no appreciable differential settlement due to soil liquefaction. The geotechnical portion of the report, however, identified the possibility of soil liquefaction and therefore required soil remediation to meet the site class D forces used in the linear elastic procedure.

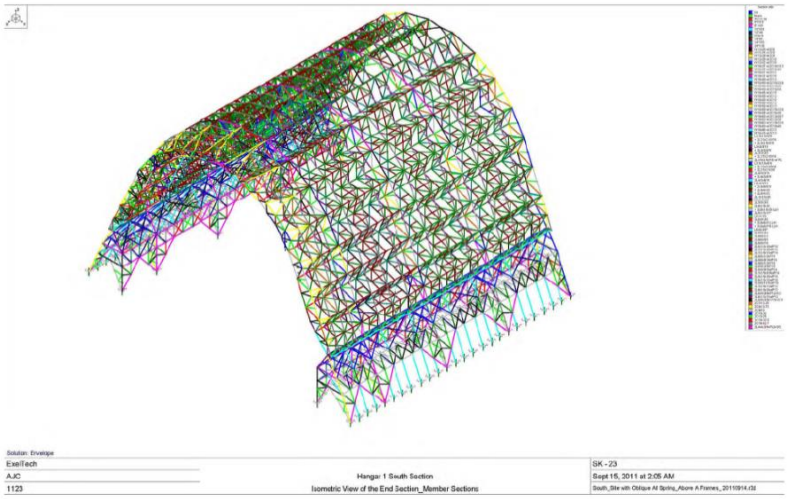

Figure 5. RISA 3D Model NASA Hangar One [4]

The methodology used in this NASA report was intended to meet the latest building codes and standards; however it did not include all possible analysis methods. Based on the information available at the time of this study, the approach used in the geotechnical analysis portion of this report was conservative with regards to the settlement potential in order to capture the maximum probable required soil and steel mitigation. The hangar had been designed well considering the time when it was built. There was very little code knowledge of the seismic loads at the time. The hangar structure had an absolute and continuous load path, including connections from every portion of the structure to the ground, and there was no evidence of distress in the structure. Additionally, the anticipated dead and live loads did not exceed those historically present. Review of this paper provided insights about consideration of different load combinations per ASCE 7-10 [10], CHBC 2010 [15] and FEMA [17]. From stated guidelines, only ASCE 7-10 [10] had been adopted to consider load combinations for Hangar Q. Furthermore, it provided an excellent demonstration of a RISA 3D model which was produced for three different cases and

was considered very useful for Hangar Q as the analysis of Hangar Q was also done incorporating RISA 3D for structural analysis.

Condition Assessment and Rehabilitation Plans, Hangar 2 and 3, Ladd Field National Historic Landmark

The main idea of the investigation of wooden Hangars 2 and 3 [5], Ladd Field National Historical Landmark, Fort Wainwright, Alaska (2008) was to perform condition assessment and rehabilitation. Field assessment and structural analyses of Fort Wainwright's Hangars 2 and 3 had been performed. As a result of assessment and analyses, a set of recommendations for the structural improvement of these facilities had been developed. These recommendations were intended as a planning guide for the determination as to whether the hangars should have been repaired or replaced. Analyses used the 2003 International Building Code (IBC) [18] as the primary basis.

Two separate analyses were performed. The first analysis addressed all gravity loading, which included live, dead, and snow loads. The second analysis addressed lateral loading, which included wind and seismic loads. There were various interpretations and opinions as to which code applied to these buildings when constructed in 1944. Candidates included the Army's United Facilities Criteria [25], the Uniform Building Code (UBC) [19] and the Naval Facilities Engineering Command (NAVFAC) Design Manuals [20].

The top chords of the trusses were compression members that had been retrofitted with confinement clamps at various locations. The maximum ratio of applied stress to allowable stress under the 2003 IBC [18] was 1.34. While analysis showed these members to be overstressed, strengthening by the addition of supplemental framing members was not recommended. As compression members

with one edge fully braced, they had a low risk for buckling. Also, they had been confined in many locations, which should have the effect of increasing the ultimate strength of the members in compression. The bottom chords of the trusses were tension members that had been retrofitted in various locations with post-tensioning rods and plates. The maximum ratio of applied to allowable stress in these members was 1.32. In order to meet the applied stress requirements of the 2003 IBC [18] these members should had been strengthened. Strengthening of these elements could have been achieved with the addition of microlam timber strengthening plates along the entire bottom chord of all 18 trusses.

Wind braces or buttresses were comprised of a primary diagonal brace and web members connecting the columns to the brace. In each brace three of these web members were overstressed due to lateral loading. These members required strengthening. In order to access these elements, a substantial amount of drywall must be removed and replaced. There were 18 trusses with wind braces at each end, and there were three web elements requiring strengthening per brace, so that a total of 108 of these members required strengthening. This article could provide strengthening methods that could be used for Hangar Q after rigorous analysis. The geotechnical investigation and analysis had resulted in the determination that both hangars were founded on soils that were susceptible to liquefaction during a seismic event. In order to secure the structures during a peak earthquake, the spread footings required retrofitting with piles.

Historic Assessment of Existing Hangar 5, Building 386, Ault Field Naval Air Station

The primary goal of the analysis of Existing Hangar 5 [6], Building 386 Ault Field Naval Air Station, Whidbey Island County, Washington (2006) was to perform

historic conditional assessment. The Navy intended to provide mission essential renovation and modernization to Building 386 (Hangar 5) at Ault Field, Naval Air Station (NAS) Whidbey Island to meet life safety requirements including anti-terrorism force protection (ATFP) improvements and replacing outdated and inefficient mechanical and electrical systems and reconfiguring and adding administration and training spaces to accommodate users.

Moreover, the Navy proposed to demolish an air traffic control tower constructed on the northwest portion of Hangar 5. The air traffic control tower was no longer used and it was not seismically safe. Hangar 5 was a concrete structure with two barrel roof bays spaced between multiple story shop and administrative areas. Hangar 5 featured two 150 x 240 feet pre-cast concrete open arch hangars that were separated by a 2-story 120 x 240 feet open shop area in the original design. Two story administrative spaces lined the perimeter of the central shop area and outside the hangar bays. These spaces were constructed with a combination of cast in place concrete frames above reinforced concrete masonry units with asbestos containing metal cladding in the transverse direction (east/west). It has a combination of concrete frames and shear walls in the longitudinal direction either north or south. The Navy evaluated the structural integrity of Hangar 5 and its ability to meet progressing mission needs.

Figure 6. Sprinkler System and Spalling from Roof System [6]

Hangar 5 had an insufficient and deteriorating lateral resisting system to resist loads due to a major seismic event in accordance with the Federal Emergency Management Agency (FEMA) [17] criteria, causing a concern for personnel and aircraft safety. The hangar required structural rehabilitation to its roof (*Figure 7)*, walls, and floor construction. The existing hangar bay barrel roof precast concrete panels had welded attachments to the concrete arches that were deficient and required repair, *Figure 6*. The precast concrete floors had cracking, requiring replacement. The hangar doors were weathered and the track system was deteriorated and was beginning to impact operations.

Figure 7. Broken Concrete in Roof [6]

In order to strengthen Hangar 5, there must be significant seismic repairs, replacement of outdated and inefficient mechanical systems, heating, ventilating and air conditioning (HVAC) system components and electrical systems. Hangar 5 structural deterioration, like Hangar Q, would impact its ability to function as intended. The deteriorated lateral resisting system hampers Hangar 5's ability to withstand an earthquake and might cause injury or death to workers inside the structure.

Woodland State Airport Hangar Condition Assessment

An elementary objective of this structural evaluation [8] was to provide alternatives for the three hangar buildings, indicated as A, B, & C, at the Woodland State Airport in Woodland, Washington. Washington State Department of Transportation (WSDOT) Aviation Division asked Berger/Abam Engineers Inc. to carry out structural assessment of three hangars. All three buildings were of wood construction with various modifications to their structure. The three Hangar buildings at the airport were built between the 1950s and 1980s.These buildings house small single engine aircraft and include space for up to fifteen airplanes. Evaluation was

based on an old structural assessment of the buildings and knowledge gained from a site visit and walk-through of the hangar buildings. Numerous structural deficiencies were discovered including vertical and lateral load-carrying deficiencies for all three buildings and structural issues with the roof members and trusses, columns, foundations, and lateral load carrying elements.

Observation and evaluation of the existing hangar construction indicated that all of the buildings were seriously limited in vertical, and/or lateral capacity, or were already beginning to fail. The major structural problems included the absence of columns, inadequate modification to the original load path of the buildings, and lack of lateral support for the structures. Hangar Buildings A and B had been deemed uninhabitable because of inadequate modifications of the existing structure. The structure of Hangar Building C had also been modified to a point that was a cause for concern. These previous modifications could potentially be repaired to provide temporary improvement to the structures.

The condition assessment report included temporary modifications like repairing or replacing columns and foundations, strengthening of the purlins that span between the roof trusses, repair of previous work done to the main building trusses, and improvement of the buildings' lateral force resisting elements. The report also included some renovation proposals to the existing buildings; because almost all structural elements were in need of repair or strengthening in the existing hangar buildings, and recognizing that all fixes would be permitted and designed per the current building code, the undertaking of repairs would quickly push the project to a full renovation. Installation of a code approved foundation system, replacement and strengthening of columns, strengthening of roof trusses and purlins, the addition of lateral load-carrying elements for both the roof and walls of the buildings were

incorporated. In addition, a geotechnical investigation would be required to address the potential for flooding and a high water table as well as the soil condition and the possibility of liquefaction. While this work would be very extensive, it would give the buildings an extended life and would ensure the life-safety condition of the buildings. The three hangar buildings at the Woodland State Airport were in need of repair to ensure their continued safety and performance. Due to deficiencies, the report concluded that methods of original construction, modifications, and inadequate repairs over the years had created problems that in some cases greatly limited or reduced the structural capacity of the buildings. Renovation proposals mentioned in this article would be taken into account during analysis of Hangar Q to come up with methods to remedy structural deficiencies.

Wind Damage to Columbia Regional Airport, Missouri

The objective of the investigation by Henry Liu and Fariborz Nateghi [23] was to determine wind damage to an existing airport as a case study. Columbia Regional Airport in Missouri was struck by winds with maximum speeds of 96 mph (43 m/s) on June 17, 1985. Parked aircraft, hangars, building glass windows and automobiles were damaged by this sudden impact of wind. After the catastrophe, an investigation was carried out which indicated that the storm included a powerful downdraft, and was not a tornado as it was originally assumed, that the aircraft tie down system had discrepancies, that a gravel road was the prominent source of damage to cars parked at the airport terminal, that the gust factor of this high wind was much higher than the usual assumptions for structural design, and so forth. Further observations were that the atmospheric pressure of the storm (*Figure 8*) evaluated was massively influenced by the wind-induced pressure of the building in which the barometer was located, and that west was the leading direction of high winds at this location of airport. Acquired

knowledge from the in depth investigation could be used to estimate possible wind damage to airport hangars.

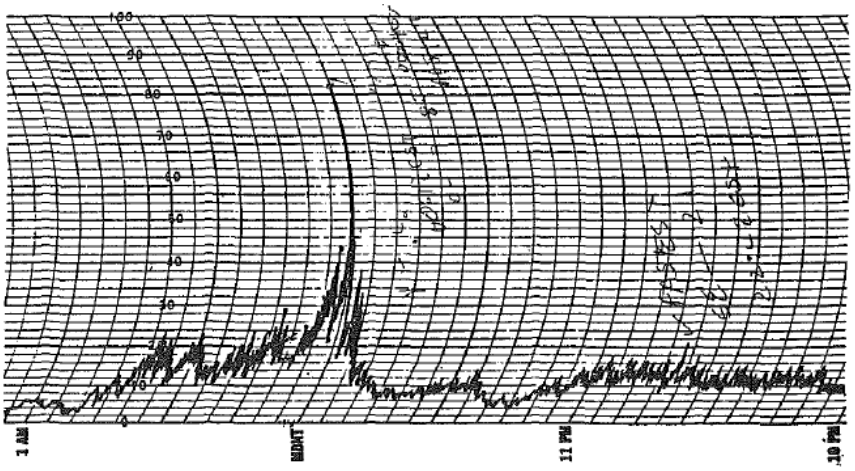

Figure 8.Wind Speed Record of Storm [23]

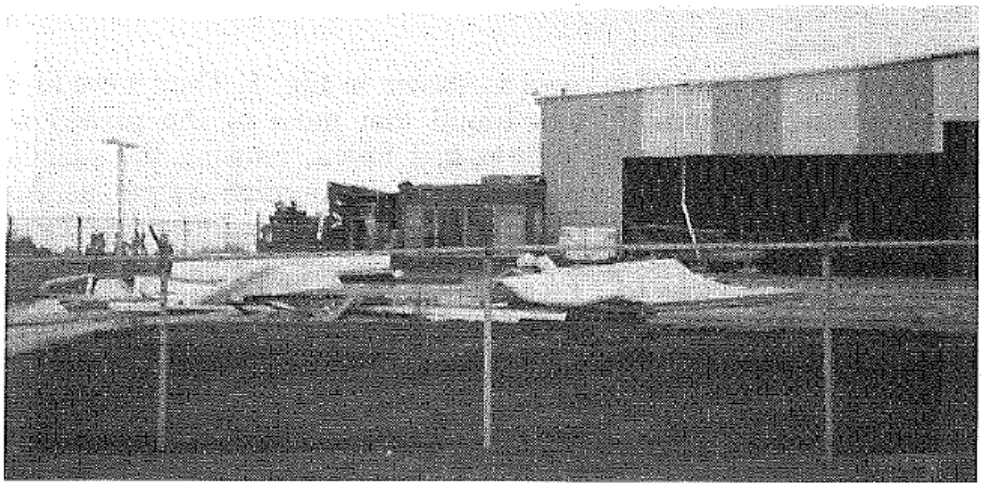

Figure 9.Aircraft Hangar and Adjacent Office Damaged by Wind [23]

The aircraft which were parked outdoors were damaged the most. Only one aircraft was damaged which was parked inside a hangar because the hangar door failed. The hangar and its adjacent building failed because of the storm (*Figure 9)*. The strongest wind in this storm was either from the west or southwest.

It was not possible to determine the wind direction with accuracy because the wind sensor readings were considered only in eight directions. Observations by Henry Liu and Fariborz Nateghi from this paper would be useful to understand about damage of aircraft hangars due to a high wind storm and could help with the wind force analysis of Hangar Q.

Chapter 3

Computer Models

The focus of the computer modeling was to analyze and check the structural stability of the hangar under various contemporary loading combinations of ASCE7-10 [10] as it stands, or as it will be rebuilt. The modeling was done in RISA 3D, which is a finite element analysis tool. The points used in RISA 3D were brought in from an AutoCAD drawing in which the points of the hangar were attained from design drawings. The model developed was an open eight truss hangar model.

Finite Element and Coordinate Axes

The finite element described in this research is a two-node isoperimetric beam element for all the steel members, which is suited to in-plane analysis of arches, specially three hinged arch structures as well as plane frame structures. A basic model of Hangar Q with the coordinate system can be seen in *Figure 10*, which shows the X-axis in the direction of width of the hangar, the Y-axis in the direction of height of the hangar, and the Z-axis in the direction of the length of the hangar.

Nodal Assumptions

Based on the original design drawings, the following boundary conditions and changes were made to the hangar:

- The nodes at the top of the piers *(Figure 10)* were modeled as pin joints. Boundary conditions assigned for these nodes in RISA 3D are shown in *Figure 11*.
- Top chord nodes in the truss were modeled as free to rotate in all three global directions (X,Y,Z) and translations were allowed in X and Y directions.

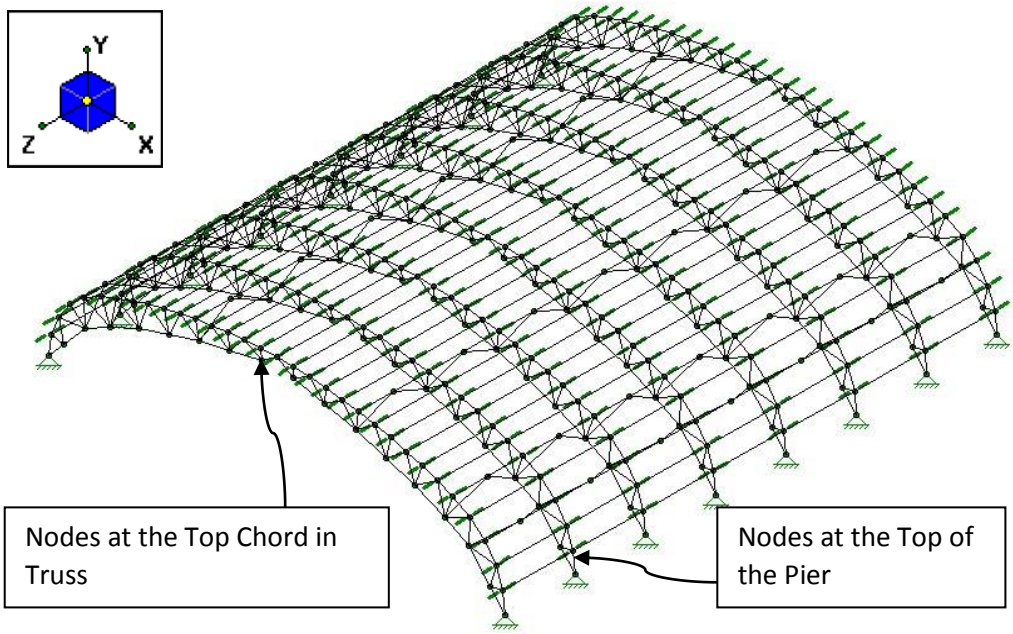

Figure 10. Basic Hangar Q Geometry with Coordinate Axes

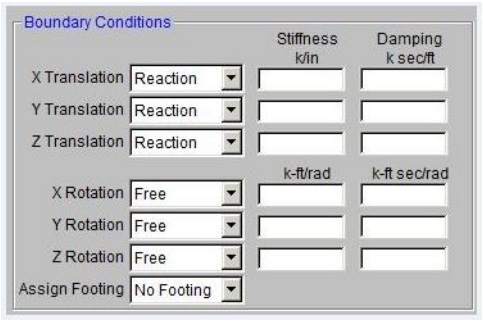

Figure 11. Boundary Conditions for Nodes at the Top of the Pier

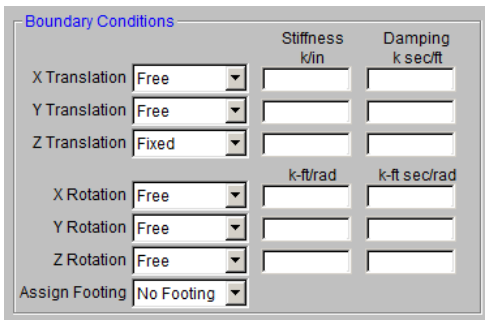

Figure 12. Boundary Conditions for Nodes along the Top chord of the Truss

- In the Z direction, the nodes along the top chord of the truss were laterally restrainted (fixed) to model the presence of the roof cladding. Refer to *Figure 12* for boundary conditions assigned to these nodes in RISA 3D.
- All other points were considered to be free in all directions.

Steel Truss Element Modeling Assumptions

- Cross-section properties may be assigned to members in one of two ways: either by choosing a shape directly from the steel database or by using a section set.
- Section sets provide a way to group members so that they have the same properties. A section set is only assigned a title for a particular type of member with the same material and geometric properties.
- As it was not possible to assign the same section sets to all steel members as hot rolled sections (HR1), they were labeled with different types of hot rolled sections. Customized labels are shown below in Table 1.
- These members of the Hangar Q were grouped into four distinct section sets.

Table 1

Section Sets Adopted in RISA 3D (before retrofitting)

#	Label	Shape	Design List	Material
1	Purlins	C7x9.8	Wide Flange	A7
2	Channels	C6x10.5	Channel	A7
3	Double Angled	LL4x4x4x0	Double Angle	A7

Table 2

Section Sets Adopted in RISA 3D (after retrofitting)

#	Label	Shape	Design List	Material
1	Purlins	W8x15	Wide Flange	A992
2	Channels	C6x10.5	Channel	A7
3	Double Angled	LL4x4x4x0	Double Angle	A7
4	WTs	Double angle with cover plate on top	W_ Tee	A7

Chapter 4

Load Cases

The structural analysis was focused on the redesign and reconstruction of an eight truss hangar. The hangar was modeled in RISA 3D and was checked for maximum global deflections (X, Y, Z) and local deflections (x, y, z) as well as maximum stresses ratios (unity checks) to evaluate its structural strength and serviceability. Analysis results are discussed in detail in Chapter 5.

RISA 3D automatically calculated the self-weight dead load for all the steel members in the model. To approximate the dead load of the steel roofing, a 0.012 ksf vertical area load was applied to all roof members. Thus, the dead load included self weight of all structural members in addition to roof loading with 14 inch overhangs on both ends of the roof.

It was also important to note that both the LRFD and ASD load combinations were used to analyze the steel truss arches and perform analysis and design of the concrete piers with the pier foundations and the concrete cross-beams.

Dead Loads

The self weight load included the weight of the steel members applied in the negative Y direction (refer *Figure 10* for geometry). The roof load included the weight of the roof assuming 0.012 ksf, applied in the negative Y direction. To accommodate the overhangs of 14 inch for roof cladding, an effective tributary area was determined and then a separate distributed load (line load) was applied to each end truss, i.e. the first and last trusses, to accurately model the effect of the roof cladding overhangs.

This overhang load was = Roof Load (ksf) * Width of Overhang (ft)

$$= (0.012 \text{ k/ft}^2)\ (14 \text{ inch}/12 \text{ inch /ft}) = 0.014 \text{ k/ft},$$

It is applied as shown in *Figure 13* and *Figure 14*.

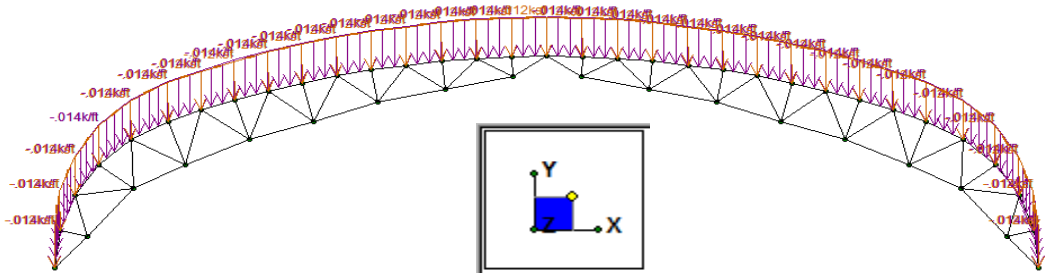

Figure 13. Roof Load with Overhang Loading on Hangar Q - Elevation

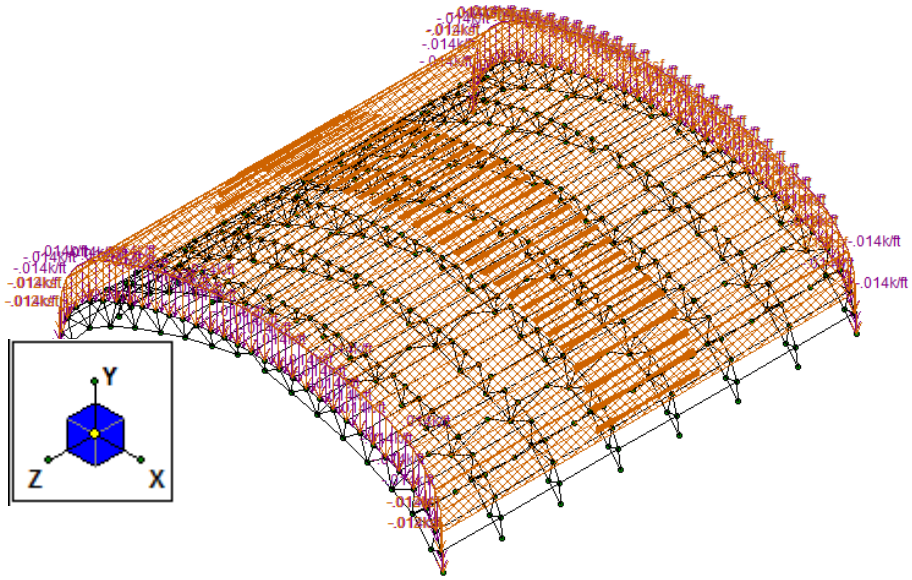

Figure 14. Roof Load with Overhang Loading on Hangar Q - Isometric

Snow Loads

The necessary calculations for snow loads were performed by following Chapter 7 using Equation 7-1 of ASCE7-10 [10], as shown below:

$$p_f = 0.7\, C_e\, C_t\, I\, p_g \qquad (7.1)$$

Where:

p_f = snow load (psf)

C_e = exposure Factor = 0.90 (Table 7.2 [10])

C_t = thermal Factor = 1.2 (Table 7.3 [10])

I = importance Factor = 1.1 (Table 7.4 [10])

p_g = ground snow load (psf) = 20 psf (Figure.7.1 [10])

Balanced and unbalanced loads were analyzed separately as per clauses 7.4.3 and 7.6.2 [10], *Figure A3* (Appendix A).

Balanced snow loads. For Hangar Q, snow loads acted on a sloping surface with curved roofs. They were assumed to act on the horizontal projection of that surface. The sloped roof snow loads, p_s, were obtained by multiplying the flat roof snow load p_f by the roof slope factor, C_s. Balanced loads were determined from the balanced load diagrams in *Figure A2* with C_s determined from the appropriate curve in *Figure A3* (Appendix A).

As per the roof slope factor for curved roofs, the portions of curved roofs having a slope exceeding 70° were considered free of snow load (i.e., $C_s = 0$). In Hangar Q, the slope from the eaves to the first two top chord members of both sides of the truss exceeded the slope 70° so that they were considered as free of snow load. As the slope at the eaves is more than 70°, it satisfied the Case 3 as shown in *Figure A3* (Appendix A).

Balanced load was calculated per eq.7.1 [10];

$p_f = 0.7\ C_e\ C_t\ I\ p_g$ = (0.7) (0.9) (1.2) (1.1) (20) = 0.016632 ksf

The adopted thermal factor was C_t =1.2 > 1.0, so it satisfied clause 7.4.2 for the cold roof slope category. Mathematically the information in *Figure A2* (Appendix A) can be represented as follows:

Cold Roofs (C_t = 1.2):

(a) Unobstructed slippery surfaces:

0° to 15° slope C_s = 1.0

15° to 70° slope C_s = 1.0 – (slope - 15°) / 55°

> 70° slope C_s = 0

(b) All other surfaces:

0° to 45° slope C_s = 1.0

45° to 70° slope C_s = 1.0 – (slope - 45°) / 25°

> 70° slope C_s = 0

There was no clear indication for the particular case of Hangar Q to determine which category of surfaces it fell into, i.e. unobstructed slippery surfaces or all other surfaces. Based on this observation, it was decided to go with all other surfaces as a more conservative loading than unobstructed slippery surfaces.

- C_s =1.0 for 0° to 45°
- C_s =1.0 (slope - 45°) / 25° for 45° to 70°
- C_s =1.0 - (56.12° – 45°) / 25° = 0.555 for 45° to 70°
- C_s = 0 for > 70°
- $p_s = p_f C_s$ = (0.016632) (1) = 0.016632 ksf = 0.017 ksf for 0° to 45°
- $p_s = p_f C_s$ = (0.016632) (0.555) = 0.00923 ksf for 45° to 70°
- $p_s = p_f C_s$ = 0 ksf for > 70°

In addition to balanced load, a snow load based on the 14 inch overhang of the members and roof at each end of the hangar must be considered, as shown in *Figure 15*, *Figure 16,* and *Figure 17.* Applied loading is mirrored so only half is shown here. For the overhang of 14 inch,

This overhang load was = Snow Load-Balanced (ksf) * Width of Overhang (ft)

(0.017) (14 inches/12 inches) = 0.0198 k/ft for 0° to 45°

(0.00923) (14 inches/12 inches) = 0.01076 k/ft for 45° to 70°

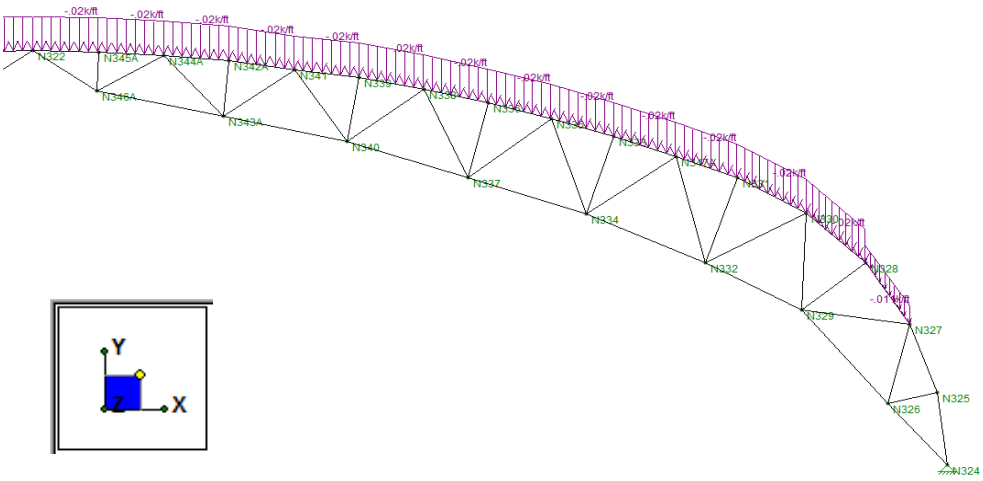

Figure 15. Snow Load-Balanced - Overhang Loading on Hangar Q - Elevation

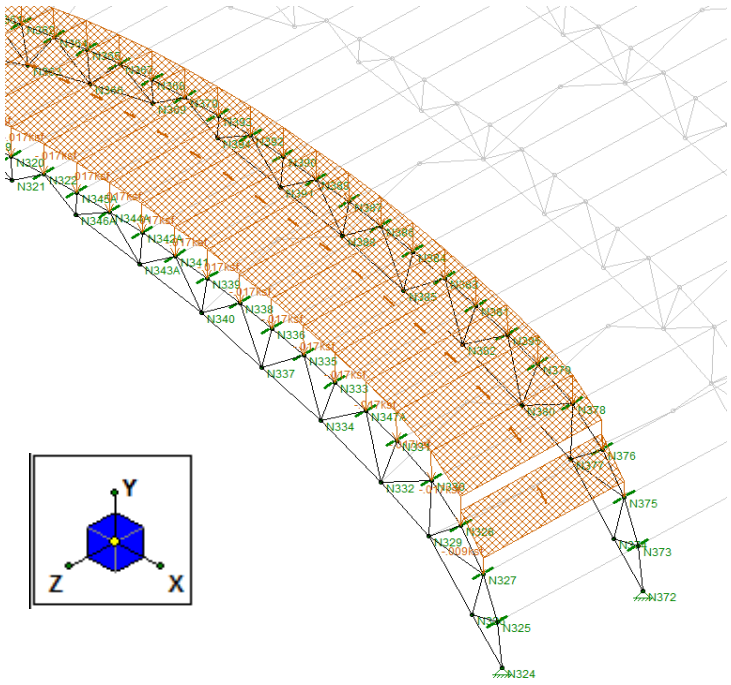

Figure 16. Snow Load-Balanced - Area Loading on Hangar Q- Isometric

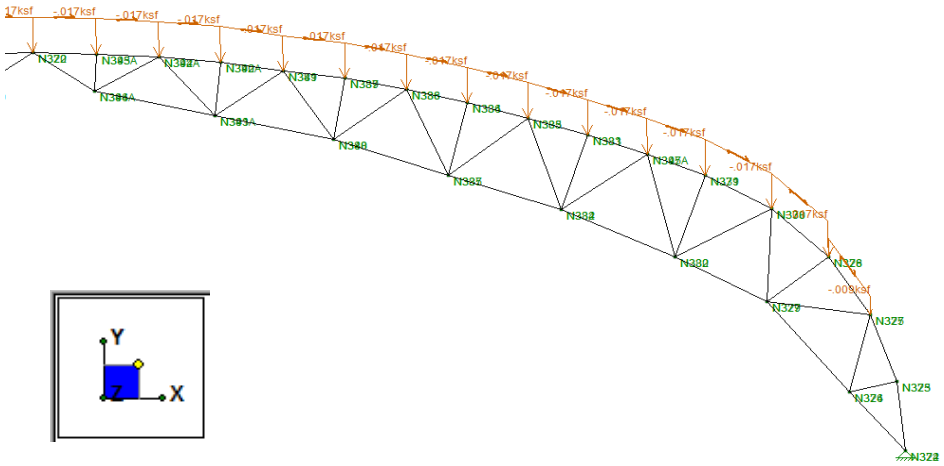

Figure 17. Snow Load-Balanced - Area Loading on Hangar Q - Elevation

Unbalanced snow loads. Curved roofs with areas having a slope exceeding 70° were again considered free of snow load, which includes the first two top chord members of the leeward side of the truss. The slope of a curved roof varied from 0° at crown to < 70° in the half portion of the roof as unbalanced loads were applied. Unbalanced loads were determined according to the loading diagrams in *Figure A3* (Appendix A). In Case 3, the windward sides were considered free of snow as usual for Cases 1 and 2, *Figure A3* (Appendix A). All these factors were considered in the slope reduction factors supported by Refs. C7-38 through C7-41 [10].Unbalanced snow load was calculated using eq.7.1 and maximum, minimum conditions:

$p_f = 0.7\ C_e\ C_t\ I\ p_g = (0.7)\ (0.9)\ (1.2)\ (1.1)\ (20) = 0.016632$ ksf

$0.5\ p_f = (0.5)\ (0.016632) = 0.00832$ ksf for Minimum value

$2\ p_f\ (C_s/C_e) = (2)\ (16.632)\ (1\ /0.9) = 0.037$ ksf for Maximum value

To calculate values due to the triangle or trapezoidal variation in the unbalanced snow loads, similar triangle properties were considered to calculate nonuniform snow load distribution over the curved roof. In addition to the unbalanced snow load, nonuniformly distributed snow load (Table 3) based on the 14 inch

overhangs of the members and roof at each end of the hangar must be included as shown in *Figure 20.*

This overhang load was = Snow Load-Unbalanced (ksf) * Width of Overhang (ft)

Table 3

Nonuniform Loading Variation of Unbalanced Snow Load on Hangar Q

Variation of unbalanced load per loading pattern	Variation of unbalanced load for overhang of 14 inch per loading pattern
0.008316 ksf - Min	0.009702 k/f- Min
0.01075 ksf	0.01254 k/f
0.01317 ksf	0.01536 k/f
0.01557 ksf	0.01816 k/f
0.018008 ksf	0.021009 k/f
0.02041 ksf	0.02381 k/f
0.02279 ksf	0.02658 k/f
0.02516 ksf	0.02935 k/f
0.02751 ksf	0.032095 k/f
0.02983 ksf	0.03480 k/f
0.03213 ksf	0.03748 k/f
0.03440 ksf	0.04013 k/f
0.03696 ksf - Max	0.04312 k/f- Max
0.02140 ksf	0.02496 k/f

(See *Figure 18* and *Figure 19* for application of these loads on a particular region of the roof)

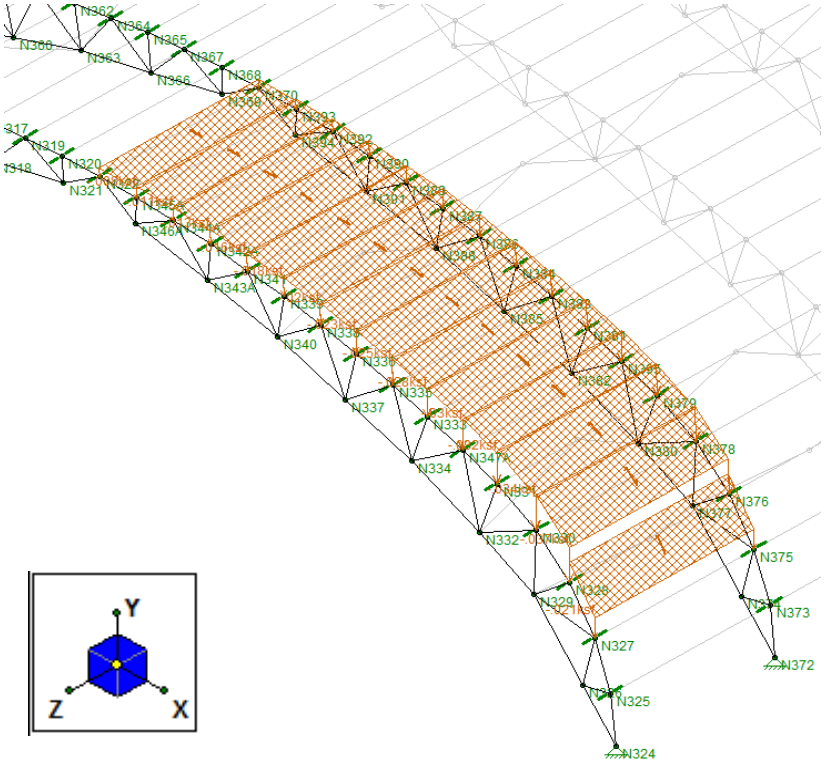

Figure 18. Snow Load-Unbalanced - Area Loading on Hangar Q - Isometric

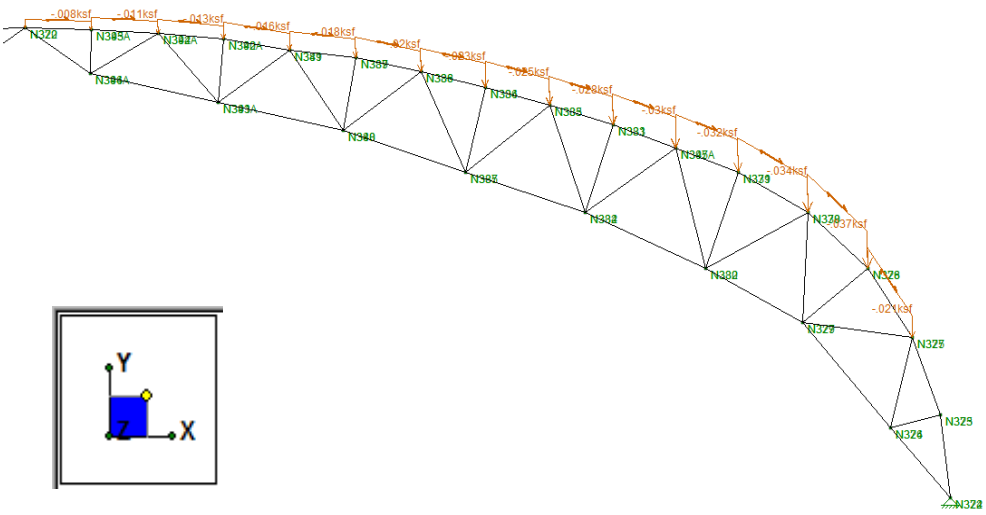

Figure 19. Snow Load-Unbalanced - Area Loading on Hangar Q - Elevation

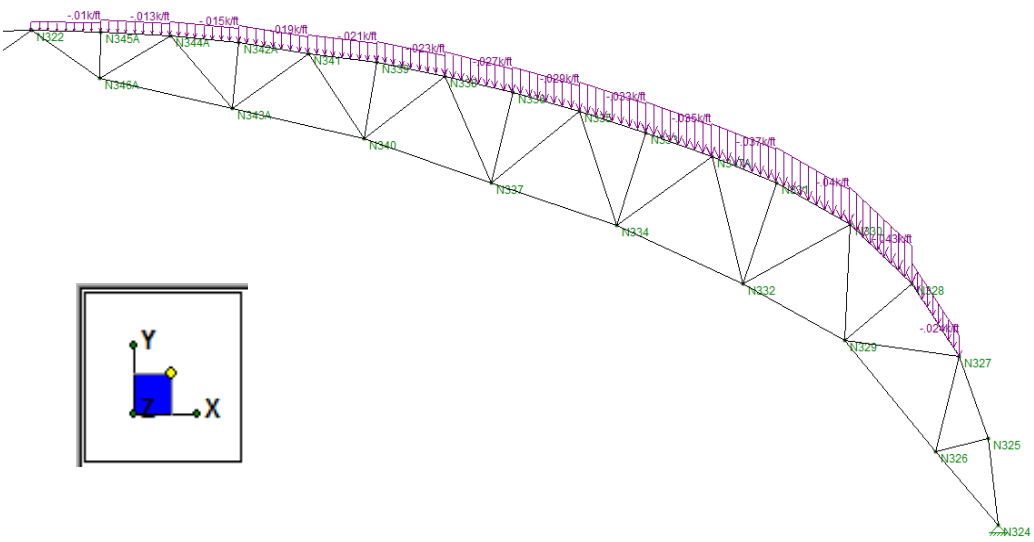

Figure 20. Snow Load-Unbalanced - Overhang Loading on Hangar Q - Elevation

Wind Loads

The necessary calculations for wind loads were performed by following Chapter 6 using Equation 6-17 of the ASCE 7-10 [10], as shown below. Hangar Q fell under Main Wind-Force Resisting System (MWFRS) type and was considered to fall under rigid buildings of all heights. Design wind pressures for the MWFRS under buildings of all heights were determined by the following equation:

$p = qGC_p - q_j(GC_{pi})$ (lb/ft^2) (6.17)

Where:

$q = q_z$ for windward walls evaluated at height z above the ground

$q = q_h$ for leeward walls, side walls, and roofs, evaluated at height h above the ground

G = gust effect factor (section 6.5.8 [10])

C_p = external pressure co-efficient (Figure 6.6 or 6.8 [10])

GC_{pi} = internal pressure coefficient (Figure 6.5 [10])

As Hangar Q was to be redesigned as an open structure, therefore $C_{pi} = 0.0$.

So $p = qGC_p$ was considered to calculate the wind load on Hangar Q. To calculate q_z and q_h per section 6.5.10 [10], velocity pressures evaluated at height z were calculated by the following equations:

$q_z = 0.0256\, K_z K_{zt} K_d V^2 I$ (lb/ft^2),

$q_h = 0.0256\, Kh\, K_{ht} K_d V^2 I$ (lb/ft^2) (6.15)

Where*:*

K_d = the wind directionality factor (defined in section 6.5.4.4 [10])

K_z = the velocity pressure exposure coefficient (defined in section 6.5.6.6 [10])

K_{zt} = the topographic factor (defined in section 6.5.7.2 [10])

q_h was the velocity pressure calculated (using Eq. 6-15 [10] at a mean roof height h).

The numerical coefficient 0.00256 was used for a design application [10]:

K_d = wind directionality factor = 0.85 (Per Table 6.4 [10])

I = importance Factor = 1.15 (Per Table 1.1 [10])

V= 3 sec gust velocity = 110 mph (Figure.6.1c [10])

K_{zt} = topographic Factor = 1.0 (Sec 6.5.7.2 [10])

K_z = velocity pressure exposure = 0.70 for 0-30 ft ht [10]; 0.76 for 31-40 ft ht [10]

By plugging in all of these values into q_z equation:

$q_z = (0.00256)\ (0.70)\ (1.0)\ (0.85)\ (110^2)\ (1.15) = 0.02120$ ksf for 0 to 30 ft ht

$q_z = q_h = (0.00256)\ (0.76)\ (1.0)\ (0.85)\ (110^2)\ (1.15) = 0.023$ ksf for 31 to 40 ft ht

q_h at mean roof height = 32 ft from spring line of roof

(Mean roof height was as shown in mansard roof *Figure 19* below)

External pressure coefficient C_p (*Figure.6.6* [14]) has two parts, which are; Windward Wall, C_p = 0.8 for all values of L/B, Leeward Wall, C_p = -0.5 for L/B = 130/140 = 0.93, where:

L = horizontal dimension of building measured parallel to wind direction

B = horizontal dimension of building measured normal to wind direction

Therefore, the following values for *p* were derived:

$p = q_z G C_p$ = (0.02120) (0.85) (0.80) = 0.01442 ksf for Windward (x)

$p = q_z G C_p$ = (0.02120) (0.85) (0.50) = 0.00901 ksf for Leeward (x)

$p = q_h G C_p$ = (0.023) (0.85) (0.80) = 0.01564 ksf for Windward (y)

$p = q_h G C_p$ = (0.023) (0.85) (0.50) = 0.009775 ksf for Leeward (y) and Roof Top

It was necessary to define five points on the arch roof to determine wind load per the mansard roof requirements. In addition to wind load, uniformly distributed wind loads based on the 14 inch overhangs of the members and roof at each end of the hangar must be factored in.

This overhang load was = Wind Load (ksf) * Width of Overhang (ft):

(0.01442) ksf (14 inch/12 inch) = 0.016823 k/ft for Windward (x)

(0.00901) ksf (14 inch/12 inch) = 0.010511 k/ft for Leeward (x)

(0.01564) ksf (14 inch/12 inch) = 0.018246 k/ft for Windward (y)

(0.009775) ksf (14 inch/12 inch) = 0.011404 k/ft for Leeward (y) and Roof Top

Two cases were defined for the wind load - Case 1 and Case 2 - which indicated only the change of direction of the wind ward (y). For Case 1, *Figure 22* and *Figure 23*, the wind load was applied downward. For Case 2, *Figure 24* and *Figure 25*, the wind load was applied upward to part of the truss of Hangar Q. These load cases are shown for the mansard roof *Figure 21*.

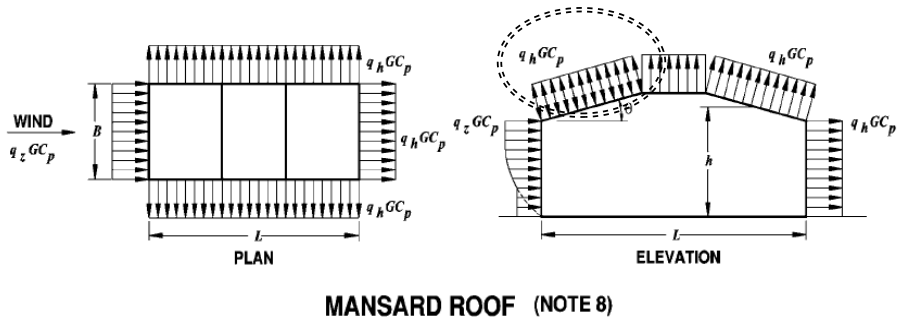

*Figure 21.*Mansard Roof Wind Load Distribution

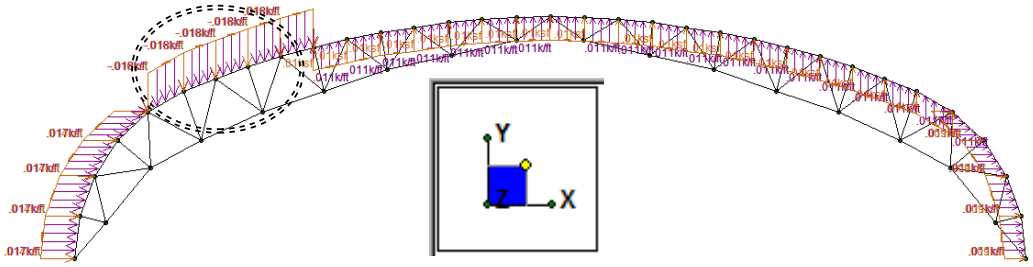

Figure 22. Wind Load Case 1 with Overhang Loading on Hangar Q - Elevation

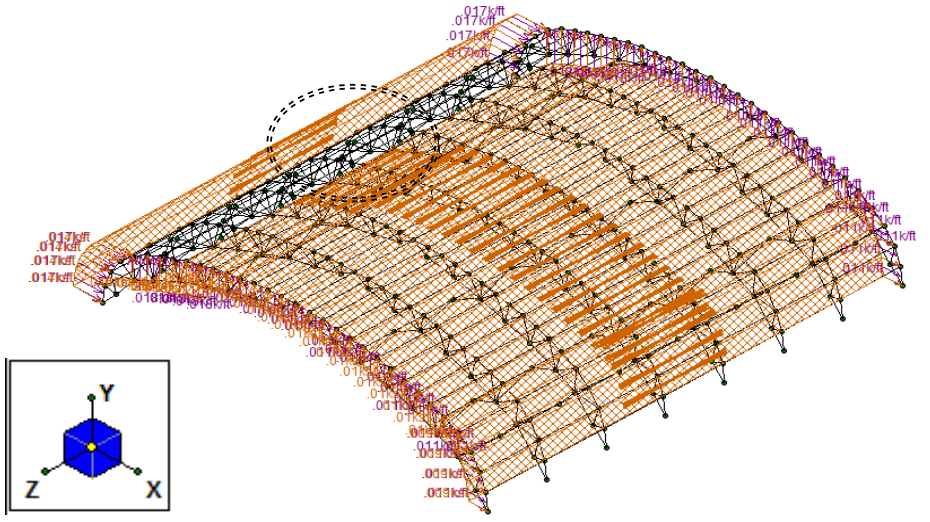

Figure 23. Wind Load Case 1 with Overhang Loading on Hangar Q - Isometric

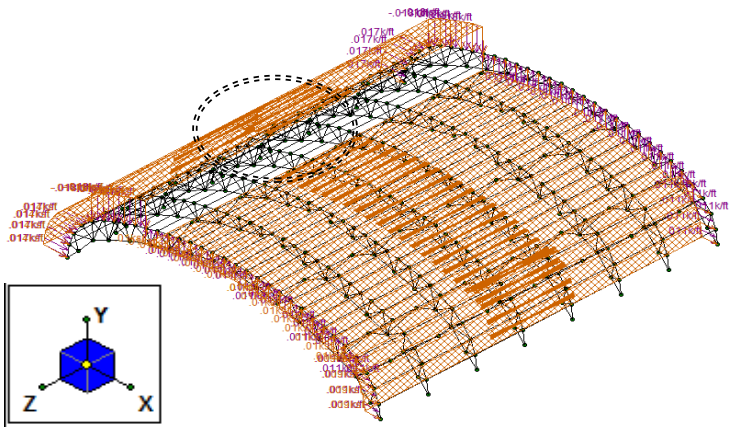

Figure 24. Wind Load Case 2 with Overhang Loading on Hangar Q - Isometric

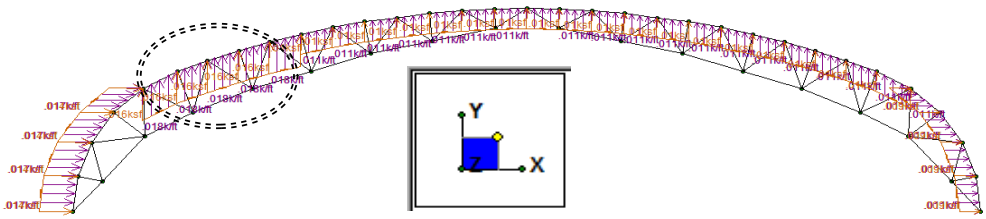

Figure 25. Wind Load Case 2 with Overhang Loading on Hangar Q - Elevation

Load Combinations

Both Allowable Strength Design (ASD) and Load and Resistance Factor Design (LRFD) loading combinations were applied in the Hangar Q analysis. It is observed that essentially each of them provides the same level of safety [10].

Basic Load Cases

1. Self Weight
2. 2. Roof Load
3. 3.Snow Load-Balanced
4. 4. Snow Load-Unbalanced
5. 5. Wind Load Case-1
6. 6. Wind Load Case-2

Allowable Strength Design (ASD) Combinations

I. D + F

II. D + H + F + L + T

III. D + H + F + (L_r or S or R)

IV. D + H + F + 0.75 (L + T) + 0.75 (L_r or S or R)

V. D + H + F + (W or 0.7E)

VI. D + H + F + 0.75 (W or 0.7E) + 0.75L + 0.75 (L_r or S or R)

VII. 0.6D + W + H

VIII. 0.6D + 0.7E + H

Where**:**

D = dead load; D_i = weight of ice

E = earthquake load; F_a = flood load

F = load due to fluids with well-defined pressures and maximum heights

H = load due to lateral earth pressure, ground water pressure

L = live load; L_r = roof live load

R = rain load; S = snow load

T = self-straining force; W = wind load

W_i = wind-on-ice determined in accordance with chapter 10 [10]

As per the ASD load combinations, the following load combinations were derived for the analysis of Hangar Q:

7. Dead Load
8. Dead Load + Snow Load (Balanced)
9. Dead Load + Snow Load (Unbalanced)
10. Dead Load + Wind Load Case 1
11. Dead Load + Wind Load Case 2

12. Dead Load + 0.75 Snow Load (Balanced) + 0.75 Wind Load Case 1
13. Dead Load + 0.75 Snow Load (Balanced) + 0.75 Wind Load Case 2
14. Dead Load + 0.75 Snow Load (Unbalanced) + 0.75 Wind Load Case 1
15. Dead Load + 0.75 Snow Load (Unbalanced) + 0.75 Wind Load Case 2
16. 0.6 Dead Load + Wind Load Case 1
17. 0.6 Dead Load + Wind Load Case 2

Load and Resistance Factor Design (LRFD) Combinations

I. U = 1.4D
II. U = 1.2D + 1.6L + 0.5 (L_r or S or R)
III. U =1.2D + 1.6 (L_r or S or R) + (1.0L or 0.5W)
IV. U = 1.2D + 1.0W + 1.0L + 0.5 (L_r or S or R)
V. U = 1.2D + 1.0E + 1.0L + 0.2S
VI. U = 0.9D + 1.0W
VII. U= 0.9D + 1.0E

As per the LRFD load combinations, the following load combinations were derived for analysis of Hangar Q:

18. 1.4 Dead Load
19. 1.2 Dead Load + 0.5 Snow Load (Balanced)
20. 1.2 Dead Load + 0.5 Snow Load (Unbalanced)
21. 1.2 Dead Load + 1.6 Snow Load (Balanced) + 0.5 Wind Load Case 1
22. 1.2 Dead Load + 1.6 Snow Load (Balanced) + 0.5 Wind Load Case 2
23. 1.2 Dead Load + 1.6 Snow Load (Unbalanced) + 0.5 Wind Load Case 1
24. 1.2 Dead Load + 1.6 Snow Load (Unbalanced) + 0.5 Wind Load Case 2
25. 1.2 Dead Load + Wind Load Case 1 + 0.5 Snow Load (Balanced)
26. 1.2 Dead Load + Wind Load Case 1 + 0.5 Snow Load (Unbalanced)

27. 1.2 Dead Load + Wind Load Case 2 + 0.5 Snow Load (Balanced)

28. 1.2 Dead Load + Wind Load Case 2 + 0.5 Snow Load (Unbalanced)

29. 1.2 Dead Load + 0.2 Snow Load (Balanced)

30. 1.2 Dead Load + 0.2 Snow Load (Unbalanced)

31. 0.9 Dead Load + Wind Load Case 1

32. 0.9 Dead Load + Wind Load Case 2

In the analysis of Hangar Q, both loading combinations - ASD and LRFD - were incorporated to determine the maximum and minimum values for the arch truss reactions at the tops of the piers. The analysis of results are presented in Chapter 5, which consisted of maximum reactions, maximum deflections, and maximum stress ratios (unity checks) for particular load combinations and also the worst cases were considered to check the failure criteria (unity check >1). The stability analysis of the foundation (Chapter 6) was carried out adopting vertical and horizontal loads derived in ASD and LRFD load combinations accordingly to check eccentricity, building pressure on soil, and location of vertical resultant force from soil. Finally, reinforced concrete design of the foundations, the piers, and the cross beams was performed per ACI 318-11 [11] and detailed in Chapter 6.

Chapter 5

Analysis of Results

Hangar Q was modelled using RISA 3D as discussed in Chapter 3 with the application of dead load, snow load, and wind load to analyze the bow string trusses and members using load combinations as per ASCE 7-10 [10], as discussed in Chapter 4. The resulting forces at the tops of the piers, *Figure 26*, were used to design the new reinforced concrete piers and their foundations, and the cross beams between the piers. Structural analysis was carried out using the steel member sections cited in the original drawings provided by DRBA. Analysis showed structural deficiencies (stress ratio >1) particularly in purlins (channel sections) and double angle members (bracings and chord members). Retrofitting of these overstressed members (stress ratio >1) were carried out by replacing purlins with wide flange sections and strengthening double angle members with steel cover plates. The factors and values used for the wind and snow loads were determined using Chapters 6 and 7 of the ASCE 7-10 [10]. The wind values in the load combinations refer to windward and leeward effects on the roof of the hangar.

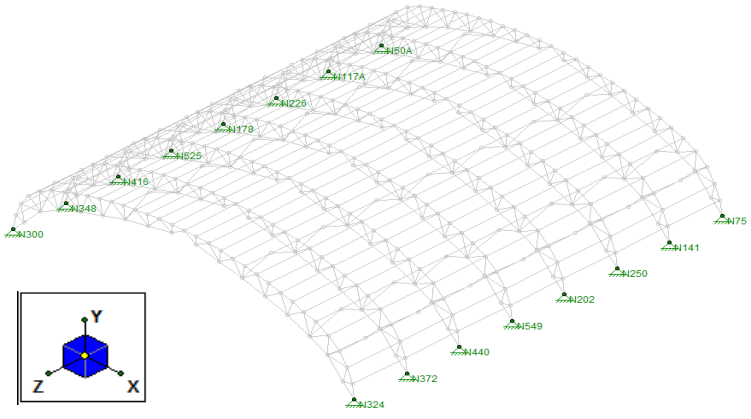

Figure 26. Joints to be considered in Designing the Pier

The maximum reactions for ASD load combinations and LRFD load combinations (LC) are presented in Tables 4 and 5, respectively, as these reactions were used as loads for the design of the concrete piers and their foundations.

Table 4

Reactions for Allowable Strength Design (ASD) Combinations

Joints	X (kips)	LC	Y (kips)	LC	Z (kips)	LC
N300	24.7	8	26.088	8	-0.301	11
N348	51.671	8	55.99	8	-0.026	11
N416	48.145	8	50.319	8	0.021	8
N525	48.109	8	51.386	8	-0.014	8
N178	48.109	8	51.386	8	0.012	8
N226	48.145	8	50.319	8	-0.021	8
N117A	51.671	8	55.99	8	0.026	11
N50A	24.7	8	26.088	8	0.301	11
Joints	X (kips)	LC	Y (kips)	LC	Z (kips)	LC
N324	-24.7	8	26.20	9	-0.455	7
N372	-51.671	8	56.01	9	0.052	12
N440	-48.145	8	50.472	9	0.021	8
N549	-48.109	8	51.639	9	-0.014	8
N202	-48.109	8	51.639	9	0.014	8
N250	-48.145	8	50.472	9	-0.021	8
N141	-51.671	8	56.01	9	-0.052	12
N75	-24.7	8	26.20	9	0.455	7

Table 5

Reactions for Load and Resistance Factor Design (LRFD) Combinations

Joints	X (kips)	LC	Y (kips)	LC	Z (kips)	LC
N300	28.285	21	34.655	21	-0.611	28
N348	59.07	21	75.656	21	0.078	28
N416	54.891	21	67.78	21	0.017	22
N525	54.913	21	69.234	21	-0.016	21
N178	54.913	21	69.234	21	0.016	21
N226	54.891	21	67.78	21	-0.017	22
N117A	59.07	21	75.656	21	-0.078	28
N50A	28.285	21	34.655	21	0.611	28
Joints	X (kips)	LC	Y (kips)	LC	Z (kips)	LC
N324	-28.276	21	34.463	21	-0.523	18
N372	-59.05	21	75.531	21	-0.061	28
N440	-54.759	21	67.72	21	-0.022	22
N549	-54.827	21	69.359	21	-0.019	21
N202	-54.827	21	69.359	21	-0.019	21
N250	-54.759	21	67.72	21	-0.022	22
N141	-59.05	21	75.531	21	-0.061	28
N76	-28.276	21	34.463	21	-0.523	18

Maximum deflections from all trusses were used to assess the deflected behavior of Hangar Q and whether they satisfied the limiting criterion for deflection. Unity checks (stress ratio) were carried out for all the members of Hangar Q using equation H1-b [12], which is already available in RISA 3D considering P-delta analysis. For the deflections in the vertical direction (Y), all the values were considered acceptable as long as they did not exceed the l/240 deflection limit, where l = span of truss or length of the hangar. This leads to allowable vertical deflections considering span (130 ft) of truss = 6.5 inches and allowable vertical deflections considering length (140 ft) of the hangar = 7 inches. Joints with maximum global deflections (*Figure 27*) and members with maximum local deflections (*Figure 28*) are shown. None of the vertical deflections exceeded the allowable limit. Drift

(deflections in X and Z directions) was also a major criteria to check the structural stability of the hangar corresponding to the height of the hangar (30 ft). Allowable range of drift was considered between H/100 to H/600 [25]. Based on the boundary conditions applied in RISA 3D, it was prudent to adopt H/200 (1.80 inches) based on [25] as an allowable drift limit. Eventually, all the deflections in the horizontal (drift) directions (X and Z) in the global and local coordinates satisfied the allowable drift limit. It is to be noted that rotations are allowed in the X, Y, and Z directions at end connections of the hangar as modeled with pinned joints for all eight trusses. Analysis results are presented (Table 5-8) in more detail.

- Allowable vertical deflection (Y, y) = l/240
- Considering the width of the truss = (130 ft * 12 inches) / 240 = 6.5 inches
- Considering the length of the truss = (140 ft * 12 inches) / 240 = 7 inches
- Allowable horizontal deflection (drift-X, x, Z, z) = H/200
- Considering the height of the hangar = (30 ft *12 inches) / 200 = 1.8 inches

Thus, Hangar Q should be safe for the maximum deflections that occurred under applied loads. The results are presented in the tables and figures below.

Table 6

Joint Deflections (Global)

LC	Global Coordinates	Deflection (in)	Nodes
12	X	0.861	N342, N464
9	Y	-1.21	N213, N396
9	Z	-0.51	N88, N337

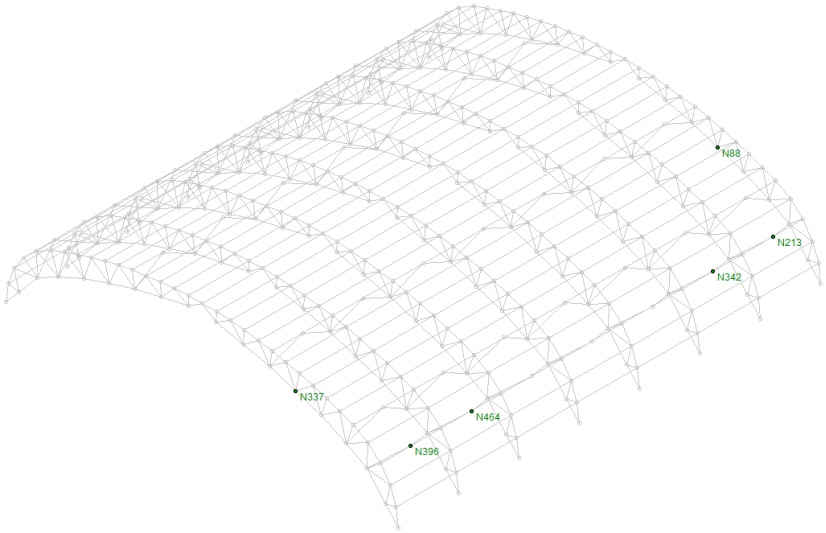

Figure 27. Joints with Maximum Global Deflections

Table 7

Member Deflections (Local)

LC	Local Coordinates	Deflection (in)	Members
9	x	-1.195	M322, M1128
9	y	-1.244	M301, M1107
10	z	1.27	M418, M1135

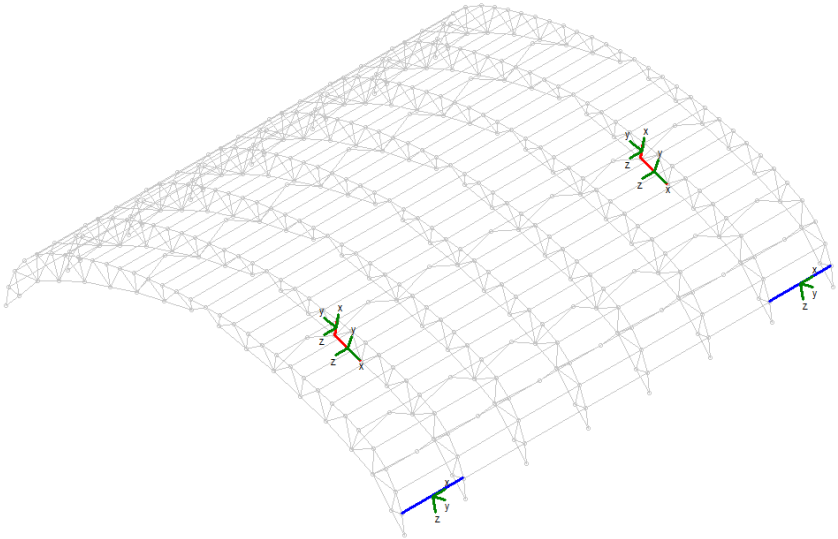

Figure 28. Members with Maximum Local Deflections

The RISA 3D results presented in Tables 6 and 7 are for joint deflections and for member deflections, respectively. Both of these deflections satisfied the allowable limit of vertical deflection and horizontal deflection (drift). For the unity check (or stress ratios), the interaction formula [12] of flexure and compression in doubly symmetric members and singly symmetric members were considered. These kind of members have constraints to bend about a geometric axis which would be limited by Equation H1-b [12]. RISA 3D has this equation by default to be considered in P-delta analysis.

Table 8

Sections Unity Check (before retrofitting)

Steel Sections	Overstressed Members (Stress Ratio >1)	LRFD (LC)	ASD (LC)
C7x9.8	M680,M1875, M1136,M1614	2.81 (25)	2.737 (10)
C6x10.5	M457, M1175	0.517 (26)	0.472 (14)
LL4x4x4x0	M535,M544, M633, M648, M1253, M1262, M1589	1.92 (21)	1.93 (12)

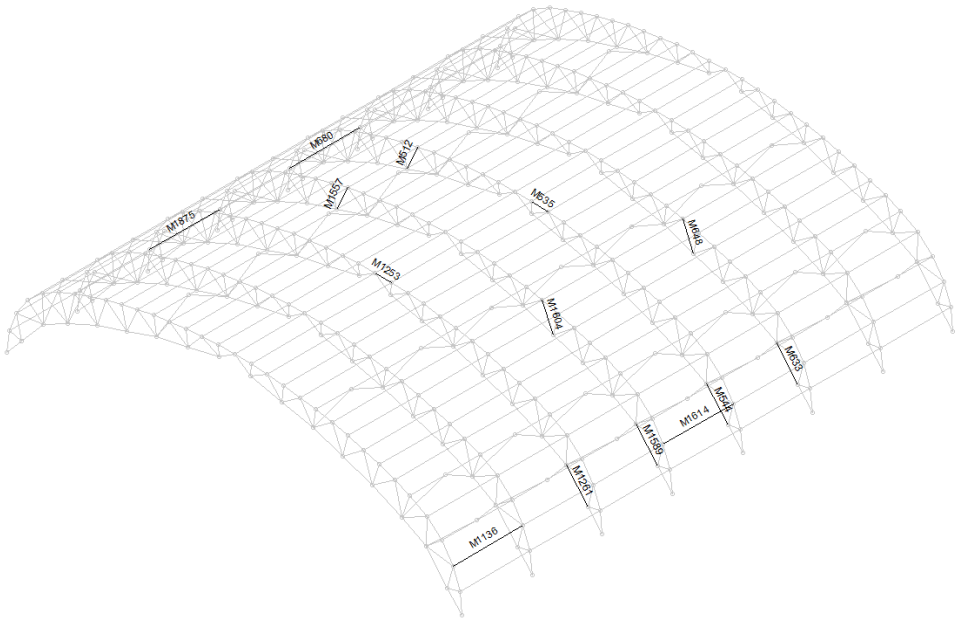

Figure 29. Some of the Retrofitted Sections

Table 9

Sections Unity Check (after retrofitting)

Steel Sections	Members with Maximum Stress Ratio <1	LRFD (LC)	ASD (LC)
W8x15	M680,M1875,M1136,M1614	0.82 (25)	0.79 (10)
C6x10.5	M457, M1175	0.46 (26)	0.43 (14)
LL4x4x4x0	M535,M544, M633,	0.86 (21)	0.84 (9)
WT	M648, M1253, M1262, M1589	0.74 (21)	0.71(8)

The members were adopted from the original design drawings (before retrofitting). Many of these members showed overstressed behavior (unity check > 1), particularly in top chord members, bottom chord members, purlins, and bracing (LL4x4x4x0) for ASD and LRFD load combinations. In analysis, it was found that there were more overstressed members but only the members listed in Table 8 (before retrofitting) and Table 9 (after retrofitting) with maximum stress ratios as shown in *Figure 29* (for clarity purpose only few members are shown. Please refer Appendix B for all retrofitted sections.). It was decided to retrofit these steel sections by replacing them with sections with larger cross section areas, moments of inertia, or adding cover plates to maintain the historic value of the truss. All of the purlins, which were originally channel sections (C7x9.8), were replaced by wide flange sections (W8x15). Cross braces (C6x10.5) between the trusses were channel sections and in good shape so modifications were not required for these steel sections.

Many of the critical double angle members (bracing and chord members) were overstressed (unity check > 1) under applied loading [10]. These overstressed double angle members were retrofitted by putting cover plates (0.5 inch thick) on top of them to control the limiting criteria (unity check < 1) (*Figure 30* and *Figure 31).* This was modeled in RISA using WT sections.

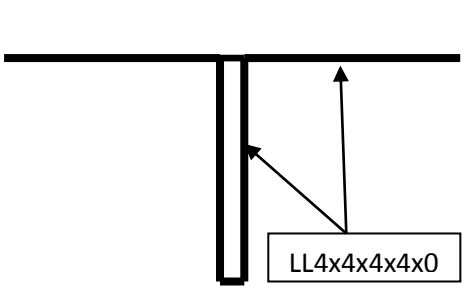

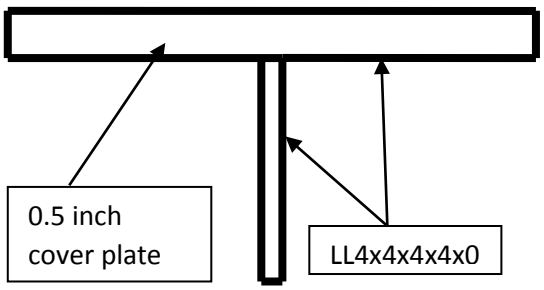

Figure 30. Original LL4x4x4x0 Section

Figure 31. Retrofitted Section

Basically, the cross sectional areas of the double angle (bracing, chord) members (LL4x4x4x0) were increased by modifying the original section with 0.5-inch cover plates (*Figure 31*) to satisfy the unity check (stress ratio < 1.0) criteria.

Chapter 6

Analysis and Design of Concrete Elements

The structural analysis and design of the foundations, piers, and cross beams were carried out using ASD and LRFD load combinations. Analysis of Hangar Q was done in RISA 3D. Basically, reactions at the ends of the trusses were used as loads on the top of the piers to design all concrete members as stated above. As a first priority, stability of the foundation was checked with its dimensions, which must satisfy the eccentricity criteria, soil pressure criteria, to get a structurally stable foundation, and to satisfy equilibrium condition under ASD load combinations.

As per the request made by DRBA, the shape of the pier (150 inches by 150 inches by 24 inches) was maintained above the ground level to preserve the historical value of the hangar. This meant that if stability conditions were not satisfied with selected foundation and pier dimensions then a trial and error method was used to achieve equilibrium by changing the foundation geometry but not the pier dimensions. To check the stability and equilibrium of the foundation geometry, a spreadsheet with variable pier dimensions was developed along with hand calculations. Furthermore, once the dimensions of the foundations were fixed, then the foundations and piers were analyzed and designed with their proper reinforcement detail. Analysis and design of the piers were performed by adopting three different approaches.

The cross beams serve to connect the tops of the piers longitudinally for stability purposes. For the beams, maximum LRFD load combinations and an assumption of five 200 lb men on top of the beam at one time as a uniformly distributed load (UDL) were applied to analyze and to come up with the design and reinforcement detail of the beams.

A consistent methodology was used in the stability analysis of the foundation, the design of the foundation, the structural analysis and reinforcement design, and the detailing of the piers. According to the discussion and consensus, suitable maximum reaction from ASD load combinations was adopted to check the stability of the foundation, i.e., the width and length of footing, the point of application of the soil pressure beneath the foundation, the eccentricity and average building pressure, and maximum building pressure. Maximum reactions from LRFD load combinations were utilized to calculate the thickness and reinforcement detail of the footing. Suitable maximum reactions from LRFD load combinations were also used to come up with the reinforcement design for the piers.

Stability Analysis of Foundation

In the stability analysis, maximum reactions from ASD load combinations were considered to check the stability of the footing by incorporating the assumed width and length of the footing. By referring to reactions from ASD load combinations, it was advisable to consider a case which provides maximum vertical load and maximum horizontal load to fix the width and length of the footing as a part of the stability analysis.

Total horizontal loads and total vertical loads were computed. In particular, total vertical load was the summation of the vertical load which was derived from the RISA 3D analysis and the dead load weight of all four sections (Table 12) of the pier and foundation (*Figure 32*, *Figure 33*). As there was no additional horizontal load acting on the pier, total horizontal load was equal to the horizontal load calculated from RISA 3D analysis by considering ASD load combinations.

The moment was computed at point A (i.e. at the heel of pier), as shown in *Figure 32*, to determine the distance to the point of application (X') of the resultant

vertical reaction and checked that it should be less than the assumed length of the foundation. The eccentricity (e) was evaluated by subtracting half of the length of the foundation from the distance of the point of application (X') of the resultant vertical reaction and ensured that it should be less than one sixth of the length of the foundation which was the criteria to keep the foundation free from developing tension at the heel of the pier. The maximum pressure acting on the soil should be less than the safe bearing pressure (sbc) of the soil as shown in the design drawings provided by DRBA. Calculations for the maximum ASD load combination are presented here. Detailed computations are described in Appendix C.

Maximum horizontal load and maximum vertical load. Total horizontal load was taken as equal to the maximum reaction in the X-direction from the analysis of the truss. So, the total horizontal load = 51.70 kips.

Total vertical load was calculated as the summation of vertical load in the Y-direction from the analysis of the truss and the dead loads due to the weights of the four sections of the pier and foundation (Table 10, *Figure 32*).

So, the total vertical load = 129.62 kips

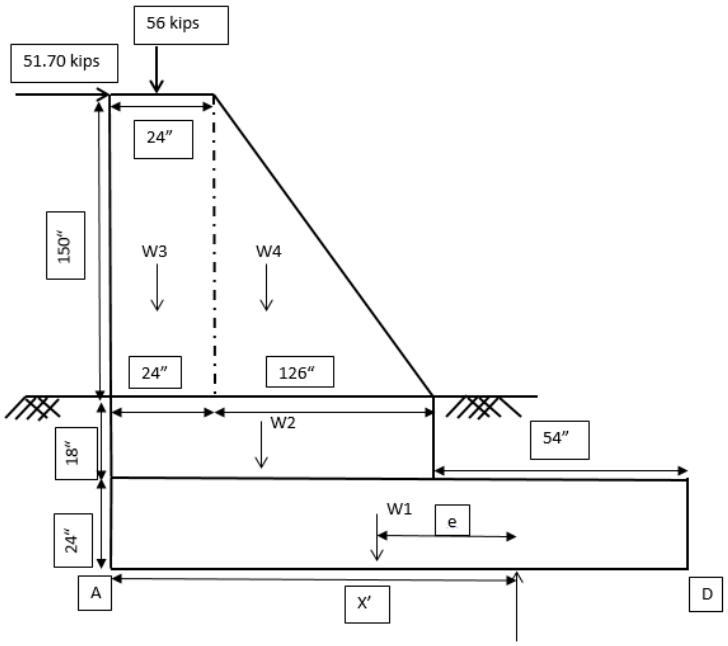

Figure 32. Elevation of Pier

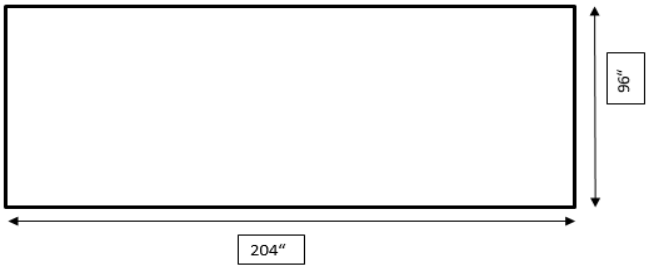

Figure 33. Foundation of Pier (ASD) Plan View

The distance of the point of application (X') of the resultant vertical reaction was computed by employing moment equilibrium at point A, considering all forces, referring to *Figure 32*. (Clockwise Moment = Negative, Counter clockwise Moment = Positive):

X' = 127.80 inches < assumed length of foundation (l) = 204 inches - from point A.

Eccentricity was found by subtracting half of the assumed length (l) from X':

e = X'- (l/2) = 25.80 inches < assumed length (l) / 6 = 34 inches

Table 10

Weight of the Sections with Lever Arm from Heel (point A)

Weight of the sections	X from A (inch)
W1 = (204*24*96*150) / (12^3) * (1000) = 40.8 kips	X1 = 102
W2 = (150*24*150) / (12^3) * (1000) = 5.625 kips	X2 = 75
W3 = (150*24*24*150) / (12^3) * (1000) = 40.8 kips	X3 = 12
W4 = (126*150*24*150) / (2) *(12^3) * (1000) = 19.70 kips	X4 = 66

As per these calculations, the length of the soil pressure (228.60 inches) acting beneath foundation was larger than assumed length of the foundation (204 inches) and e < l/6, so it would be a trapezoidal pressure distribution from the soil, as in *Figure 34*.

.

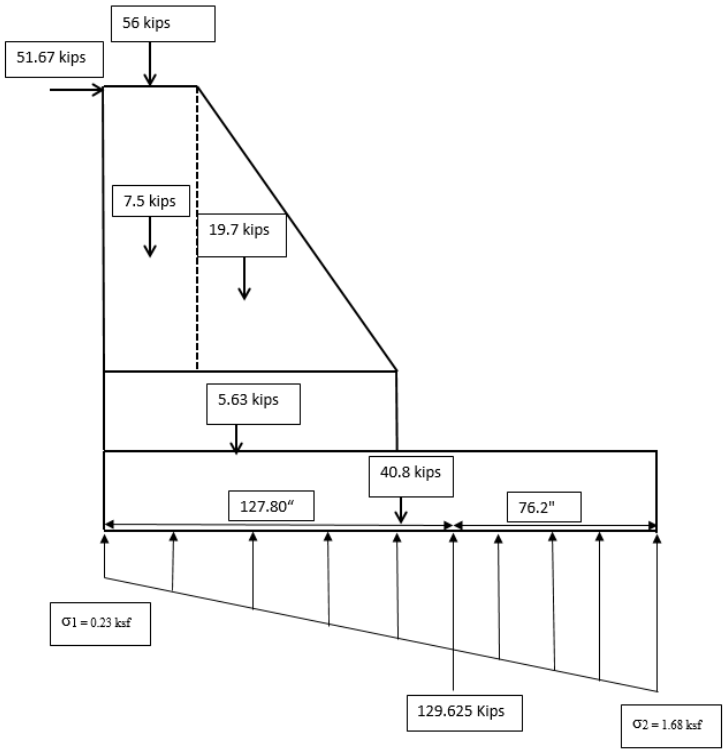

Figure 34. Soil Pressure Distribution beneath Foundation

Here, it was necessary to determine average building pressure and maximum building pressure to check that none of them exceeded the limiting soil bearing pressure. The average building pressure acting on the foundation from the top was

determined considering total vertical load as mentioned earlier and (*Figure 33*) area of foundation. Allowable soil bearing pressure was used as 3 ksf from provided drawings.

Total vertical load = 129.62 kips; acting on an area = 136 ft^2

Average building pressure = load /area = 0.9531 ksf < 3 ksf

Maximum building pressure was calculated as:

(204 *96) σ_1 + (σ_2 - σ_1) (0.5*204*96) = 129.62 kips; considering forces

σ_1 (204*96*102) + (σ_2 - σ_1) (0.5*204*96*0.67*204) = (129.62*127.80); considering moments

Solving simultaneously the equation of forces and equation of moments;

σ_1 = 0.23 ksf , σ_2 = 1.68 ksf (*Figure 34*) which are less than 3 ksf, so foundation geometry is stable under maximum ASD load combinations.

Structural Analysis and Design of Pier Foundation

Based on the pier and foundation geometry, *Figure 35* and *Figure 36*, it was decided to design the pier foundation as a spread footing. The upward soil pressure under the spread footing tended to bend the foundation upward as a fixed cantilever beam. The foundation was designed as shallow cantilever beams for the moments and shears involved.

The thickness of the footing was assumed to be 24 inches (2 ft) considering the depth of the frost line to be 33 inches (2 ft 9 inch) [9] and from that the adopted depth of the excavation which was 42 inches (3ft 6 inches).The weight of the concrete (W_c) and the weight of the soil (W_s) were calculated by taking their unit weights and depth of the footing into account, i.e. 150 pcf , 110 pcf, respectively so their weights are as: W_c = 300 psf , W_s = 165 psf.

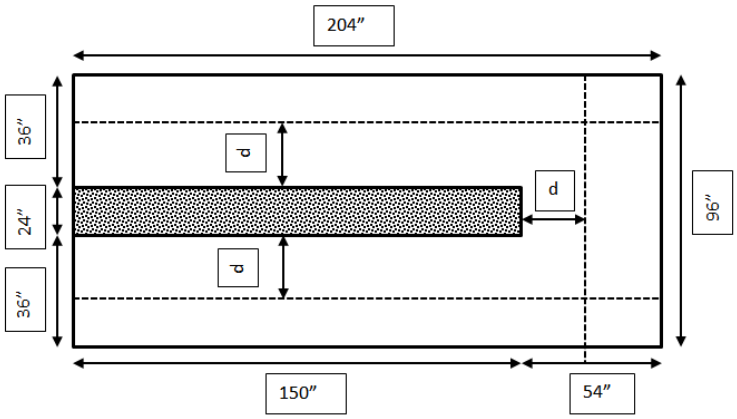

Figure 35. Plan of Foundation

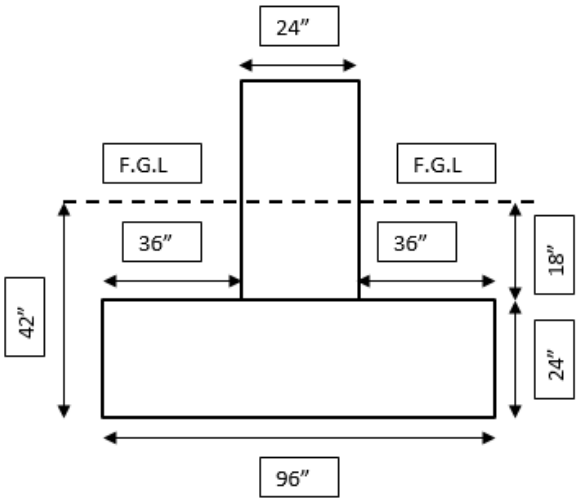

Figure 36. Section of Foundation

Effective soil pressure was derived (q_{eff} = 2.535 ksf) by subtracting the weight of the concrete and the weight of soil from the allowable safe bearing pressure (3.00 ksf). Net upward pressure (q_u = 4.056 ksf) was calculated by considering load factor 1.6 (conservatively). The depth of reinforcement was taken to be d = 19.50 inches. The thickness of the footing was checked assuming a one way shear concept at a distance *d* from the edge of the wall as shown in *Figure 35*, and it was found to be less than the depth of the reinforcement which was the limiting criteria for the

thickness of the footing. The shear forces assuming a one way shear concept were computed by considering net upward pressure and overhang in a particular direction. The depth of the footing by one way shear was derived as follows:

$d = V_u / (\emptyset\ 2 \sqrt{f_c} b)$

V_u = 11.661 kips; d = 11.828 inches < 19.5 inches for shorter direction

V_u = 5.577 kips; d= 5.656 inches < 19.5 inches for longer direction

The bending moments were also computed at the edge of the spread footing utilizing net upward pressure. Moment arms were taken as overhang distances in respective directions, *Figure 32*.

M_u = 41.067 kip-ft for the shorter direction;

M_u = 18.252 kip-ft for the longer direction

The percentage of steel reinforcement (ρ) was calculated to determine the area of steel, which was computed by multiplying the percentage of steel (ρ) within the area (bd, *Figure 35*) of the pier. Three basic equations to calculate minimum area of steel which included, area of steel via flexure, area of steel via shrinkage, area of steel via bending moment were employed. From these equations, the area of steel via flexure governed the design of the footing reinforcement. R_u for the footing was computed to find percentage of steel (ρ) of the footing considering bending moments and overhang dimensions in respective directions.

R_u = 0.11 ksi for the shorter direction;

R_u = 0.048 ksi for the longer direction

The percentage of steel required in both directions was:

ρ = 0.002088 for the shorter direction;

ρ = 0.000898 for the longer direction

The area of steel was calculated following three different approaches [11]:

A_s = ρbd = 0.49 inch^2/ft; minimum for bending moment; d = depth of reinforcement,

A_s = 0.0018bh = 0.52 inch^2/ft width; minimum for shrinkage;

h = depth of footing,

A_s = (200bd) / f_y = 0.78 inch^2/ft width; minimum for flexure

The numbers of bars were computed at the bottom of the footing in the shorter and longer directions according to the given geometry of the foundation. For the mesh of bars in the top of the footing, 50% of the total bending moment was adopted as suggested in 21.5.2.2 [11] for flexural longitudinal reinforcement. It says "positive moment strength at the joint face shall be not less than one-half (50%) of the negative moment strength provided at that face of the joint." It means that reversal of stresses (compression-tension) is possible at both the faces of the footing, i.e. top and bottom of the footing slabs as described. As per given clause 21.5.2.2 [11], compression and tension could reverse their directions during application of lateral loads on the footing or any structural element. The area of steel and the number of bars in the top of the slab were computed similarly as the bottom of the slab. Considering the maximum area from above three equations and using #8 bars (area of one #8 bar = 0.79 inch^2). Required number of bar (n) per ft was calculated as; n = 0.987 ≈ 1 bar/ft

Thus, #8 bar @ 1 ft c/c were used in both directions.

The number of bars in a particular direction was found as follows:

n -1 = (length of footing – 2 (cover)) /12

n -1 = 16.5; n=17.5 ≈ 18, placed in shorter direction

n -1 = (width of footing - 2 (cover)) /12 = 7.5;

n= 8.5 ≈ 9, placed in longer direction

Bottom slab bars were spaced as #8 @ 12 inches c/c in both directions.

For design of reinforcement details, refer to *Figure 34*, *Figure 35*, and *Figure 36*.

The area of the top slab bars was taken as 50% of the area provided in the bottom of the slab due to possible reversal of stresses of compression and tension at top and bottom face of footing [11]:

A_s provided for top slab = 0.5 (A_s provided for bottom slab) = 0.39 inch^2; *Figure 37, 38*. N = A_s provided for top slab/ area of #6 bars = 0.886 ≈ 1 bar/ft

Thus, 1 bar/ft c/c was used in both directions, so #6 @ 12 inches c/c were placed in the both directions.

The bearing stresses at the base of the wall and the top of the footing were checked versus bearing strength. The bearing strength N_1, at the base of the wall, N_2 bearing strength at the top of the footing is given as;

$N_1 = Ø\ (0.85\ f_c\ A_1)$;

$N_2 = N_1 \sqrt{\frac{A_2}{A_1}} \leq 2N_1$;

Where, areas A_1 and A_2 were calculated incorporating the thickness of the wall, the length of the footing, and the width of the wall per foot.

Area A_1 = 2 ft^2; Area A_2 = 17 ft^2

$N_1 = Ø\ (0.85\ f_c\ A_1)$ = 477.36 kips

$N_2 = N_1 \sqrt{\frac{A_2}{A_1}} \leq 2N_1$; but N_2 = 1391.73 kips > 2 (477.36)

So, N2 = $2N_1$ = 954.7 kips > 46.03 kips, it is OK.

So, the footing was adequate in bearing stress.

Minimum dowel steel bars were superseded due to practical aspect of design and constructability and in lieu of that, the main pier reinforcements were extended to the bottom slab reinforcement of the footing and tied up into them. Minimum temperature and shrinkage reinforcement also superseded reinforcement provided with full length in both directions for the bottom and top of the slab in the footing. Available development length was derived based on the provided geometry and the

cover. The required development length was derived per equations given in 12.2.2 [11]. Sufficient development length was not available according to calculations so a standard hook was provided to get the required bond and anchorage of reinforcement with concrete. The available development length was derived taking the length of the footing into account, the thickness of the footing, and the cover.

Available development length (for shorter direction bars) = 33 inches

Available development length (for longer direction bars) = 51 inches

$l_d = (f_y d_b) / (20\sqrt{f_c})$ [15] = 54. 77 inches > 51 inches, for #8 bars, NOT OK

$l_d = (f_y d_b) / (25\sqrt{f_c})$ [15] = 32.86 inches < 33 inches, for #6 bars, it is OK

Adequate development length was not available for #8 bars so, the design was supposed to have hooks to introduce the necessary tension, development length referring to 12.5.2 [11].

Development length of standard hooks in tension:

$l_{dh} = 0.02\ d_b\ \Psi_e\ f_y / \lambda\ \sqrt{f_c}$:

l_{dh} = 21.90 inches < 51 inches for #8 bars, it is OK

The dimensions given for hooks were developed to protect members against splitting of the concrete or bar breakage, no matter what concrete strengths, bar sizes, or bar stresses were used. Either the 90° hook which has an extension of 12 bar diameters ($12d_b$) at the free end or the 180° hook which has an extension of 4 bar diameters ($4d_b$) could be used at the free end but either of this should not be less than 2.5 inches. The radii and diameters shown were measured on the inside of the bends. 90° hook was used for #8 and #6 bars for the footing. (Appendix C)

$12d_b$, $D = 6d_b$, $r = D/2$

for #8 bar $12d_b$ = 12 inches, D = 6 inches, r = 3 inches

Total Length bar = (thickness of wall) + $2(l_{dh})$ + $12d_b$ + r

Total length of one #8 bar with 90° hook = 82.8 inches in shorter direction;

Finally, according to total length of bars computed, detailing of reinforcement was carried out as shown in figures below.

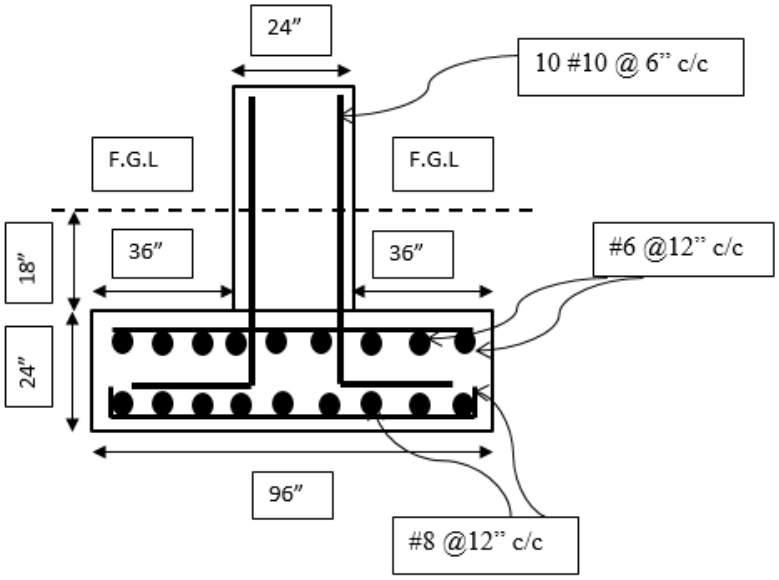

Figure 37. Reinforcement Detail of Footing - Section

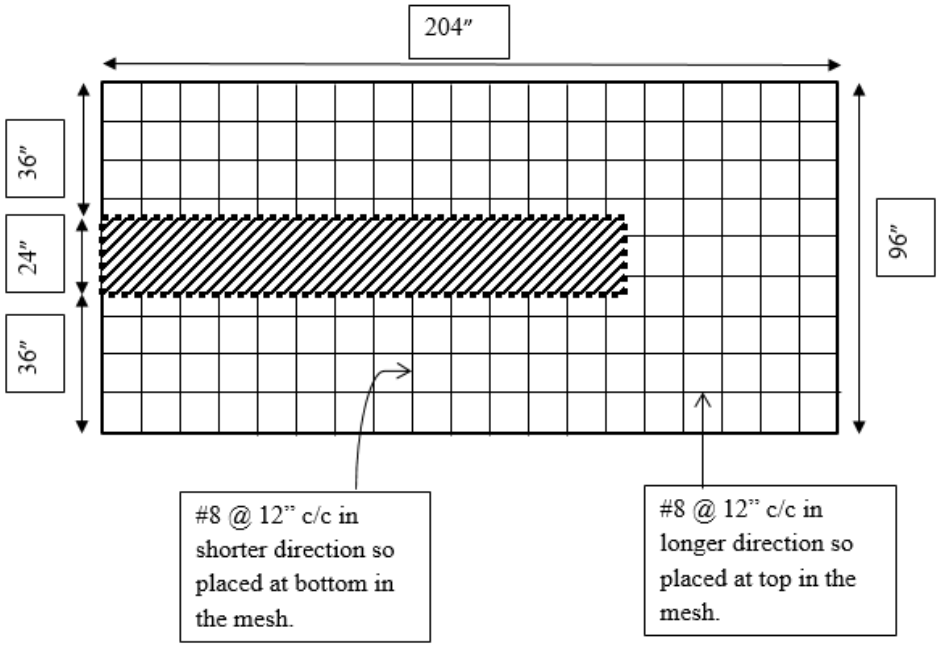

Figure 38. Reinforcement Detail of Footing at Bottom of Slab

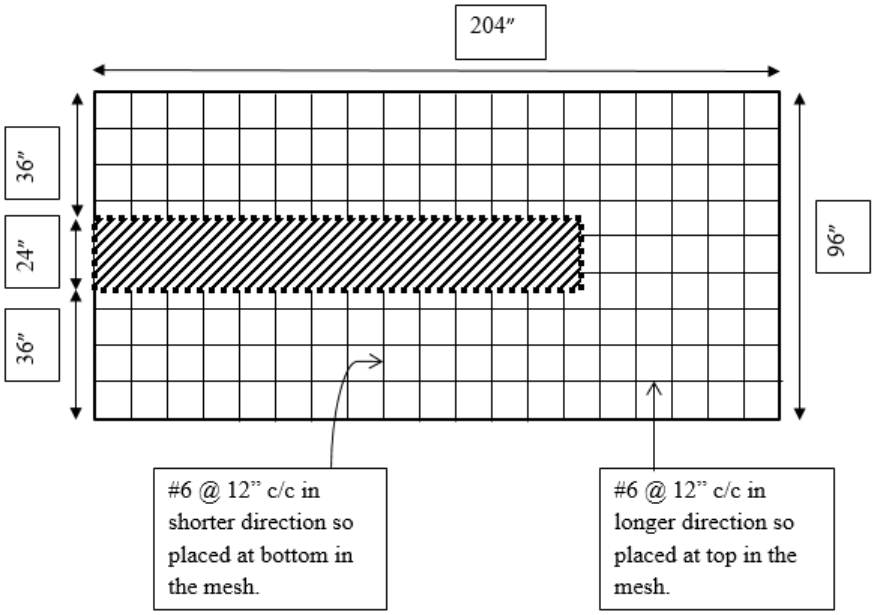

Figure 39. Reinforcement Detail of Footing at Top of Slab

Analysis and Design of Pier

Reinforcement details for pier were derived by adopting three different approaches as listed below.

1. Cantilever beam method
2. Non-linear strain distribution method
3. Shear wall method

Cantilever beam method. In this approach, the pier was considered (*Figure 40*) as a reinforced concrete cantilever beam [3] to analyze and design the reinforcement details. Here, a maximum value from LRFD load combinations was applied as a concentrated load to design pier reinforcement. Four different sections were introduced to consider precisely the behavior of the cantilever beam with varying depth, two of them were at the two ends (1-1 and 4-4) and the remaining two of them were at distance of 50 inches (2-2 and 3-3) apart as shown in *Figure 41*. Each section was analyzed and designed separately and then the reinforcement details were

determined. In these calculations, the yield stresses of steel was f_y = 60 ksi, compressive strength of concrete f'_c = 3000 psi, resistance factors ($Ø$) for flexure = 0.9 and for shear = 0.75, concrete cover = 2 inches on both sides, and λ = 1.0 for normal weight concrete.

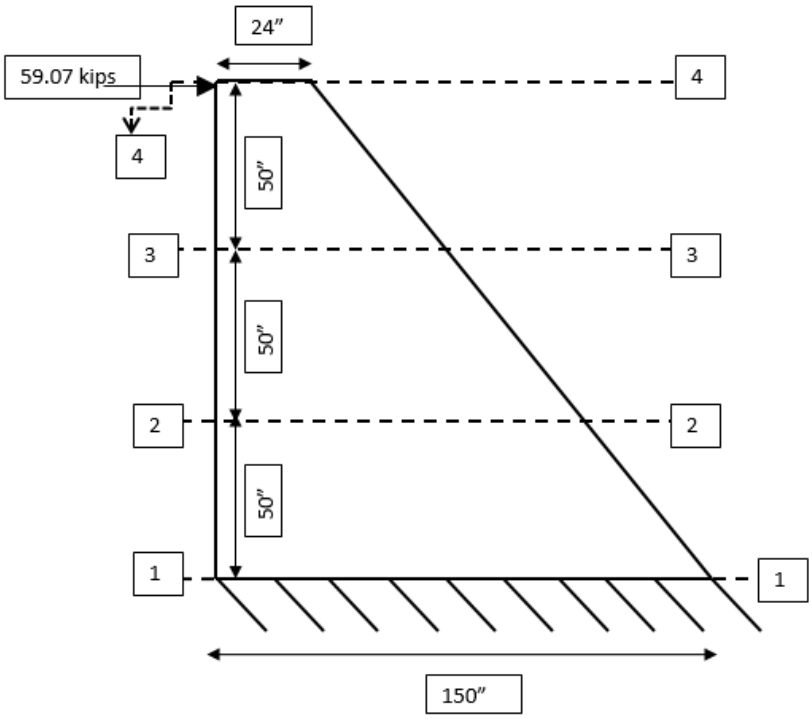

Figure 40. Pier as Cantilever Beam

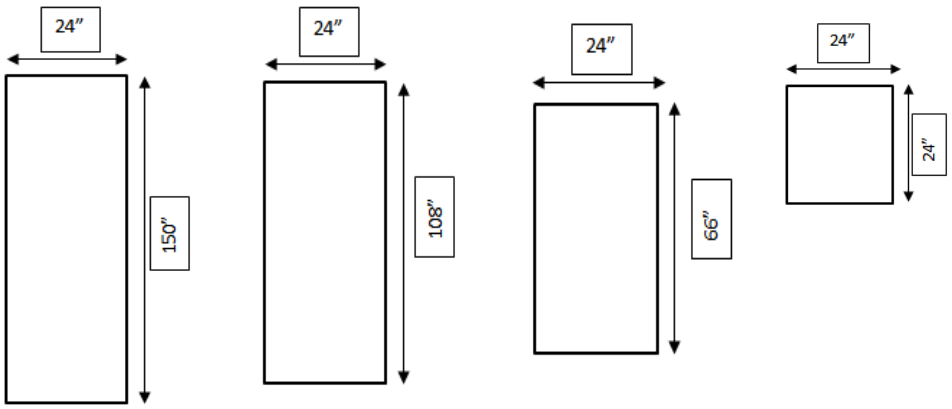

Sec 1-1 Sec 2-2 Sec 3-3 Sec 4-4

Figure 41. Sections of Pier as Cantilever Beam

However, only the summary of calculation for sec 1-1 and sec 3-3 were presented here, other calculations for sec 2-2 and sec 4-4 were similar and are presented in Appendix C.

Design of the beam for flexure (sec 1-1). To analyze and design the cantilever beam in flexure at sec 1-1 the basic dimensions were used as shown in *Figure 40* and *41***.** The nominal moment of section (M_n) was calculated taking into account the point load (*Figure 40*) and moment arm from sec 1-1 to the point load with M_n = 9845 kip-inches.

The area of steel was calculated using three discrete equations:

$A_s \geq [(0.85 f_c' \, b \, d) / f_y] * [1 - \sqrt{1 - (2 M_n) / (0.85 f_c' \, b \, d^2)}]$; $A_s \geq 1.28$ inch^2

Minimum area 1; $A_s \geq (3\sqrt{f'_c} bd) / f_y$; $A_s \geq 9.60$ inch^2

Minimum area 2; $A_s \geq (200bd) / f_y$ $A_s \geq 11.68$ inch^2

The area of steel was derived using the minimum area 2 equation which governed.

10 - #10 bar were adopted, A_s = 12.7 inch^2 > required A_s = 11.68 inch^2 so it is OK.

To calculate the lever arm between tension and compression forces, first it was required to compute the depth of compression (a):

$a = (A_s f_y) / (0.85 f_c' \, b)$ = 12.45 inches;

Lever arm = (d - $a/2$)

The nominal bending strength was found in order to verify that the section is sufficient to resist moment:

$M_n = Ø \, A_s f_y \, (d - a/2)$ = 95857.695 kip-inches > M_u = (9845*0.9) = 8860.5 kip-inches

Thus, the section is sufficient and adequate.

Design of the beam for shear (sec 1-1). To analyze and design the cantilever beam in shear at sec 1-1 the basic dimensions were used as shown in *Figure 40* and

41. The factored shear force was calculated considering the maximum load on pier from LRFD:

Factored shear force, V_u = 94.512 kips. The factored moment was computed taking distance of load from support as a moment arm:

Factored moment M_n = 14176.8 kip-inch

The nominal shear load was calculated incorporating $\emptyset$ = 0.75

Nominal shear load V_n = 126.016 kips

The shear force carried by the concrete, V_c = 383.84 kips

$V_n < (V_c / 2)$ thus, shear reinforcement is not required.

The shear force carried by the steel was computed by subtracting the shear carried by the concrete from the nominal shear load; V_s = -257.824 kips.

The negative sign indicated that theoretically it was not required to have shear reinforcement so minimum shear reinforcement was provided as if $V_n < (V_c / 2)$.

For minimum spacing of stirrups should be considered from either half of section (d/2) depth or 24 inches, i.e. s_{max} = 24 inches.

Minimum area of shear reinforcement was given as:

$A_{vmin} = (0.75 \sqrt{f'_c}\, b_w s) / f_{yt}$ or $(50 b_w s) / f_{yt}$; greater value should be adopted.

A_v min/s = 0.016 inch^2/ inch or 0.020 inch^2 /inch

So A_v min/s = 0.020 inch^2 /inch = 0.24 inch^2/ft.

Design of the beam for flexure (sec 3-3). To analyze and design the cantilever beam in flexure at sec 3-3 the basic dimensions were used as shown in *Figure 40* and *41*. The nominal moment of section (M_n) was calculated taking into account the point load and the moment arm from sec 3-3 to the point load:

M_n = 3281.67 kip-inches

The area of steel was calculated using three discrete equations:

$A_s \geq (0.85 f_c' b d) / f_y [1- \sqrt{1 - (2 M_n) / (0.85 f_c' b d^2)}]$; $A_s \geq 0.98$ inch^2;

Minimum area 1; $A_s \geq (3\sqrt{f'_c} bd) / f_y$; $A_s \geq 4.075$ inch^2

Minimum area 2; $A_s \geq (200bd) / f_y$; $A_s \geq 4.96$ inch^2 controls

The area of steel was derived using the minimum area 2 equation, which governed

4 - #10 bar were adopted, $A_s = 5.08$ inch^2 > governed $A_s = 4.96$ inch^2 so it is OK;

To calculate the lever arm between the tension and compression forces, first it was required to compute the depth of compression (a):

$a = (A_s f_y) / (0.85 f_c' b) = 4.98$ inches;

Lever arm = $(d - a/2)$

The nominal strength was calculated to verify the section is sufficient to resist moment:

$M_n = Ø A_s f_y (d - a/2) = 16324.78$ kip-inch > 2953.50 kip-inch

Therefore, the section is sufficient.

Design of the beam for shear (sec 3-3). To analyze and design the cantilever beam in shear at sec 3-3 the basic dimensions were used as shown in *Figure 40* and *41*. The factored shear force was calculated considering the maximum load on the pier from LRFD factored force $V_u = 94.512$ kips**.** The factored moment was computed taking the distance of the load from the support as a moment arm:

Factored moment $M_n = 4725.6$ kip-inches

The nominal shear load was worked out incorporating $Ø = 0.75$:

Nominal shear load $V_n = 126.016$ kips

Shear force carried by concrete, $V_c = 163.002$ kips

$V_n > (V_c / 2)$ so shear reinforcement is required.

The shear force carried by the steel was computed subtracting shear carried by the concrete from the nominal shear load; $V_s = -36.986$ kips

V_s negative value showed that theoretically concrete was strong enough to withstand shear without shear reinforcement so minimum shear reinforcement should be provided here:

$A_{vmin} = (0.75 \sqrt{f'_c}\, b_w\, s) / f_{yt}$ or $(50 b_w s) / f_{yt}$

A_v min/s = 0.016 inch^2/ inch or 0.020 inch^2 / inch

So A_v min/s = 0.020 inch^2 / inch

Required area $A_v/s = V_s/ f_{yt}\, d$

A_v/s = 0.078 inch^2 /inch > A_v min/s = 0.020 inch^2 / inch = 0.24 inch^2/ft;

Non-linear strain distribution method. Deep beams are structural elements loaded as beams but having a large depth to thickness ratio and a shear span to depth ratio not exceeding 2 for concentrated load and 4 for distributed load, where the shear span is the clear span of the beam for distributed load. Floor slabs under horizontal loads, wall slabs under vertical loads, short-span beams carrying heavy loads, and some shear walls are examples of this type of structural element. Geometry of deep beams act non-linearly as two dimensional members rather than one-dimensional members and are subjected to a two-dimensional state of stress. As a result, plane sections before bending do not necessarily remain plane after bending. The resulting strain distribution is no longer considered linear, and shear deformations that are neglected in normal beams become significant compared to pure flexure. Consequently, the stress block becomes nonlinear even at the elastic stage. At the limit state of ultimate load, the compressive stress distribution in the concrete would no longer follow the same shape or intensity [2].

In this approach, the pier was analyzed and designed as a deep beam (*Figure 42*) using non-linear strain distribution methodology. Here also maximum reactions of LRFD load combinations were considered in this approach. In non-linear distribution, it is required to identify the critical section to see whether maximum moment occurs there or at the base (support) to determine reinforcement. However in chapter 6, only determination of the reinforcement at the support or base is explained, while the other calculations are presented in Appendix C.

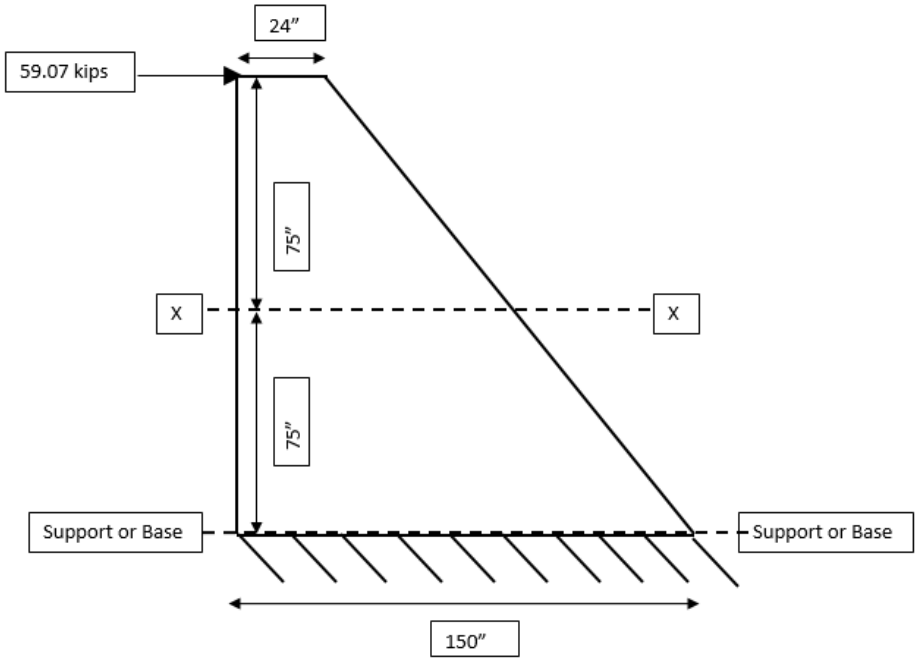

Figure 42. Pier as a Deep Beam for Section at Base/Support

The non-linear strain distribution approach was adopted to design the pier as a deep beam. Flexure design was carried out first incorporating the width of the beam (b_w = 2 ft), the height of the beam (h = 12.5 ft), and the shear span to face of support distance (a =12.5 ft). The depth of the beam (d = 0.9h) was computed as per the assumption for this non-linear strain distribution approach. The ratio of the shear span to the depth of the beam (a/d = 1.11) which must be less than the ratio for the concentrated load (a/d = 2) on a deep beam. Furthermore, the shear force and the

bending moment were calculated at the critical section x-x and at the support to get the maximum moment and shear values in the deep beam:

V_u(x-x) = 59.07 kips; M_u(x-x) = 369.19 kip-ft; M_u at support = 738.375 kip-ft

The shear force at the critical section x-x was less than $Ø\ 10\ (\sqrt{f_c'})b_w\ d$ = 1330.96 kips and thus it is OK. The ratio (a/h = 1) of shear span (a) to height of beam (h) was taken in to account and it was less than to the ratio of the concentrated load (a/h = 2) for a deep beam. The lever arm between the tension and compression forces was derived:

$jd = 0.2(a+ 2h)$ = 7.5 ft.

The area of vertical tensile reinforcement was calculated using three discrete equations:

$A_s = M_u / Ø\ f_y jd$

A_s = 0.92 inch^2 for M_u(x-x) = 369.19 kip-ft;

A_s = 1.82 inch^2 for M_u at support = 738.375 kip-ft

$A_s = (3\sqrt{f'_c}bd) / f_y$ = 8.873 inch^2

$A_s = 200b_w d/f_y$ = 10.80 inch^2

The area of steel derived using equation $200b_w d/f_y$, governed.

10 - #10 bars were chosen as vertical tension reinforcement.

Therefore, A_s (Provided) = 12.70 inch^2 > required A_s = 10.80 inch^2,

The point up to which A_s is to be distributed in the tension zone (segment) of the beam is; $Y = 0.25h-0.05a < 0.20h$; putting h = 150 inches and a = 150 inches

Y= 30 inches ≤ 30 inches. It indicated that the first 30-inch distance along the support of the pier was in the tension zone and the remaining 120-inch distance was in the compression zone (*Figure 42A*). The spacing for the tension steel was calculated to be

6 inches c/c, so 5 bars on each face of the pier were placed. The percentage of vertical tension steel was calculated, $\rho_w = A_s / (b_w d) = 0.40\ \% = 0.0040$

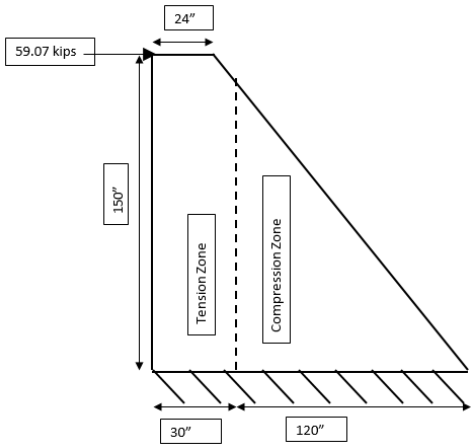

Figure 43. Tension and Compression Zone in Deep beam

Vertical reinforcement for the compression zone (Figure 43) may be adopted arbitrarily as the same as of the tension reinforcement from stress block diagram (tension = compression) and constructability point of view. Thus, the area of steel for compression reinforcement was adopted as = 12.70 inch^2. As vertical compression reinforcement, 16 - #7 bars (8 bars on each face) were placed at 15 inch c/c spacing for the remaining 120 inches.

The shear carried by the concrete was calculated using the equation below:

$V_c = K(1.9 (\sqrt{f_c}' + 2500\ \rho_w (V_u\, d / M_u)\, b_w\, d \leq 6 (\sqrt{f_c}'\, b_w\, d)$

Where $K = (3.5 – 2.5 (M_u / V_u\, d)$ = 2.11 for M_u(x-x) = 369.19 kip-ft

and $K = (3.5 – 2.5 (M_u / V_u\, d)$ = 0.72 < 1, for M_u at support = 738.375 kip-ft

for K=2.11 , V_c = 904.37 kips ≤ 1064.77 kips

for K=1, V_c = 382.90 kips ≤ 1064.77 kips

Ø V_c /2 = (678.27) / 2 = 339.14 kips for K = 2.11

Ø V_c /2 = (287.17) / 2 = 143.58 kips for K =1

V_u = 59.07 kips < 339.14 kips and 143.58 kips

As per these calculations, V_c was adequate in both cases. The applied load (shear) on the deep beam was less than shear carried by concrete. Hence, no design shear reinforcement was required, but as per the requirement of deep beam, this should have minimum shear reinforcement for the present case.

The minimum horizontal shear reinforcement was calculated as, $A_{vh} = 0.0015 b_w s_v = 0.43$ inch^2. The maximum vertical spacing (s_v) for horizontal shear reinforcement was as: s_v = min (d/5 inch or 12 inch) = 12 inches. #5 horizontal bars were placed at a vertical spacing of 12 inches c/c at both faces of the deep beam, so the area provided for horizontal reinforcement, A_{vh} (provided) = 0.62 inch^2. The minimum vertical shear reinforcement was computed as: $A_v = 0.0025 b_w s_v = 0.72$ inch^2. The maximum horizontal spacing s_h = min (d/5 inches or 12 inches) = 12 inches. #4 vertical bars were placed at horizontal spacing of 12 inches c/c at both faces of the pier so the area provided for vertical reinforcement; A_v (provided) = 0.80 inch^2. Temperature and shrinkage reinforcement was also derived for the pier using three different equations given in ACI 318-11 [11] as follow: $A_s = 0.0020bh = 0.58$ inch^2; $A_s = 0.0018bh = 0.52$ inch^2; $A_s = 0.0014bh = 0.40$ inch^2.

The area provided for minimum shear reinforcement (horizontal or vertical) was greater than the area required for temperature and shrinkage reinforcement, so there was no need to have temperature and shrinkage reinforcement as minimum shear reinforcement superseded temperature and shrinkage reinforcement. For better constructability, it was preferable to have reinforcement in the compression zone (on both faces) which would replace the vertical compression reinforcement (16 - #7 @ 15 inches c/c) and vertical shear reinforcement (#4 @ 12 inches c/c). Finally, for better constructability, #7 @ 12 inches c/c was adopted in lieu of vertical compression reinforcement and vertical shear reinforcement.

Shear wall method. In this method, the pier was considered as a shear wall and designed accordingly. Identical material properties, dimensions and loading (*Figure 44*) were adopted as in previous calculations.

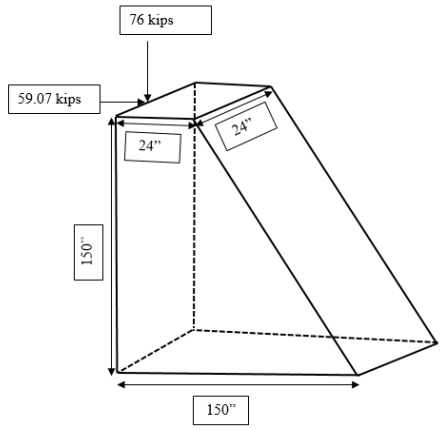

Figure 44. Pier as Shear Wall

As a primary constraint, the thickness of the wall was checked using equations provided in ACI section 11.9.3 [11] and as limiting criteria, shear force computed was more than applied load (*Figure 44*), so thickness of wall was OK:

V_u = Ø10 ($\sqrt{f_c'}$) hd = 1183.08 kips > applied shear load (V_u) = 59.07 kips

After the thickness check, the shear carried by concrete was calculated using equations provided in ACI section 11.9.6. as follows, with the smaller value considered as governing (for detailed calculation refer Appendix C):

(a) $V_c = 3.3\lambda (\sqrt{f_c'})\, hd + (N_u d/4\, l_w) = 535.75$ kips

(b) $V_c = [0.6\, \lambda \sqrt{f_c'} + l_w (1.25\, \lambda \sqrt{f_c'} + 0.2\, N_u / l_w h) / (M_u/V_u) - (l_w/2)]\, hd$

V_u = 59.07 kips; M_u = 369.19 kip-ft put in aforesaid equation (b).

V_c = 94.64 kips + infinity = infinity; because second term of equation (b) gives denominator zero so it would be infinity solution.

So option (a) was the governing value of V_c for wall.

An important factor in shear design is the requirement for shear reinforcement. As the factored shear carried by the concrete (195.21 kips) was more than the applied shear load (59.07 kips) as a limiting criteria to provide shear reinforcement, which indicated no requirement of shear reinforcement.

$ØV_c / 2 = 195.21$ kips > 59.07 kips. It is OK. Shear reinforcement was not required.

Vertical (longitudinal) reinforcement detailing was carried out per ACI 14.3.2:

$\rho_l = A_{v,\,vert}/hs_1 = 0.0015bh$

Spacing s_1 was considered to be a minimum of 3h or d/5, so $s_1 = 18$ inches. Therefore, typical 12 inches c/c spacing was adopted, $s_1 = 12$ inches to get $A_{v,\,vert} = 0.43$ inch^2

#5 bars were placed at a horizontal spacing of 12 inches c/c

So $A_{v,vert}$ (provided) = 0.62 inch^2.

Horizontal (transverse) reinforcement detailing was carried out per ACI 14.3.3:

$\rho_t = A_{v,horiz}/hs_2 = 0.0025bh$

Spacing s_2 was considered to be a minimum of 3h or d/5 = 120/5 = 24 inches

So $s_2 = 18$ inches. Therefore, typical 12 inches c/c spacing was considered:

$s_2 = 12$ inches to get $A_{v,\,horiz} = 0.72$ inch^2

#4 bars were provided at a vertical spacing of 12 inches c/c:

$A_{v,horiz}$ (provided) = 0.8 inch^2

Vertical flexural reinforcement was calculated based on the bending moment at the base of the wall to find out the percentage of steel for flexure reinforcement:

$M_u = 738.375$ kip-ft at base of wall, $M_u/\varphi bd^2 = 28.49$ lb/inch^2

$\rho = \rho_{min}$ for flexure = 0.0033 (ref. Appendix A, Table A12)

$A_s = \rho bd = 9.504$ inch^2; 8 #10 bars were placed as flexure reinforcement at each end assuming V_u could come from either direction.

Reinforcement detailing from all three methods are summarized in Table 11. It was decided to use the most conservative structurally sound and stable reinforcement detail which can sustain anticipated worst loading combinations in analysis. Therefore, according to the design of reinforcement derived via the deep beam concept following the non-linear approach was adopted [3]. In future, strut and tie model methodology could be incorporated to design more precise and economical reinforcement details of pier as a deep beam in lieu of non-linear strain distribution approach.

Table 11

Summary of Reinforcement Detail from Three Different Approaches

Linear Approach (Cantilever Beam Concept)			
Sec 1-1	Sec 2-2	Sec 3-3	Sec 4-4
10 #10	8 #10	4 #10	2 #10
Flexure Reinforcement for all four sections			
#4 @ 20 inch c/c or lesser spacing- Shear Reinforcement			

Non-Linear Approach (Deep Beam Concept)
#10 @ 6 inch c/c- Vertical Tension Reinforcement
#7@12 inch c/c- Vertical Compression and Shear Reinforcement
#5 @12 inch c/c - Horizontal Shear Reinforcement

RCC Shear Wall (Wall Concept)
8 #10- Flexure Reinforcement
#4 @12 inch c/c -Vertical Shear Reinforcement
#5 @12 inch c/c - Horizontal Shear Reinforcement

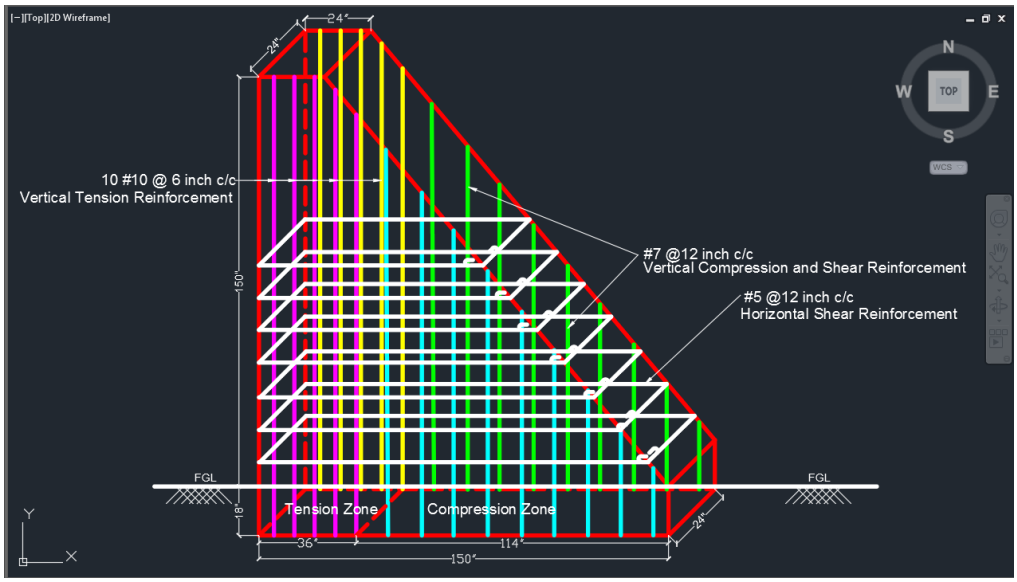

Figure 45. Recommended Reinforcement Detailing for Pier

Cross Beam Analysis and Design

The cross beams connect the tops of the piers. The purpose of the cross beams is to maintain the correct spacing of the truss bases. Thus, the cross beams serve to stabilize the tops of the piers relative to each other in the longitudinal direction.

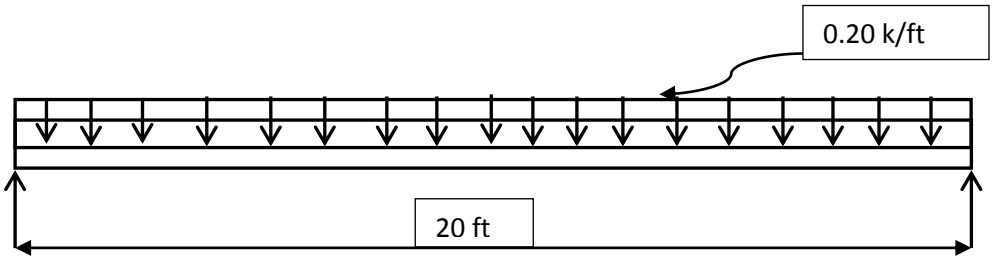

Figure 46. Design of Cross Beam on Top of Pier

Using LRFD and an assumed live load of five 200 lb men on top of the beam at one time, it was designed for a worst case scenario (*Figure 46*). The beam does not appear to be taking any vertical load from the hangar and is considered to be a continuous beam running from pier to pier. Assumed dimensions of the beam are as follows.

b = 12 inch, h = 8 inch, span = 20 ft = 240 inch center to center spacing,

Diameter of bar = 0.50 inch for #4 bars

d = 8 – 1.5 – (0.50/2) – 0.50 = 5.75 inches

Self-Weight (Dead Load of Beam) = 150 lb/ft^3 * (8/12 ft) * (12/12 ft) * (20 ft)

= 2000 lb = 2 kips

= (2 kips/ 20 ft) = 0.1 kips/ft *1.2 = 0.12 kips/ft

Self-Weight (Dead Load of Beam) = 0.12 kips/ft

Live Load on Beam = (5 * 200 * 1.6) = 1600 lb = 1.6 kips

So, uniformly distributed live load = 1.6 kips / 20ft = 0.080 kips/ft,

This load was applied as a uniformly distributed load.

Total Load on Beam, w = DL + LL = 0.12 kips/ft + 0.080 kips/ft = 0.20 kips/ft

Maximum Moment in the beam = wl^2/8 = (0.20 * (20)^2) / 8 = 10 kips-ft

As per assumption, the bottom is in tension and the top is in compression.

Max Shear = V = (wl) /2 = 2 kips as a reaction on each support. (*Figure 42*)

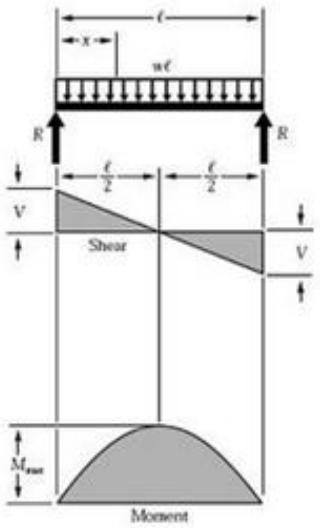

$$R = V \quad \ldots\ldots\ldots\ldots\ldots = \frac{w\ell}{2}$$

$$V_x \quad \ldots\ldots\ldots\ldots\ldots = w\left(\frac{\ell}{2} - x\right)$$

$$M_{max}\ \text{(at center)} \quad \ldots\ldots\ldots = \frac{w\ell^2}{8}$$

$$M_x \quad \ldots\ldots\ldots\ldots\ldots = \frac{wx}{2}(\ell - x)$$

$$\Delta_{max}\ \text{(at center)} \quad \ldots\ldots\ldots = \frac{5w\ell^4}{384\,EI}$$

$$\Delta_x \quad \ldots\ldots\ldots\ldots\ldots = \frac{wx}{24\,EI}(\ell^3 - 2\ell x^2 + x^3)$$

Figure 47. Simply Supported Beam Shear Force and Bending Moment Diagram

The design of the reinforcement for the concrete beam will be as follows:

Nominal moment $M_n = M_u / Ø$

M_n = (10 * 12) / 0.90 = 133.34 kips – inches

$M_n = A_s f_y (d - a/2)$ and $a = (A_s f_y) / (0.85 f_c' b)$

133.34 kips-inches = A_s * 60 (5.75 – 1.22 A_s)

$A_s^2 – 4.713 A_s + 1.821 = 0$

By solving the quadratic equations:

A_s = 8.523 inch^2 or 0.23 inch^2; two solutions from the quadratic equations. Most feasible value should be considered to get sound structural reinforcement**,**

so A_s = 0.23 inch^2 was adopted.

Check for A_s min:

1) A_s min 1 = $(3\sqrt{f_c'}\, bd) / f_y$ or 2) A_s min 2 = (200bd) / f_y

1) $A_s$min 1 = 0.217 inch^2 or 2) A_s min 2 = 0.265 inch^2

Among these three values, A_s =0.265 inch^2 was considered as the required reinforcement area to be detailed. The number of bars, n = 2 - #4 bars as bottom tension bar

Check for Cover:

[8 - (0.50*2) - (1.5*2)] / 2 = 2 inches > minimum =1.5 inches so it is OK.

As the cross beam follows regular beam criteria (width to depth ratio < 1) and it only holds the pier and truss but does not transfer any kind of load, there was no requirement of minimum shear reinforcement.

Now, the calculations for development length are as follows. First and foremost, it is required to calculate available development length to compare with actual development length.

$l_d = f_y d_b \Psi_t \Psi_e / 25\sqrt{f_c'}$

l_d = (60000*0.50*1.0*1.0) / (25*54.77) = 21.91 inches,

Where:

Ψ_t = bar-location factor = 1.0; for bottom bars per ACI 12.2.4 [11].

Ψ_e = coating factor = 1.0; for uncoated and galvanized reinforcement per ACI 12.2.4 [1].

As it was designed as a simply supported beam so development l_d is OK.

The reinforcement of the cross beam could experience drastic temperature differences. Therefore, it was necessary to carry out the thermal expansion check for the beam which could affect the load bearing capacity of the steel bars. These calculations are as follows:

$\alpha (\Delta T) = (P) / (AE)$;

α = thermal expansion coefficient = (4.1 to 7.3) * $10^{(-6)}$/ °F; [11]

ΔT = maximum seasonal temperature difference = 120 - 0 = 120 °F [11]

P = load (kips)

A = area of provided reinforcement ($inch^2$)

E = concrete modulus = 29000 psi [11]

So, $P = (\alpha) * (\Delta T) * (AE)$:

$P = (7.3 * 10^{(-6)} * 120) *(0.1963*2*29000) = 9.97$ kips

The yield load of steel = (yield stress of steel) * (area of steel bars provided)

The yield load of steel = (60) * (0.1963*2) = 23.56 kips > 9.97 kips so it is OK.

Cross beam is OK in thermal expansion.

Chapter 7

Summary

Structural analysis was carried out using RISA 3D to check the structural strength and stability of the roof trusses of Hangar Q under the application of various loads considering ASCE 7-10 [10]. The steel trusses of Hangar Q were modelled as three hinged arches, so boundary conditions were employed through nodal assumptions (Chapter 3) to get the proper geometry. Two node isoparametric finite elements were utilized to model the members in the trusses. Through the section set definition, it was not possible to assign the same section sets to all steel members as hot rolled sections (HR1), so they were labeled with different types of hot rolled sections likewise purlins, channels, double angles, and WTs' in RISA 3D. The self-weight of Hangar Q was automatically calculated in RISA 3D. The basic loads that were applied on the roof trusses of Hangar Q included dead loads, snow loads, vertical wind loads, and lateral wind loads. The loads due to the 14 inch overhang of the roof on both ends of Hangar Q (i.e., beyond the first truss and last truss) were taken into account.

The analysis included the selection of coefficients like the exposure factor, the thermal factor, and the gust effect factor, and other parameters such as the wind directionality factor, the velocity pressure exposure co-efficient, and the topographic factor to calculate snow loads and wind loads. Mansard roof geometry was considered in order to apply the wind load distribution on Hangar Q as per ASCE 7-10[10]. Load combinations were incorporated and derived for this analysis using Allowable Strength Design (ASD) and Load and Resistance Factor Design (LRFD) as prescribed in ASCE 7-10 [10]. The maximum reactions from these load combinations were derived at the end hinge of the arch trusses and taken as the applied forces on the top

of the concrete piers in order to analyze and design the piers and their foundations. The joint deflection (global coordinates), member deflection (local coordinates), and unity check (stress ratio check) of steel sections were considered to evaluate the structural strength and safety of Hangar Q. The aim of this evaluation was to check the structural stability of Hangar Q for steel sections provided in DRBA drawings with recent code provisions. In the analysis, it was observed that some of the original steel sections in Hangar Q were structurally deficient (i.e. maximum deflection was higher than the maximum allowable deflection and some of the steel members did not satisfy stress ratio criteria (stress ratio <1)). This analysis revealed that some members were overstressed (stress ratio >1) and that the structure was not able to sustain applied external loadings according to contemporary load combinations [10]. Eventually, to derive a stable and sound structure, retrofitting and replacement of excessively deflected members and overstressed members were carried out. These steel sections were retrofitted considering replacement and strengthening according to the structural requirements. Channel sections of purlins were replaced with wide flange sections. Most of the overstressed (stress ratio >1) double angle members were required to have a larger cross section area to resist higher stresses. In order to bear higher stresses, cross section areas of double angle members were increased by adding plates (retrofitting) at the top of the section, utilizing WT sections in RISA 3D as noted in Chapter-5.

After retrofitting of all deficient and overstressed steel sections, maximum deflection (global and local) and maximum stress ratios satisfied their allowable limits indicating that Hangar Q was safe and structurally stable. The unity check (stress ratio) considered the interaction of flexure and compression in doubly and singly symmetric sections [12].

The reinforced concrete pier foundations, piers, and cross beams were analyzed and designed using the maximum reactions from the end hinges of the trusses as applied forces. For historical reasons, it was mandatory to keep intact the dimensions of the piers (i.e., 150 inches high, 150 inches long, and 24 inches thick) above ground level. The stability analysis of the pier foundations had to be checked and validated considering the eccentricity criteria and the building pressure criteria. This led to a trial and error procedure to arrive at the final geometry of the pier foundation. The maximum reactions from ASD load combinations were adopted to check all criteria for stability. The thickness of the foundation and the reinforcement design of the piers were derived employing maximum concentrated loads from LRFD load combinations. The length and depth of the pier foundations were derived based on the maximum ASD load combinations. In the stability analysis of the pier foundations, a worst load case was analyzed which contained maximum horizontal load and maximum vertical load

The structural analysis and design of the pier foundations were carried out considering the structure to be a spread footing. The thickness of the pier foundation relative to ground level was based on the frost depth [9] in the Millville region. The net upward soil pressure was calculated through the effective soil pressure and the length and width of the foundation were derived based on ASD load combinations. The thickness of the pier foundations was derived based on one way shear checks. The area of reinforcement was computed using equations as per ACI 318-11 [11]. Due to the consideration of possible reversal of stresses i.e. compression and tension at the top and bottom faces of the pier foundations, the reinforcement for the top of the pier foundations was adopted as 50% of the area of reinforcement for the bottom of the pier foundations. The pier foundations were found to be safe in bearing stress.

Temperature and shrinkage reinforcement for the pier foundations were not required as designed reinforcement based on bending was greater than the temperature and shrinkage reinforcement. Designed reinforcement was placed over the full length and width of the footing in both directions of the pier foundation. There was no sufficient development length available, so hooks were detailed to provide tension development length. Details of reinforcement were presented in Chapter 6.

The structural analysis and design of the piers were performed considering three discrete methods:

1. Cantilever beam method.
2. Non-linear strain distribution method (deep beam concept).
3. Shear wall method.

Table 10 (Chapter 6) presents a summary of the reinforcement design and detail for the piers. Reinforcement details derived from the non-linear strain distribution method governed the design.

The cross beams were designed as simply supported and provide longitudinal connections between the tops of the piers. The objective of these beams was to stabilize and hold the piers longitudinally. The calculations for the cross beams are cited in Chapter 6.

Chapter 8

Conclusions

The existing structure of Hangar Q consists of bow string steel trusses along with a steel roof supported on concrete piers. During the field inspection of Hangar Q at Millville Airport, problems were identified with consideration of DRBA recommendations to keep intact the historical value of this monumental structure. Most of the purlins, chord members, and bracing members of the trusses showed their structural deficiencies (maximum deflection more than maximum allowable deflection) when analyzed in RISA 3D. Reinforcement in the cross beams, which run from pier to pier to hold them longitudinally, and in the piers were severely corroded.

Over time, due to the expansion of corroding steel in the concrete members, tensile stresses were created which caused cracking, delamination, and spalling of concrete. In particular, the concrete piers showed extensive distressed behavior along with severe cracking, concrete degradation, and deterioration, probably due to the alkali-silica reaction in the concrete. Scaling of concrete, i.e., small pock marks in the concrete surface and exposing aggregate underneath, was also observed which occurred due to the freeze—thaw cycle in concrete.

Detailed drawings for the steel members of the truss along with connection details were provided by DRBA. Due to the lack of structural drawings for the concrete piers and their foundations, checking the structural adequacy of these members was a challenge. Therefore, because of this and the DRBA desire to move Hangar Q to a new location, the reinforced concrete piers, foundations, and cross beams were to redesigned and rebuilt using state-of-the-art standards and materials.

To meet the overall goal of strength evaluation, structural analysis in RISA 3D was performed for the most dominant loading combinations. A significant number of

purlins, chord members, and bracing members did not meet allowable deflection criteria and allowable stress ratio (unity check) criteria per both ASD and LRFD loading combinations [10].

The deficiencies cited in Chapter 5 are to be expected considering the design of the Hangar Q was carried out at a time, in 1940s, when there was very limited knowledge of the wind loads, snow loads, and their combinations on building or other structures. Retrofitting (or strengthening) work (Chapter 5) performed in relation to this Hangar Q would need to conform to the most recent AISC code [12]. It was revealed through analysis that Hangar Q required major structural retrofitting to its overstressed and deficient truss members to achieve structural adequacy to meet contemporary code provisions and to ensure their continued safety and performance. For structurally inadequate steel members, purlins were replaced and for significantly deficient members, chord and bracing members were retrofitted to keep the historic status of Hangar Q intact.

Through the analysis, it was already clear that structurally deficient truss members did not have sufficient cross sectional area to resist stresses due to applied loadings. To strengthen these members to achieve structural adequacy under state-of-the-art loading combinations, retrofitting schemes were carried out which eliminated high stresses by increasing cross sectional areas via putting 0.5 inch thick cover plates on the top of the deficient chord and bracing members.

Eventually, the stability of the pier foundation was checked against all failure critera which included eccentricity criteria and building pressure criteria and the dimensions of the foundation (width and length) were derived considering maximum ASD loading combination. Thickness and reinforcement of the foundation were worked out utilizing maximum LRFD loading combination. According to guidelines

set by DRBA, it was advisable to have the same pier geometry (150-inch width x 150-inch height x 24-inch thickness) to maintain the historic value of the structure. The analysis and design of the pier was carried out using three different methods as explained in Chapter 6, from which the final design was governed by the deep beam concept using a non-linear strain distribution approach. The cross beams have a standardize design to hold the piers together.

Chapter 9

Future Scope of Work

- As explained in Chapter 6, three different approaches have been employed to design and detail the pier and final design of reinforcement was governed via non-linear approach using the deep beam concept. In future, the strut and tie model could be checked versus the non-linear deep beam approach to design the pier.
- Presently, overstressed members in Hangar Q were retrofitted putting cover plate (0.5 inch) on top of the respective steel sections. In future, other retrofitting methodology could be developed.

References

[1] Arthur T. DeGaetano, Daniel S. Wilks, and Megan Mckay, "Atlas of Soil Freezing Depth Extremes for the Northeastern United States," Northeast Regional Climate Centre, Ithaca, New York, 1996.

[2] Bowers et. al., "Condition Assessment and Rehabilitation Plans, Hangar 2 and 3 Ladd Field National Historic Landmark Fort Wainwright, Alaska," U.S. Army Medical Research Acquisition Activity, 820 Chandler Street Fort Detrick, MD, 2008.

[3] Brain S. Maxwell, PE, SE, "Woodland State Airport Hangar Review," Berger/Abam Engineers Inc., Portland, Oregon, 2008.

[4] *Building Code Requirements for Structural Concrete*, American Concrete Institute (ACI) Standard, ACI 318, 2011.

[5] *California Historic Building Code (CHBC)*, California Building Standards Commission, International Code Council, 2010.

[6] *Construction Engineering Technical Order (CETO)*, Dept. of National Defense Canada (DND), 1985.

[7] Edward G. Nawy, "Shear and Diagonal Tension in Beams," in *Reinforced Concrete – A Fundamental Approach*, 5th Edition, Upper Saddle River, NJ, 2005, Ch *6*, Sec *6.9*, pp *171-181*.

[8] Ghassan K. Al-Chaar, Jason Ericksen, and Pramod Desai, "Case Study: Structural Evaluation of Steel Truss Aircraft Hangars at Corpus Christi Army Depot, Texas," US Army Corps of Engineers Construction Engineering Research Laboratories, 1999.

[9] H. C. Foo and G. Akhras, "Strengthening Requirements of Old, Timber Warren Trusses," *Journal of Performance of Constructed Facilities*, vol.*10*, pp *127-134*, 1996.

[10] H. C. Foo, W.C. Li, and G. Akhras, "Behaviour of a Double Parallel Chord Warren Truss at the Central Column," *Military Engineering Research Group Rep*., Royal Military College of Canada, Kingston, Ontario, Canada, pp *1-19*, 1993.

[11] Henry Liu and Fariborz Nateghi, "Wind Damage to Airport: Lessons Learned," *Journal of Aerospace Engineering*, vol.*1*, pp *105-116*, 1988.

[12] *Instructor's Solutions Manual Reinforced Concrete – A Fundamental Approach*, 6th Edition, Pearson Education, Upper Saddle River, NJ, 2009, pp *39*, *59-64*, *85-87*, *215-216*.

[13] *International Building Code (IBC)*, International Code Council, 2003.

[14] Jack C. McCormac, Russell H. Brown, " Footings," "Walls," in *Design of Reinforced Concrete*, 9th Edition, Hoboken, NJ, 2014, Ch *12*, Sec *12.5*, pp *352-357*, Ch *18*, Sec *18.6*, pp *558-562*.

[15] Lawrence G. Griffis, "Serviceability Limit States Under Wind Load," in Engineering Journal, American Institute of Steel Construction, pp1-16, 1993.

[16] *Minimum Design Loads for Buildings and Other Structures*, American Society of Civil Engineers (ASCE) Standard, ASCE 7-10, 2010.

[17] *National Earthquake Hazard Reduction Program (NEHRP), Commentary on the Guidelines for the Seismic Rehabilitation of Buildings*, Federal Emergency Management Agency (FEMA) 274, 1997.

[18] *National Research Council of Canada*. National Building Code of Canada, Ottawa, Ontario, Canada, 1985.

[19] *Naval Facilities Engineering Command Design Manual*, 7.02, Naval Facilities Engineering Command (NAVFAC), 1986.

[20] Navy Staff, "Historic Assessment of Existing Hangar 5, Buildings 386," Ault Field, Naval Air Station, Whidbey Island, Island County, Washington, 2006.

[21] Office of Inspector General, "Condition Assessment and Rehabilitation Plan Hangar One," NASA Headquarters and Ames Research Centre, California, 2011.

[22] *Seismic Rehabilitation of Existing Buildings*, American Society of Civil Engineers (ASCE) Standard, ASCE 41, 2007.

[23] *Steel Construction Manual*, American Institute of Steel Construction (AISC) Standard, AISC 360, 2011.

[24] *Uniform Building Code (UBC)*, International Conference of Building Officials, 1997.

[25] *United Facilities Criteria (UFC)*, UFC 3-301-01, 1 June 2013, Change 3, 12 September 2016.

Appendix A

Loads Considered in Analysis

Appendix A presents the loads that were applied to the computer model of Hangar Q to check structural stability (joint deflection, member deflection, and unity check (stress ratio)). These loads include snow loads and wind loads in addition to self-weight and roof loads for Hangar Q.

Snow Loads

Ground snow loads (P_g), to be used in the determination of design snow loads for roofs shall be as set forth in *Figure 7.1* [10] for the contiguous United States and Table 7.1 [10] for Alaska. Site-specific case studies shall be made to determine ground snow loads in areas designated C_s in Figure 7.1 [10]. Ground snow loads for sites at elevations above the limits indicated in Figure 7.1 [10] and for all sites within the C_s areas shall be approved by the authority having jurisdiction. Ground snow load determination for such sites shall be based on an extreme value statistical analysis of data available in the vicinity of the site using a value with a 2 percent annual probability of being exceeded (50-year mean recurrence interval). Snow loads are zero for Hawaii, except in mountainous regions as determined by the authority having jurisdiction.

Sloped roof snow loads (P_s) acting on a sloping surface shall be assumed to act on the horizontal projection of that surface. The sloped roof snow load, P_s, shall be obtained by multiplying the flat roof snow load, P_f, with the roof slope factor, C_s, i.e., $P_s = C_s P_f$ [10]. Values of the thermal factor C_t, for warm roofs, cold roofs, curved roofs, and multiple roofs are determined from Sections 7.4.1 through 7.4.4 [10]. The thermal factor, C_t, from Table 7.3 [10] determines if a roof is cold or warm. Slippery surface values shall be used only where the roof's surface is unobstructed and

sufficient space is available below the eaves to accept all the sliding snow. A roof shall be considered unobstructed if no objects exist on it that prevent snow on it from sliding. Slippery surfaces shall include metal, slate, glass, and bituminous, rubber, and plastic membranes with a smooth surface. Membranes with an imbedded aggregate or mineral granule surface shall not be considered smooth. Asphalt shingles, wood shingles, and shakes shall not be considered slippery.

Cold roof slope factor, C_s, for cold roofs with a $C_t > 1.0$ shall be determined from Table 7.3 [10]. For cold roofs with $C_t = 1.1$ and an unobstructed slippery surface that will allow snow to slide off the eaves, the roof slope factor, C_s, shall be determined using the dashed line in *Figure 7.2b* [10]. For all other cold roofs with $C_t = 1.1$, the solid line in Figure 7.2b [10] shall be used to determine the roof slope factor, C_s. For cold roofs with $C_t = 1.2$ and an unobstructed slippery surface that will allow snow to slide off the eaves, the roof slope factor, C_s, shall be determined using the dashed line on *Figure 7-2c* [10]. For all other cold roofs with $C_t = 1.2$, the solid line in Figure 7-2c [10] shall be used to determine the roof slope factor, C_s.

Roof slope factor for curved roofs in which portions of curved roofs having a slope exceeding 70° shall be considered free of snow load (i.e., $C_s = 0$). Balanced loads shall be determined from the balanced load diagrams in Figure 7.3 [10] with C_s determined from the appropriate curve in *Figure 7.2* [10].

Unbalanced snow loads for curved roof portions having a slope exceeding 70° shall be considered free of snow load. If the slope of a straight line from the eaves (or the 70° point, if present) to the crown is less than 10° or greater than 60°, unbalanced snow loads shall not be taken into account. Unbalanced loads shall be determined according to the loading diagrams in *Figure 7.3* [10]. In all cases the windward side shall be considered free of snow. If the ground or another roof abuts a Case II or Case

III (see *Figure 7.3*[10]) curved roof at or within 3 feet (0.91 m) of its eaves, the snow load shall not be decreased between the 30° point and the eaves, but shall remain constant at the 30° point value. This distribution is shown as a dashed line in Figure 7.3 [10].

Snow loads decrease as the slopes of roofs increase. Generally, less snow accumulates on a sloped roof because of wind action. Also, such roofs may shed some of the snow that accumulates on them by sliding and improved drainage of meltwater. The ability of a sloped roof to shed snow load by sliding is related to the absence of obstructions not only on the roof but also below it, the temperature of the roof, and the slipperiness of its surface. It is difficult to define slippery in quantitative terms. For that reason a list of roof surfaces that qualify as slippery and others that do not, are presented in the standard. Most common roof surfaces are on that list. The slipperiness of other surfaces is best determined by comparisons with those surfaces. Some tile roofs contain built-in protrusions or have a rough surface that prevents snow from sliding. However, snow will slide off other smooth surfaced tile roofs. When a surface may or may not be slippery, the implications of treating it either as a slippery or non-slippery surface should be determined. Because valleys obstruct sliding on slippery surfaced roofs, the dashed lines in Figs. 7.2 a, b, and c [10] should not be used in such roof areas. Discontinuous heating of a building may reduce the ability of a sloped roof to shed snow by sliding, because meltwater created during heated periods may refreeze on the roof's surface during periods when the building is not heated, thereby locking the snow to the roof. All these factors are considered in the slope reduction factors presented in *Figure 7.2* [10] and are supported by (Refs. C7-38 through C7-411) [10]. The thermal resistance requirements have been added to the unobstructed slippery surfaces curve in *Figure 7.2a* [10] to prevent its use for

roofs on which ice dams often form because ice dams prevent snow from sliding. Mathematically the information in *Figure 7.2* [10] can be represented as follows:

Cold Roofs (C_t = 1.2):

(c) Unobstructed slippery surfaces:

0° - 15° slope $C_s = 1.0$

15° - 70° slope $C_s = 1.0 – (slope - 15°) / 55°$

> 70° slope $C_s = 0$

(d) All other surfaces:

0° - 45° slope $C_s = 1.0$

45° - 70° slope $C_s = 1.0 – (slope - 45°) / 25°$

> 70° slope $C_s = 0$

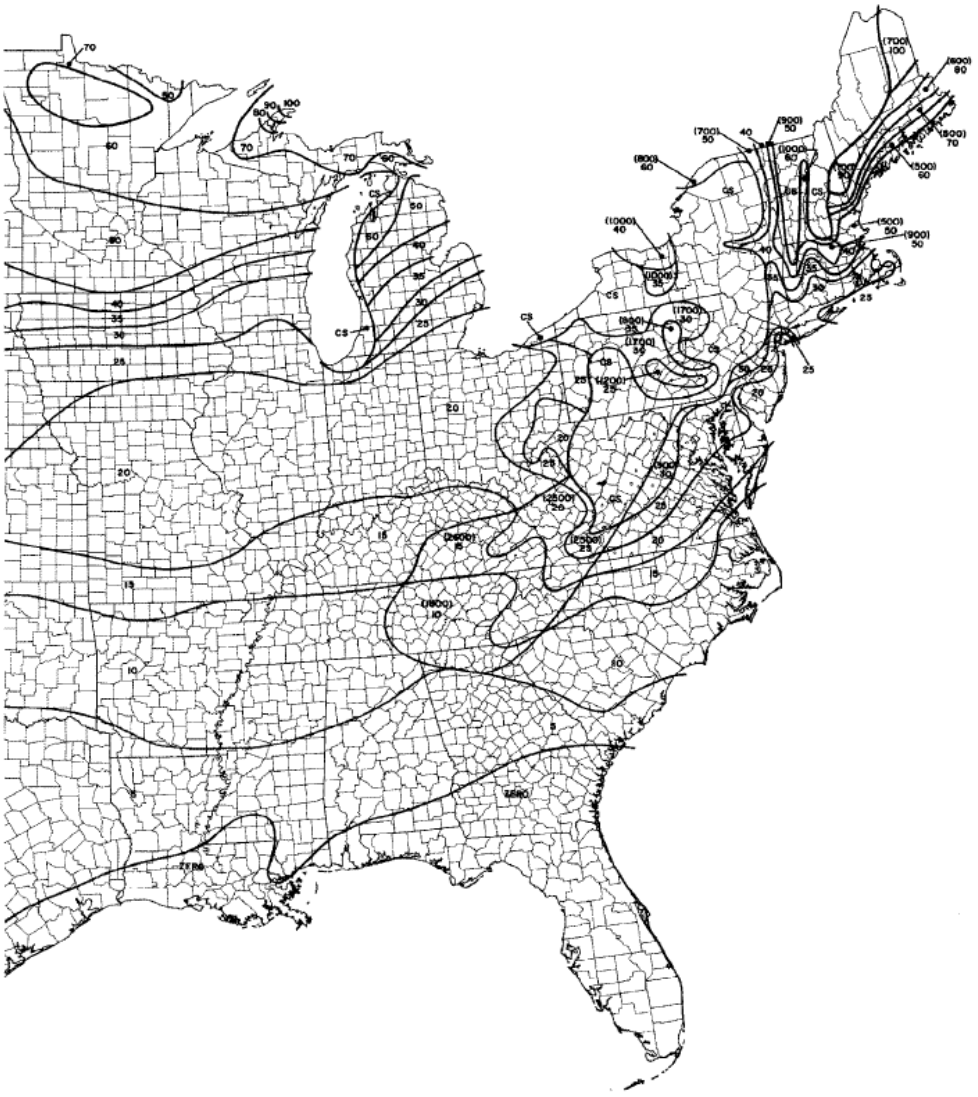

FIGURE 7-1 (continued) GROUND SNOW LOADS, p_g, FOR THE UNITED STATES (LB/FT^2)

Figure A1. Ground Snow Loads

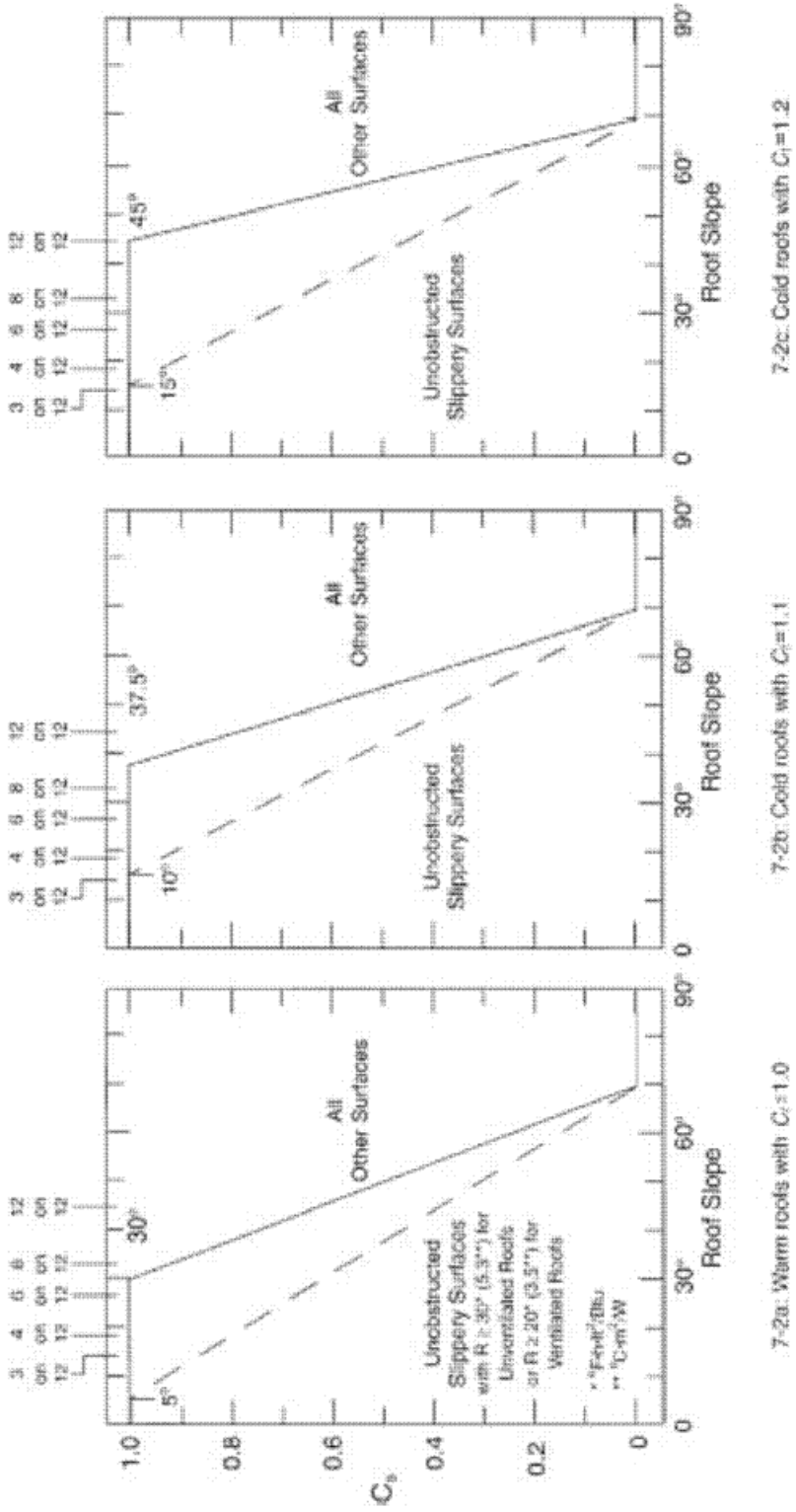

FIGURE 7-2 GRAPHS FOR DETERMINING ROOF SLOPE FACTOR C_s, FOR WARM AND COLD ROOFS (SEE TABLE 7-3 FOR C_t DEFINITIONS)

Figure A2. Graphs for Determining Roof Slope Factor

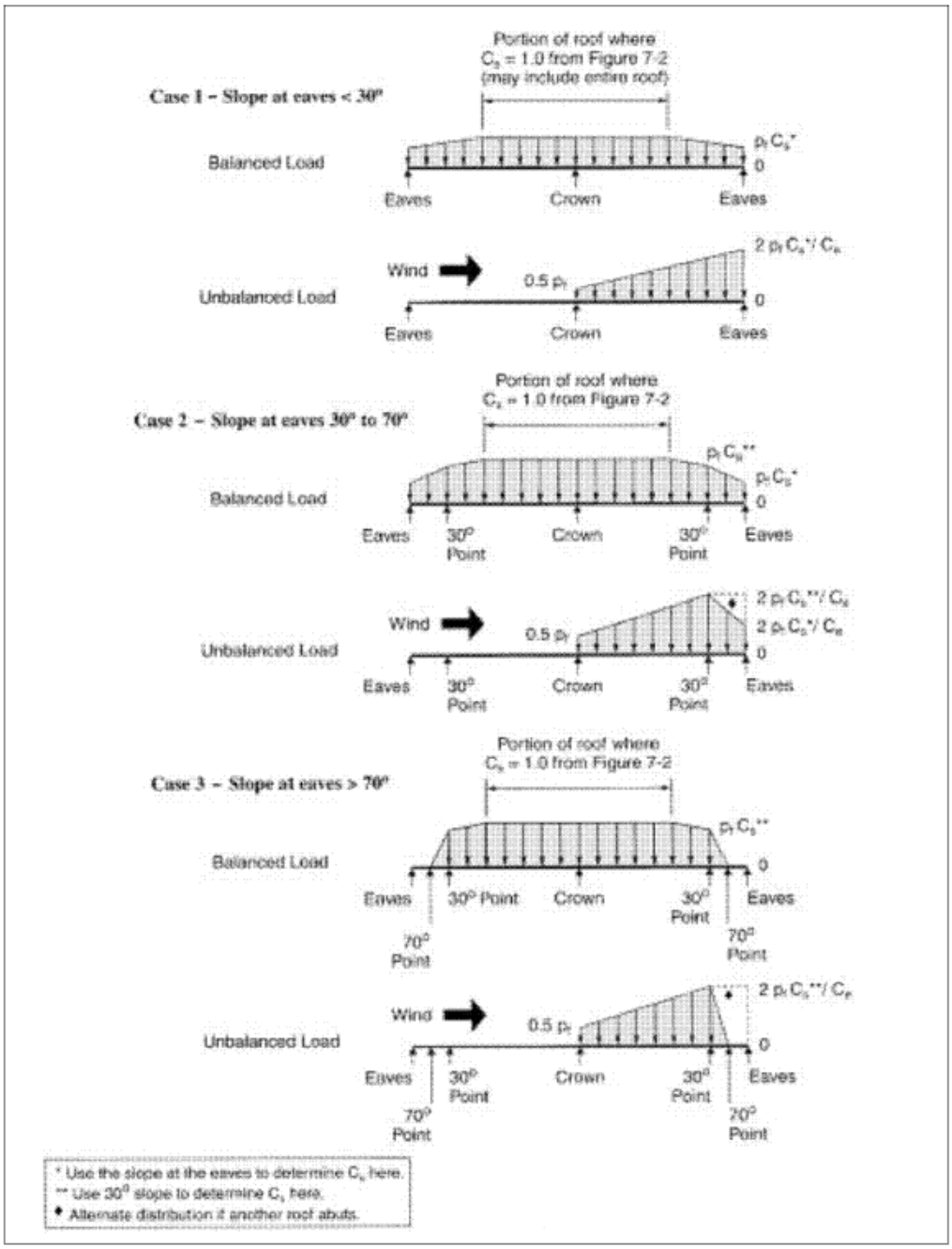

FIGURE 7-3 BALANCED AND UNBALANCED LOADS FOR CURVED ROOFS

Figure A3. Balanced and Unbalanced Loads for Curved Roofs

The terrain category and roof exposure condition (Table A1) chosen shall be representative of the anticipated conditions during the life of the structure. An exposure factor shall be determined for each roof of a structure.

Table A1

Exposure Factor

TABLE 7-2 EXPOSURE FACTOR, C_e

Terrain Category	Exposure of Roof[a] Fully Exposed	Partially Exposed	Sheltered
B (see Section 6.5.6)	0.9	1.0	1.2
C (see Section 6.5.6)	0.9	1.0	1.1
D (see Section 6.5.6)	0.8	0.9	1.0
Above the treeline in windswept mountainous areas.	0.7	0.8	N/A
In Alaska, in areas where trees do not exist within a 2-mile (3 km) radius of the site.	0.7	0.8	N/A

[a]Definitions: Partially Exposed: All roofs except as indicated in the following text. Fully Exposed: Roofs exposed on all sides with no shelter[b] afforded by terrain, higher structures, or trees. Roofs that contain several large pieces of mechanical equipment, parapets that extend above the height of the balanced snow load (h_b), or other obstructions are not in this category. Sheltered: Roofs located tight in among conifers that qualify as obstructions.

[b]Obstructions within a distance of $10h_0$ provide shelter, where h_0 is the height of the obstruction above the roof level. If the only obstructions are a few deciduous trees that are leafless in winter, the fully exposed category shall be used. Note that these are heights above the roof. Heights used to establish the terrain category in Section 6.5.3 are heights above the ground.

Table A2

Thermal Factor

TABLE 7-3 THERMAL FACTOR, C_t

Thermal Condition[a]	C_t
All structures except as indicated below:	1.0
Structures kept just above freezing and others with cold, ventilated roofs in which the thermal resistance (R-value) between the ventilated space and the heated space exceeds 25 °F× *h*× ft²/Btu (4.4 K × m²/W).	1.1
Unheated structures and structures intentionally kept below freezing.	1.2
Continuously heated greenhouses[b] with a roof having a thermal resistance (R-value) less than 2.0 °F× *h*× ft²/Btu (0.4 K × m²/W)	0.85

[a]These conditions shall be representative of the anticipated conditions during winters for the life of the structure.

[b]Greenhouses with a constantly maintained interior temperature of 50°F (10°C) or more at any point 3 feet above the floor level during winters and having either a maintenance attendant on duty at all times or a temperature alarm system to provide warning in the event of a heating failure.

Table A3

Importance Factor

TABLE 7-4 IMPORTANCE FACTOR, *I* (SNOW LOADS)

Category[a]	*I*
I	0.8
II	1.0
III	1.1
IV	1.2

[a]See Section 1.5 and Table 1-1.

Table A4

Occupancy Category of Buildings and Their Structures for Flood, Wind, Snow, Earthquake and Ice Loads

TABLE 1-1 OCCUPANCY CATEGORY OF BUILDINGS AND OTHER STRUCTURES FOR FLOOD, WIND, SNOW, EARTHQUAKE, AND ICE LOADS

Nature of Occupancy	Occupancy Category
Buildings and other structures that represent a low hazard to human life in the event of failure, including, but not limited to: • Agricultural facilities • Certain temporary facilities • Minor storage facilities	I
All buildings and other structures except those listed in Occupancy Categories I, III, and IV	II
Buildings and other structures that represent a substantial hazard to human life in the event of failure, including, but not limited to: • Buildings and other structures where more than 300 people congregate in one area • Buildings and other structures with daycare facilities with a capacity greater than 150 • Buildings and other structures with elementary school or secondary school facilities with a capacity greater than 250 • Buildings and other structures with a capacity greater than 500 for colleges or adult education facilities • Health care facilities with a capacity of 50 or more resident patients, but not having surgery or emergency treatment facilities • Jails and detention facilities Buildings and other structures, not included in Occupancy Category IV, with potential to cause a substantial economic impact and/or mass disruption of day-to-day civilian life in the event of failure, including, but not limited to: • Power generating stations[a] • Water treatment facilities • Sewage treatment facilities • Telecommunication centers Buildings and other structures not included in Occupancy Category IV (including, but not limited to, facilities that manufacture, process, handle, store, use, or dispose of such substances as hazardous fuels, hazardous chemicals, hazardous waste, or explosives) containing sufficient quantities of toxic or explosive substances to be dangerous to the public if released. Buildings and other structures containing toxic or explosive substances shall be eligible for classification as Occupancy Category II structures if it can be demonstrated to the satisfaction of the authority having jurisdiction by a hazard assessment as described in Section 1.5.2 that a release of the toxic or explosive substances does not pose a threat to the public.	III
Buildings and other structures designated as essential facilities, including, but not limited to: • Hospitals and other health care facilities having surgery or emergency treatment facilities • Fire, rescue, ambulance, and police stations and emergency vehicle garages • Designated earthquake, hurricane, or other emergency shelters • Designated emergency preparedness, communication, and operation centers and other facilities required for emergency response • Power generating stations and other public utility facilities required in an emergency • Ancillary structures (including, but not limited to, communication towers, fuel storage tanks, cooling towers, electrical substation structures, fire water storage tanks or other structures housing or supporting water, or other fire-suppression material or equipment) required for operation of Occupancy Category IV structures during an emergency • Aviation control towers, air traffic control centers, and emergency aircraft hangars • Water storage facilities and pump structures required to maintain water pressure for fire suppression • Buildings and other structures having critical national defense functions Buildings and other structures (including, but not limited to, facilities that manufacture, process, handle, store, use, or dispose of such substances as hazardous fuels, hazardous chemicals, or hazardous waste) containing highly toxic substances where the quantity of the material exceeds a threshold quantity established by the authority having jurisdiction. Buildings and other structures containing highly toxic substances shall be eligible for classification as Occupancy Category II structures if it can be demonstrated to the satisfaction of the authority having jurisdiction by a hazard assessment as described in Section 1.5.2 that a release of the highly toxic substances does not pose a threat to the public. This reduced classification shall not be permitted if the buildings or other structures also function as essential facilities.	IV

Wind Loads

A building or other structure whose fundamental frequency is greater than or equal to 1 Hz is to be considered a rigid structure. The main wind force resisting system is defined as an assemblage of structural elements assigned to provide support and stability for the overall structure. The system generally receives wind loading from more than one surface. Mean roof height, h, is computed as an average of the roof eave height and the height to the highest point on the roof surface, except that, for roof angles of less than or equal to 10° the mean roof height shall be the roof eave height.

For rigid structures as defined in clause 6.5.8.1 in Section 6.2 [10], the gust-effect factor shall be taken as 0.85.

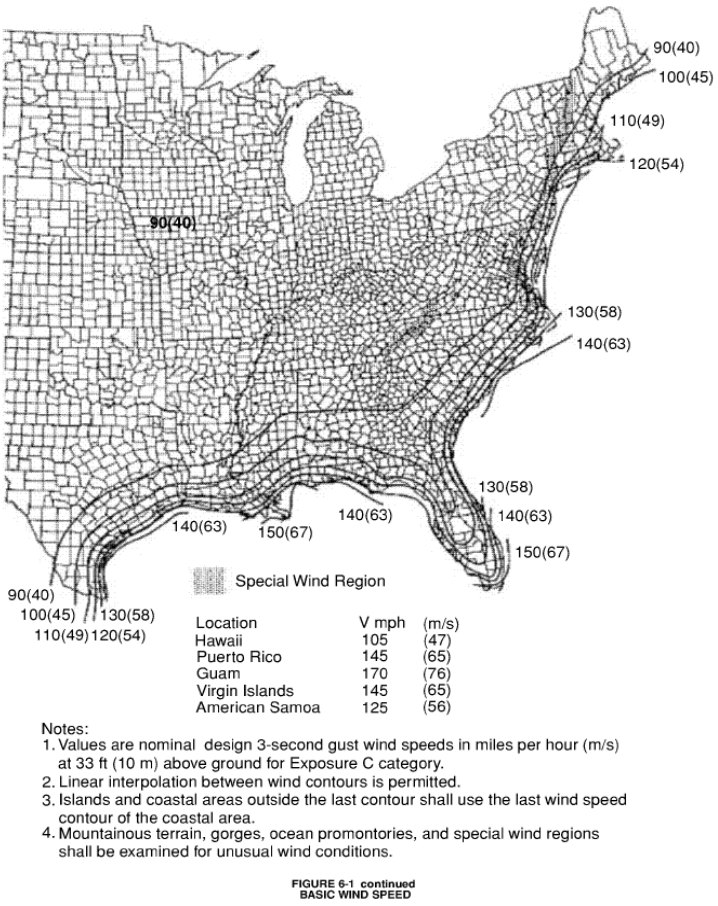

Figure A4. Basic Wind Speed

Topographic factor, K_{zt}, shall be calculated using the wind speed-up effect included in the calculation of design wind loads utilizing the factor, $K_{zt} = (1+ K_1K_2K_3)^2$ where K_1, K_2, and K_3 are given in *Figure 6.4* [10]. If site conditions of structures do not meet all the conditions specified in Section 6.5.7.1 [10], then $K_{zt} = 1.0$.

Table A5

Internal Pressure Coefficient

Main Wind Force Res. Sys. / Comp and Clad. – Method 2		All Heights
Figure 6-5	Internal Pressure Coefficient, GC_{pi}	**Walls & Roofs**
Enclosed, Partially Enclosed, and Open Buildings		

Enclosure Classification	GC_{pi}
Open Buildings	0.00
Partially Enclosed Buildings	+0.55 -0.55
Enclosed Buildings	+0.18 -0.18

Notes:

1. Plus and minus signs signify pressures acting toward and away from the internal surfaces, respectively.
2. Values of GC_{pi} shall be used with q_z or q_h as specified in 6.5.12.
3. Two cases shall be considered to determine the critical load requirements for the appropriate condition:
   (i) a positive value of GC_{pi} applied to all internal surfaces
   (ii) a negative value of GC_{pi} applied to all internal surfaces

Main Wind Force Resisting System – Method 2		All Heights
Figure 6-6	External Pressure Coefficients, C_p	Walls & Roofs
Enclosed, Partially Enclosed Buildings		

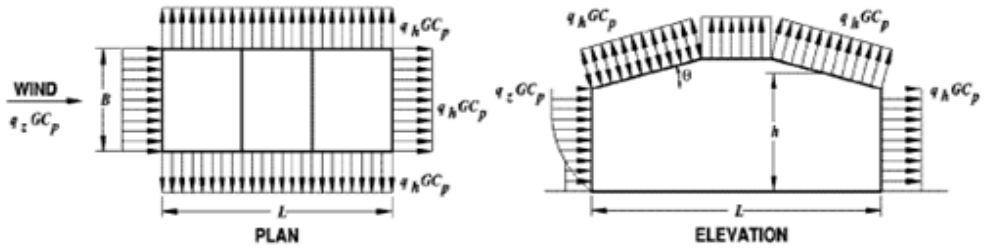

MANSARD ROOF (NOTE 8)

Figure A5. Mansard Roof

Table A6

External Pressure Coefficient

Main Wind Force Resisting System – Method 2		All Heights
Figure 6-6 (con't)	External Pressure Coefficients, C_p	Walls & Roofs
Enclosed, Partially Enclosed Buildings		

Wall Pressure Coefficients, C_p			
Surface	**L/B**	**C_p**	**Use With**
Windward Wall	All values	0.8	q_z
Leeward Wall	0-1	-0.5	q_h
	2	-0.3	
	≥4	-0.2	
Side Wall	All values	-0.7	q_h

Notes:

1. Plus and minus signs signify pressures acting toward and away from the surfaces, respectively.
2. Linear interpolation is permitted for values of *L/B*, *h/L* and θ other than shown. Interpolation shall only be carried out between values of the same sign. Where no value of the same sign is given, assume 0.0 for interpolation purposes.
3. Where two values of C_p are listed, this indicates that the windward roof slope is subjected to either positive or negative pressures and the roof structure shall be designed for both conditions. Interpolation for intermediate ratios of h/L in this case shall only be carried out between C_p values of like sign.
4. For monoslope roofs, entire roof surface is either a windward or leeward surface.
5. For flexible buildings use appropriate G_f as determined by Section 6.5.8.
6. Refer to Figure 6-7 for domes and Figure 6-8 for arched roofs.
7. Notation:
   B: Horizontal dimension of building, in feet (meter), measured normal to wind direction.
   L: Horizontal dimension of building, in feet (meter), measured parallel to wind direction.
   h: Mean roof height in feet (meters), except that eave height shall be used for θ ≤ 10 degrees.
   z: Height above ground, in feet (meters).
   G: Gust effect factor.
   q_z,q_h: Velocity pressure, in pounds per square foot (N/m^2), evaluated at respective height.
   θ: Angle of plane of roof from horizontal, in degrees.
8. For mansard roofs, the top horizontal surface and leeward inclined surface shall be treated as leeward surfaces from the table.
9. Except for MWFRS's at the roof consisting of moment resisting frames, the total horizontal shear shall not be less than that determined by neglecting wind forces on roof surfaces.

Table A7

Importance Factor for Wind Loads

Importance Factor, I (Wind Loads)

Table 6-1

Category	Non-Hurricane Prone Regions and Hurricane Prone Regions with V = 85-100 mph and Alaska	Hurricane Prone Regions with V > 100 mph
I	0.87	0.77
II	1.00	1.00
III	1.15	1.15
IV	1.15	1.15

Note:

1. The building and structure classification categories are listed in Table 1-1.

Table A8

Velocity Pressure Exposure Coefficient

Velocity Pressure Exposure Coefficients, K_h and K_z

Table 6-3

Height above ground level, z		Exposure (Note 1)			
		B		C	D
ft	(m)	Case 1	Case 2	Cases 1 & 2	Cases 1 & 2
0-15	(0-4.6)	0.70	0.57	0.85	1.03
20	(6.1)	0.70	0.62	0.90	1.08
25	(7.6)	0.70	0.66	0.94	1.12
30	(9.1)	0.70	0.70	0.98	1.16
40	(12.2)	0.76	0.76	1.04	1.22
50	(15.2)	0.81	0.81	1.09	1.27
60	(18)	0.85	0.85	1.13	1.31
70	(21.3)	0.89	0.89	1.17	1.34
80	(24.4)	0.93	0.93	1.21	1.38
90	(27.4)	0.96	0.96	1.24	1.40
100	(30.5)	0.99	0.99	1.26	1.43
120	(36.6)	1.04	1.04	1.31	1.48
140	(42.7)	1.09	1.09	1.36	1.52
160	(48.8)	1.13	1.13	1.39	1.55
180	(54.9)	1.17	1.17	1.43	1.58
200	(61.0)	1.20	1.20	1.46	1.61
250	(76.2)	1.28	1.28	1.53	1.68
300	(91.4)	1.35	1.35	1.59	1.73
350	(106.7)	1.41	1.41	1.64	1.78
400	(121.9)	1.47	1.47	1.69	1.82
450	(137.2)	1.52	1.52	1.73	1.86
500	(152.4)	1.56	1.56	1.77	1.89

Notes:

1. **Case 1:** a. All components and cladding.
   b. Main wind force resisting system in low-rise buildings designed using Figure 6-10.
   Case 2: a. All main wind force resisting systems in buildings except those in low-rise buildings designed using Figure 6-10.
   b. All main wind force resisting systems in other structures.
2. The velocity pressure exposure coefficient K_z may be determined from the following formula:
   For 15 ft. $\le z \le z_g$ For $z < 15$ ft.
   $K_z = 2.01\ (z/z_g)^{2\alpha}$ $K_z = 2.01\ (15/z_g)^{2\alpha}$
   Note: z shall not be taken less than 30 feet for Case 1 in exposure B.
3. α and z_g are tabulated in Table 6-2.
4. Linear interpolation for intermediate values of height z is acceptable.
5. Exposure categories are defined in 6.5.6.

Table A9

Wind Directionally Factor

Wind Directionality Factor, K_d

Table 6-4

Structure Type	Directionality Factor K_d*
Buildings	
Main Wind Force Resisting System	0.85
Components and Cladding	0.85
Arched Roofs	0.85
Chimneys, Tanks, and Similar Structures	
Square	0.90
Hexagonal	0.95
Round	0.95
Solid Signs	0.85
Open Signs and Lattice Framework	0.85
Trussed Towers	
Triangular, square, rectangular	0.85
All other cross sections	0.95

*Directionality Factor K_d has been calibrated with combinations of loads specified in Section 2. This factor shall only be applied when used in conjunction with load combinations specified in 2.3 and 2.4.

Appendix B

Detailed Output of Analysis

Appendix B contains the results of the computer analysis for reactions, deflections (joint and member) and unity check (stress ratio) of truss members with respect to each load case that were considered in the analysis and design of Hangar Q. These results are presented in tables that follow. It also has list of retrofitted sections.

Table B1

Reactions for Self Weight

LC	Joint	X [k]	Y [k]	Z [k]	MX [k-ft]	MY [k-ft]	MZ [k-ft]
1	N324	-5.81	6.62	-0.04	0	0	0
1	N372	-9.01	10.36	0.00	0	0	0
1	N440	-8.62	9.70	0.00	0	0	0
1	N549	-8.62	9.83	0.00	0	0	0
1	N202	-8.62	9.83	0.00	0	0	0
1	N250	-8.62	9.70	0.00	0	0	0
1	N141	-9.01	10.36	0.00	0	0	0
1	N75	-5.81	6.62	0.04	0	0	0
1	N300	5.81	6.62	-0.04	0	0	0
1	N348	9.01	10.36	0.00	0	0	0
1	N416	8.62	9.70	0.00	0	0	0
1	N525	8.62	9.83	0.00	0	0	0
1	N178	8.62	9.83	0.00	0	0	0
1	N226	8.62	9.70	0.00	0	0	0
1	N117A	9.01	10.36	0.00	0	0	0
1	N50A	5.81	6.62	0.04	0	0	0

Table B2

Reactions for Roof Load

LC	Joint	X [k]	Y [k]	Z [k]	MX [k-ft]	MY [k-ft]	MZ [k-ft]
2	N324	-7.91	9.13	-0.27	0	0	0
2	N372	-17.64	20.88	0.01	0	0	0
2	N440	-16.41	18.77	0.00	0	0	0
2	N549	-16.39	19.16	0.00	0	0	0
2	N202	-16.39	19.16	0.00	0	0	0
2	N250	-16.41	18.77	0.00	0	0	0
2	N141	-17.64	20.88	-0.01	0	0	0
2	N75	-7.91	9.13	0.27	0	0	0
2	N300	7.91	9.13	-0.27	0	0	0
2	N348	17.64	20.88	0.01	0	0	0
2	N416	16.41	18.77	0.00	0	0	0
2	N525	16.39	19.16	0.00	0	0	0
2	N178	16.39	19.16	0.00	0	0	0
2	N226	16.41	18.77	0.00	0	0	0
2	N117A	17.64	20.88	-0.01	0	0	0
2	N50A	7.91	9.13	0.27	0	0	0

Table B3

Reactions for Snow Load (Balanced)

LC	Joint	X [k]	Y [k]	Z [k]	MX [k-ft]	MY [k-ft]	MZ [k-ft]
3	N324	-10.98	10.37	0.02	0	0	0
3	N372	-24.84	24.70	-0.01	0	0	0
3	N440	-22.99	21.88	0.01	0	0	0
3	N549	-22.97	22.39	-0.01	0	0	0
3	N202	-22.97	22.39	0.01	0	0	0
3	N250	-22.99	21.88	-0.01	0	0	0
3	N141	-24.84	24.70	0.01	0	0	0
3	N75	-10.98	10.37	-0.02	0	0	0
3	N300	10.98	10.37	0.02	0	0	0
3	N348	24.84	24.70	-0.01	0	0	0
3	N416	22.99	21.88	0.01	0	0	0
3	N525	22.97	22.39	-0.01	0	0	0
3	N178	22.97	22.39	0.01	0	0	0
3	N226	22.99	21.88	-0.01	0	0	0
3	N117A	24.84	24.70	0.01	0	0	0
3	N50A	10.98	10.37	-0.02	0	0	0

Table B4

Reactions for Snow Load (Unbalanced)

LC	Joint	X [k]	Y [k]	Z [k]	MX [k-ft]	MY [k-ft]	MZ [k-ft]
4	N324	-6.15	12.02	0.04	0	0	0
4	N372	-13.75	27.20	-0.01	0	0	0
4	N440	-12.42	24.84	0.00	0	0	0
4	N549	-12.64	25.15	0.00	0	0	0
4	N202	-12.64	25.15	0.00	0	0	0
4	N250	-12.42	24.84	0.00	0	0	0
4	N141	-13.75	27.20	0.01	0	0	0
4	N75	-6.15	12.02	-0.04	0	0	0
4	N300	5.96	2.56	-0.01	0	0	0
4	N348	13.68	7.55	-0.01	0	0	0
4	N416	12.66	5.72	0.01	0	0	0
4	N525	12.65	6.30	0.00	0	0	0
4	N178	12.65	6.30	0.00	0	0	0
4	N226	12.66	5.72	-0.01	0	0	0
4	N117A	13.68	7.55	0.01	0	0	0
4	N50A	5.96	2.56	0.01	0	0	0

Table B5

Reactions for Wind Load Case-1

LC	Joint	X [k]	Y [k]	Z [k]	MX [k-ft]	MY [k-ft]	MZ [k-ft]
5	N324	2.07	-3.86	0.08	0	0	0
5	N372	4.79	-9.18	-0.02	0	0	0
5	N440	4.57	-8.51	0.01	0	0	0
5	N549	4.39	-8.43	0.00	0	0	0
5	N202	4.39	-8.43	0.00	0	0	0
5	N250	4.57	-8.51	-0.01	0	0	0
5	N141	4.79	-9.18	0.02	0	0	0
5	N75	2.07	-3.86	-0.08	0	0	0
5	N300	-7.19	-0.99	-0.14	0	0	0
5	N348	-15.89	-1.73	0.03	0	0	0
5	N416	-14.96	-1.68	-0.01	0	0	0
5	N525	-14.87	-1.70	0.00	0	0	0
5	N178	-14.87	-1.70	0.00	0	0	0
5	N226	-14.96	-1.68	0.01	0	0	0
5	N117A	-15.89	-1.73	-0.03	0	0	0
5	N50A	-7.19	-0.99	0.14	0	0	0

Table B6

Reactions for Wind Load Case-2

LC	Joint	X [k]	Y [k]	Z [k]	MX [k-ft]	MY [k-ft]	MZ [k-ft]
6	N324	4.49	-4.85	0.08	0	0	0
6	N372	10.41	-12.34	-0.02	0	0	0
6	N440	9.73	-10.79	0.00	0	0	0
6	N549	9.57	-10.99	0.00	0	0	0
6	N202	9.57	-10.99	0.00	0	0	0
6	N250	9.73	-10.79	0.00	0	0	0
6	N141	10.41	-12.34	0.02	0	0	0
6	N75	4.49	-4.85	-0.08	0	0	0
6	N300	-9.60	-7.07	-0.15	0	0	0
6	N348	-21.73	-16.02	0.04	0	0	0
6	N416	-19.88	-14.50	-0.01	0	0	0
6	N525	-20.07	-14.76	0.00	0	0	0
6	N178	-20.07	-14.76	0.00	0	0	0
6	N226	-19.88	-14.50	0.01	0	0	0
6	N117A	-21.73	-16.02	-0.04	0	0	0
6	N50A	-9.60	-7.07	0.15	0	0	0

Table B7

Reactions for Dead Load

LC	Joint	X [k]	Y [k]	Z [k]	MX [k-ft]	MY [k-ft]	MZ [k-ft]
7	N324	-13.72	15.74	-0.30	0	0	0
7	N372	-26.68	31.25	0.01	0	0	0
7	N440	-25.05	28.46	0.01	0	0	0
7	N549	-25.03	28.99	-0.01	0	0	0
7	N202	-25.03	28.99	0.01	0	0	0
7	N250	-25.05	28.46	-0.01	0	0	0
7	N141	-26.68	31.25	-0.01	0	0	0
7	N75	-13.72	15.74	0.30	0	0	0
7	N300	13.72	15.74	-0.30	0	0	0
7	N348	26.68	31.25	0.01	0	0	0
7	N416	25.05	28.46	0.01	0	0	0
7	N525	25.03	28.99	-0.01	0	0	0
7	N178	25.03	28.99	0.01	0	0	0
7	N226	25.05	28.46	-0.01	0	0	0
7	N117A	26.68	31.25	-0.01	0	0	0
7	N50A	13.72	15.74	0.30	0	0	0

Table B8

Reactions for Dead Load + Snow Load (Balanced)

LC	Joint	X [k]	Y [k]	Z [k]	MX [k-ft]	MY [k-ft]	MZ [k-ft]
8	N324	-24.70	26.09	-0.27	0	0	0
8	N372	-51.67	55.99	-0.02	0	0	0
8	N440	-48.15	50.32	0.02	0	0	0
8	N549	-48.11	51.39	-0.01	0	0	0
8	N202	-48.11	51.39	0.01	0	0	0
8	N250	-48.15	50.32	-0.02	0	0	0
8	N141	-51.67	55.99	0.02	0	0	0
8	N75	-24.70	26.09	0.27	0	0	0
8	N300	24.70	26.09	-0.27	0	0	0
8	N348	51.67	55.99	-0.02	0	0	0
8	N416	48.15	50.32	0.02	0	0	0
8	N525	48.11	51.39	-0.01	0	0	0
8	N178	48.11	51.39	0.01	0	0	0
8	N226	48.15	50.32	-0.02	0	0	0
8	N117A	51.67	55.99	0.02	0	0	0
8	N50A	24.70	26.09	0.27	0	0	0

Table B9

Reactions for Dead Load + Snow Load (Unbalanced)

LC	Joint	X [k]	Y [k]	Z [k]	MX [k-ft]	MY [k-ft]	MZ [k-ft]
9	N324	-19.86	27.72	-0.23	0	0	0
9	N372	-40.49	58.46	-0.01	0	0	0
9	N440	-37.50	53.26	0.01	0	0	0
9	N549	-37.70	54.11	-0.01	0	0	0
9	N202	-37.70	54.11	0.01	0	0	0
9	N250	-37.50	53.26	-0.01	0	0	0
9	N141	-40.49	58.46	0.01	0	0	0
9	N75	-19.86	27.72	0.23	0	0	0
9	N300	19.67	18.31	-0.32	0	0	0
9	N348	40.42	38.85	-0.02	0	0	0
9	N416	37.74	34.19	0.02	0	0	0
9	N525	37.72	35.33	-0.01	0	0	0
9	N178	37.72	35.33	0.01	0	0	0
9	N226	37.74	34.19	-0.02	0	0	0
9	N117A	40.42	38.85	0.02	0	0	0
9	N50A	19.67	18.31	0.32	0	0	0

Table B10

Reactions for Dead Load + Wind Load Case-1

LC	Joint	X [k]	Y [k]	Z [k]	MX [k-ft]	MY [k-ft]	MZ [k-ft]
10	N324	-11.64	11.90	-0.24	0	0	0
10	N372	-21.82	22.07	-0.01	0	0	0
10	N440	-20.41	19.96	0.01	0	0	0
10	N549	-20.58	20.58	0.00	0	0	0
10	N202	-20.58	20.58	0.00	0	0	0
10	N250	-20.41	19.96	-0.01	0	0	0
10	N141	-21.82	22.07	0.01	0	0	0
10	N75	-11.64	11.90	0.24	0	0	0
10	N300	6.53	14.75	-0.43	0	0	0
10	N348	10.71	29.51	0.04	0	0	0
10	N416	10.03	26.78	-0.01	0	0	0
10	N525	10.10	27.28	0.00	0	0	0
10	N178	10.10	27.28	0.00	0	0	0
10	N226	10.03	26.78	0.01	0	0	0
10	N117A	10.71	29.51	-0.04	0	0	0
10	N50A	6.53	14.75	0.43	0	0	0

Table B11

Reactions for Dead Load + Wind Load Case-2

LC	Joint	X [k]	Y [k]	Z [k]	MX [k-ft]	MY [k-ft]	MZ [k-ft]
11	N324	-9.22	10.90	-0.23	0	0	0
11	N372	-16.21	18.90	-0.01	0	0	0
11	N440	-15.27	17.67	0.00	0	0	0
11	N549	-15.41	18.01	0.00	0	0	0
11	N202	-15.41	18.01	0.00	0	0	0
11	N250	-15.27	17.67	0.00	0	0	0
11	N141	-16.21	18.90	0.01	0	0	0
11	N75	-9.22	10.90	0.23	0	0	0
11	N300	4.11	8.68	-0.46	0	0	0
11	N348	4.88	15.21	0.05	0	0	0
11	N416	5.13	13.96	-0.01	0	0	0
11	N525	4.91	14.23	0.00	0	0	0
11	N178	4.91	14.23	0.00	0	0	0
11	N226	5.13	13.96	0.01	0	0	0
11	N117A	4.88	15.21	-0.05	0	0	0
11	N50A	4.11	8.68	0.46	0	0	0

Table B12

Reactions for Dead Load + Snow Load (Balanced) + Wind Load Case-1

LC	Joint	X [k]	Y [k]	Z [k]	MX [k-ft]	MY [k-ft]	MZ [k-ft]
12	N324	-20.39	20.63	-0.24	0	0	0
12	N372	-41.72	42.92	-0.03	0	0	0
12	N440	-38.84	38.49	0.02	0	0	0
12	N549	-38.95	39.49	-0.01	0	0	0
12	N202	-38.95	39.49	0.01	0	0	0
12	N250	-38.84	38.49	-0.02	0	0	0
12	N141	-41.72	42.92	0.03	0	0	0
12	N75	-20.39	20.63	0.24	0	0	0
12	N300	16.57	22.75	-0.36	0	0	0
12	N348	33.37	48.48	0.02	0	0	0
12	N416	31.05	43.59	0.01	0	0	0
12	N525	31.09	44.49	-0.01	0	0	0
12	N178	31.09	44.49	0.01	0	0	0
12	N226	31.05	43.59	-0.01	0	0	0
12	N117A	33.37	48.48	-0.02	0	0	0
12	N50A	16.57	22.75	0.36	0	0	0

Table B13

Reactions for Dead Load + Snow Load (Balanced) + Wind Load Case-2

LC	Joint	X [k]	Y [k]	Z [k]	MX [k-ft]	MY [k-ft]	MZ [k-ft]
13	N324	-18.58	19.88	-0.24	0	0	0
13	N372	-37.50	40.53	-0.02	0	0	0
13	N440	-34.98	36.77	0.01	0	0	0
13	N549	-35.07	37.55	-0.01	0	0	0
13	N202	-35.07	37.55	0.01	0	0	0
13	N250	-34.98	36.77	-0.01	0	0	0
13	N141	-37.50	40.53	0.02	0	0	0
13	N75	-18.58	19.88	0.24	0	0	0
13	N300	14.76	18.22	-0.39	0	0	0
13	N348	28.99	37.76	0.02	0	0	0
13	N416	27.39	33.99	0.01	0	0	0
13	N525	27.20	34.71	-0.01	0	0	0
13	N178	27.20	34.71	0.01	0	0	0
13	N226	27.39	33.99	-0.01	0	0	0
13	N117A	28.99	37.76	-0.02	0	0	0
13	N50A	14.76	18.22	0.39	0	0	0

Table B14

Reactions for Dead Load + Snow Load (Unbalanced) + Wind Load Case-1

LC	Joint	X [k]	Y [k]	Z [k]	MX [k-ft]	MY [k-ft]	MZ [k-ft]
14	N324	-16.76	21.85	-0.21	0	0	0
14	N372	-33.37	44.78	-0.02	0	0	0
14	N440	-30.90	40.70	0.01	0	0	0
14	N549	-31.19	41.54	-0.01	0	0	0
14	N202	-31.19	41.54	0.01	0	0	0
14	N250	-30.90	40.70	-0.01	0	0	0
14	N141	-33.37	44.78	0.02	0	0	0
14	N75	-16.76	21.85	0.21	0	0	0
14	N300	12.79	16.91	-0.39	0	0	0
14	N348	24.98	35.63	0.02	0	0	0
14	N416	23.29	31.49	0.01	0	0	0
14	N525	23.34	32.45	-0.01	0	0	0
14	N178	23.34	32.45	0.01	0	0	0
14	N226	23.29	31.49	-0.01	0	0	0
14	N117A	24.98	35.63	-0.02	0	0	0
14	N50A	12.79	16.91	0.39	0	0	0

Table B15

Reactions for Dead Load + Snow Load (Unbalanced) + Wind Load Case-2

LC	Joint	X [k]	Y [k]	Z [k]	MX [k-ft]	MY [k-ft]	MZ [k-ft]
15	N324	-14.96	21.11	-0.21	0	0	0
15	N372	-29.17	42.40	-0.01	0	0	0
15	N440	-27.05	38.99	0.01	0	0	0
15	N549	-27.31	39.61	-0.01	0	0	0
15	N202	-27.31	39.61	0.01	0	0	0
15	N250	-27.05	38.99	-0.01	0	0	0
15	N141	-29.17	42.40	0.01	0	0	0
15	N75	-14.96	21.11	0.21	0	0	0
15	N300	10.98	12.37	-0.42	0	0	0
15	N348	20.61	24.90	0.03	0	0	0
15	N416	19.62	21.88	0.01	0	0	0
15	N525	19.45	22.66	-0.01	0	0	0
15	N178	19.45	22.66	0.01	0	0	0
15	N226	19.62	21.88	-0.01	0	0	0
15	N117A	20.61	24.90	-0.03	0	0	0
15	N50A	10.98	12.37	0.42	0	0	0

Table B16

Reactions for 0.6 Dead Load + Wind Load Case-1

LC	Joint	X [k]	Y [k]	Z [k]	MX [k-ft]	MY [k-ft]	MZ [k-ft]
16	N324	-6.15	5.59	-0.11	0	0	0
16	N372	-11.16	9.57	-0.02	0	0	0
16	N440	-10.41	8.57	0.01	0	0	0
16	N549	-10.58	8.97	0.00	0	0	0
16	N202	-10.58	8.97	0.00	0	0	0
16	N250	-10.41	8.57	-0.01	0	0	0
16	N141	-11.16	9.57	0.02	0	0	0
16	N75	-6.15	5.59	0.11	0	0	0
16	N300	1.04	8.46	-0.32	0	0	0
16	N348	0.06	17.01	0.04	0	0	0
16	N416	0.02	15.40	-0.01	0	0	0
16	N525	0.10	15.69	0.00	0	0	0
16	N178	0.10	15.69	0.00	0	0	0
16	N226	0.02	15.40	0.01	0	0	0
16	N117A	0.06	17.01	-0.04	0	0	0
16	N50A	1.04	8.46	0.32	0	0	0

Table B17

Reactions for 0.6 Dead Load + Wind Load Case-2

LC	Joint	X [k]	Y [k]	Z [k]	MX [k-ft]	MY [k-ft]	MZ [k-ft]
17	N324	-3.74	4.60	-0.11	0	0	0
17	N372	-5.56	6.41	-0.01	0	0	0
17	N440	-5.27	6.29	0.00	0	0	0
17	N549	-5.41	6.41	0.00	0	0	0
17	N202	-5.41	6.41	0.00	0	0	0
17	N250	-5.27	6.29	0.00	0	0	0
17	N141	-5.56	6.41	0.01	0	0	0
17	N75	-3.74	4.60	0.11	0	0	0
17	N300	-1.38	2.38	-0.34	0	0	0
17	N348	-5.77	2.72	0.05	0	0	0
17	N416	-4.88	2.58	-0.01	0	0	0
17	N525	-5.08	2.64	0.00	0	0	0
17	N178	-5.08	2.64	0.00	0	0	0
17	N226	-4.88	2.58	0.01	0	0	0
17	N117A	-5.77	2.72	-0.05	0	0	0
17	N50A	-1.38	2.38	0.34	0	0	0

Table B18

Reactions for 1.4 Dead Load

LC	Joint	X [k]	Y [k]	Z [k]	MX [k-ft]	MY [k-ft]	MZ [k-ft]
18	N324	-19.21	22.03	-0.42	0	0	0
18	N372	-37.39	43.76	0.00	0	0	0
18	N440	-35.10	39.84	0.01	0	0	0
18	N549	-35.07	40.59	-0.01	0	0	0
18	N202	-35.07	40.59	0.01	0	0	0
18	N250	-35.10	39.84	-0.01	0	0	0
18	N141	-37.39	43.76	0.00	0	0	0
18	N75	-19.21	22.03	0.42	0	0	0
18	N300	19.21	22.03	-0.42	0	0	0
18	N348	37.39	43.76	0.00	0	0	0
18	N416	35.10	39.84	0.01	0	0	0
18	N525	35.07	40.59	-0.01	0	0	0
18	N178	35.07	40.59	0.01	0	0	0
18	N226	35.10	39.84	-0.01	0	0	0
18	N117A	37.39	43.76	0.00	0	0	0
18	N50A	19.21	22.03	0.42	0	0	0

Table B19

Reactions for 1.2 Dead Load + 0.5 Snow Load (B)

LC	Joint	X [k]	Y [k]	Z [k]	MX [k-ft]	MY [k-ft]	MZ [k-ft]
19	N324	-21.96	24.06	-0.35	0	0	0
19	N372	-44.53	49.87	-0.01	0	0	0
19	N440	-41.62	45.08	0.02	0	0	0
19	N549	-41.59	45.99	-0.01	0	0	0
19	N202	-41.59	45.99	0.01	0	0	0
19	N250	-41.62	45.08	-0.02	0	0	0
19	N141	-44.53	49.87	0.01	0	0	0
19	N75	-21.96	24.06	0.35	0	0	0
19	N300	21.96	24.06	-0.35	0	0	0
19	N348	44.53	49.87	-0.01	0	0	0
19	N416	41.62	45.08	0.02	0	0	0
19	N525	41.59	45.99	-0.01	0	0	0
19	N178	41.59	45.99	0.01	0	0	0
19	N226	41.62	45.08	-0.02	0	0	0
19	N117A	44.53	49.87	0.01	0	0	0
19	N50A	21.96	24.06	0.35	0	0	0

Table B20

Reactions for 1.2 Dead Load + 0.5 Snow Load (UB)

LC	Joint	X [k]	Y [k]	Z [k]	MX [k-ft]	MY [k-ft]	MZ [k-ft]
20	N324	-19.54	24.88	-0.32	0	0	0
20	N372	-38.94	51.11	0.00	0	0	0
20	N440	-36.30	46.55	0.01	0	0	0
20	N549	-36.39	47.35	-0.01	0	0	0
20	N202	-36.39	47.35	0.01	0	0	0
20	N250	-36.30	46.55	-0.01	0	0	0
20	N141	-38.94	51.11	0.00	0	0	0
20	N75	-19.54	24.88	0.32	0	0	0
20	N300	19.44	20.17	-0.37	0	0	0
20	N348	38.91	41.30	-0.01	0	0	0
20	N416	36.43	37.02	0.02	0	0	0
20	N525	36.40	37.96	-0.01	0	0	0
20	N178	36.40	37.96	0.01	0	0	0
20	N226	36.43	37.02	-0.02	0	0	0
20	N117A	38.91	41.30	0.01	0	0	0
20	N50A	19.44	20.17	0.37	0	0	0

Table B21

Reactions for 1.2 Dead Load + 1.6 Snow Load (B) + 0.8 Wind Load Case-1

LC	Joint	X [k]	Y [k]	Z [k]	MX [k-ft]	MY [k-ft]	MZ [k-ft]
21	N324	-32.35	32.38	-0.29	0	0	0
21	N372	-68.14	69.79	-0.06	0	0	0
21	N440	-63.29	62.34	0.04	0	0	0
21	N549	-63.41	63.92	-0.02	0	0	0
21	N202	-63.41	63.92	0.02	0	0	0
21	N250	-63.29	62.34	-0.04	0	0	0
21	N141	-68.14	69.79	0.06	0	0	0
21	N75	-32.35	32.38	0.29	0	0	0
21	N300	28.29	34.61	-0.37	0	0	0
21	N348	59.22	75.69	-0.02	0	0	0
21	N416	54.99	67.74	0.03	0	0	0
21	N525	55.02	69.23	-0.02	0	0	0
21	N178	55.02	69.23	0.02	0	0	0
21	N226	54.99	67.74	-0.03	0	0	0
21	N117A	59.22	75.69	0.02	0	0	0
21	N50A	28.29	34.61	0.37	0	0	0

Table B22

Reactions for 1.2 Dead Load + 1.6 Snow Load (B) + 0.8 Wind Load Case-2

LC	Joint	X [k]	Y [k]	Z [k]	MX [k-ft]	MY [k-ft]	MZ [k-ft]
22	N324	-30.43	31.57	-0.27	0	0	0
22	N372	-63.64	67.21	-0.05	0	0	0
22	N440	-59.18	60.50	0.03	0	0	0
22	N549	-59.27	61.84	-0.02	0	0	0
22	N202	-59.27	61.84	0.02	0	0	0
22	N250	-59.18	60.50	-0.03	0	0	0
22	N141	-63.64	67.21	0.05	0	0	0
22	N75	-30.43	31.57	0.27	0	0	0
22	N300	26.36	29.79	-0.41	0	0	0
22	N348	54.54	64.25	-0.02	0	0	0
22	N416	51.09	57.53	0.03	0	0	0
22	N525	50.86	58.80	-0.02	0	0	0
22	N178	50.86	58.80	0.02	0	0	0
22	N226	51.09	57.53	-0.03	0	0	0
22	N117A	54.54	64.25	0.02	0	0	0
22	N50A	26.36	29.79	0.41	0	0	0

Table B23

Reactions for 1.2 Dead Load + 1.6 Snow Load (UB) + 0.8 Wind Load Case-1

LC	Joint	X [k]	Y [k]	Z [k]	MX [k-ft]	MY [k-ft]	MZ [k-ft]
23	N324	-24.61	34.96	-0.19	0	0	0
23	N372	-50.24	73.72	-0.03	0	0	0
23	N440	-46.26	67.03	0.02	0	0	0
23	N549	-46.76	68.26	-0.02	0	0	0
23	N202	-46.76	68.26	0.02	0	0	0
23	N250	-46.26	67.03	-0.02	0	0	0
23	N141	-50.24	73.72	0.03	0	0	0
23	N75	-24.61	34.96	0.19	0	0	0
23	N300	20.23	22.18	-0.46	0	0	0
23	N348	41.23	48.28	-0.01	0	0	0
23	N416	38.36	41.96	0.02	0	0	0
23	N525	38.40	43.55	-0.01	0	0	0
23	N178	38.40	43.55	0.01	0	0	0
23	N226	38.36	41.96	-0.02	0	0	0
23	N117A	41.23	48.28	0.01	0	0	0
23	N50A	20.23	22.18	0.46	0	0	0

Table B24

Reactions for 1.2 Dead Load + 1.6 Snow Load (UB) + 0.8 Wind Load Case-2

LC	Joint	X [k]	Y [k]	Z [k]	MX [k-ft]	MY [k-ft]	MZ [k-ft]
24	N324	-22.69	34.16	-0.19	0	0	0
24	N372	-45.76	71.17	-0.02	0	0	0
24	N440	-42.15	65.20	0.01	0	0	0
24	N549	-42.63	66.20	-0.01	0	0	0
24	N202	-42.63	66.20	0.01	0	0	0
24	N250	-42.15	65.20	-0.01	0	0	0
24	N141	-45.76	71.17	0.02	0	0	0
24	N75	-22.69	34.17	0.19	0	0	0
24	N300	18.30	17.35	-0.49	0	0	0
24	N348	36.56	36.83	0.00	0	0	0
24	N416	34.45	31.73	0.02	0	0	0
24	N525	34.25	33.12	-0.01	0	0	0
24	N178	34.25	33.12	0.01	0	0	0
24	N226	34.45	31.73	-0.02	0	0	0
24	N117A	36.56	36.83	0.00	0	0	0
24	N50A	18.30	17.35	0.49	0	0	0

Table B25

Reactions for 1.2 Dead Load + 1.6 Wind Load Case-1 + 0.5 Snow Load (B)

LC	Joint	X [k]	Y [k]	Z [k]	MX [k-ft]	MY [k-ft]	MZ [k-ft]
25	N324	-18.62	17.93	-0.26	0	0	0
25	N372	-36.68	35.20	-0.04	0	0	0
25	N440	-34.13	31.50	0.02	0	0	0
25	N549	-34.41	32.54	-0.01	0	0	0
25	N202	-34.41	32.54	0.01	0	0	0
25	N250	-34.13	31.50	-0.02	0	0	0
25	N141	-36.68	35.20	0.04	0	0	0
25	N75	-18.62	17.93	0.26	0	0	0
25	N300	10.45	22.47	-0.54	0	0	0
25	N348	18.89	47.05	0.06	0	0	0
25	N416	17.52	42.37	-0.01	0	0	0
25	N525	17.64	43.23	-0.01	0	0	0
25	N178	17.64	43.23	0.01	0	0	0
25	N226	17.52	42.37	0.01	0	0	0
25	N117A	18.89	47.05	-0.06	0	0	0
25	N50A	10.45	22.47	0.54	0	0	0

Table B26

Reactions for 1.2 Dead Load + 1.6 Wind Load Case-1 + 0.5 Snow Load (UB)

LC	Joint	X [k]	Y [k]	Z [k]	MX [k-ft]	MY [k-ft]	MZ [k-ft]
26	N324	-16.20	18.74	-0.24	0	0	0
26	N372	-31.14	36.44	-0.03	0	0	0
26	N440	-28.86	32.97	0.01	0	0	0
26	N549	-29.25	33.90	-0.01	0	0	0
26	N202	-29.25	33.90	0.01	0	0	0
26	N250	-28.86	32.97	-0.01	0	0	0
26	N141	-31.14	36.44	0.03	0	0	0
26	N75	-16.20	18.74	0.24	0	0	0
26	N300	7.94	18.57	-0.56	0	0	0
26	N348	13.32	38.49	0.06	0	0	0
26	N416	12.36	34.31	-0.01	0	0	0
26	N525	12.49	35.20	0.00	0	0	0
26	N178	12.49	35.20	0.00	0	0	0
26	N226	12.36	34.31	0.01	0	0	0
26	N117A	13.32	38.49	-0.06	0	0	0
26	N50A	7.94	18.57	0.56	0	0	0

Table B27

Reactions for 1.2 Dead Load + 1.6 Wind Load Case-2 + 0.5 Snow Load (B)

LC	Joint	X [k]	Y [k]	Z [k]	MX [k-ft]	MY [k-ft]	MZ [k-ft]
27	N324	-14.76	16.33	-0.24	0	0	0
27	N372	-27.70	30.10	-0.02	0	0	0
27	N440	-25.91	27.83	0.01	0	0	0
27	N549	-26.14	28.41	0.00	0	0	0
27	N202	-26.14	28.41	0.00	0	0	0
27	N250	-25.91	27.83	-0.01	0	0	0
27	N141	-27.70	30.10	0.02	0	0	0
27	N75	-14.76	16.33	0.24	0	0	0
27	N300	6.59	12.78	-0.59	0	0	0
27	N348	9.56	24.19	0.07	0	0	0
27	N416	9.69	21.89	-0.01	0	0	0
27	N525	9.34	22.37	0.00	0	0	0
27	N178	9.34	22.37	0.00	0	0	0
27	N226	9.69	21.89	0.01	0	0	0
27	N117A	9.56	24.19	-0.07	0	0	0
27	N50A	6.59	12.78	0.59	0	0	0

Table B28

Reactions for 1.2 Dead Load + 1.6 Wind Load Case-2 + 0.5 Snow Load (UB)

LC	Joint	X [k]	Y [k]	Z [k]	MX [k-ft]	MY [k-ft]	MZ [k-ft]
28	N324	-12.35	17.15	-0.22	0	0	0
28	N372	-22.17	31.36	-0.02	0	0	0
28	N440	-20.64	29.31	0.01	0	0	0
28	N549	-20.98	29.79	0.00	0	0	0
28	N202	-20.98	29.79	0.00	0	0	0
28	N250	-20.64	29.31	-0.01	0	0	0
28	N141	-22.17	31.36	0.02	0	0	0
28	N75	-12.35	17.15	0.22	0	0	0
28	N300	4.08	8.87	-0.61	0	0	0
28	N348	4.00	15.63	0.08	0	0	0
28	N416	4.53	13.81	-0.01	0	0	0
28	N525	4.19	14.33	0.00	0	0	0
28	N178	4.19	14.33	0.00	0	0	0
28	N226	4.53	13.81	0.01	0	0	0
28	N117A	4.00	15.63	-0.08	0	0	0
28	N50A	4.08	8.87	0.61	0	0	0

Table B29

Reactions for 1.2 Dead Load + 0.2 Snow Load (B)

LC	Joint	X [k]	Y [k]	Z [k]	MX [k-ft]	MY [k-ft]	MZ [k-ft]
29	N324	-18.66	20.96	-0.35	0	0	0
29	N372	-37.03	42.45	0.00	0	0	0
29	N440	-34.69	38.52	0.01	0	0	0
29	N549	-34.66	39.27	-0.01	0	0	0
29	N202	-34.66	39.27	0.01	0	0	0
29	N250	-34.69	38.52	-0.01	0	0	0
29	N141	-37.03	42.45	0.00	0	0	0
29	N75	-18.66	20.96	0.35	0	0	0
29	N300	18.66	20.96	-0.35	0	0	0
29	N348	37.03	42.45	0.00	0	0	0
29	N416	34.69	38.52	0.01	0	0	0
29	N525	34.66	39.27	-0.01	0	0	0
29	N178	34.66	39.27	0.01	0	0	0
29	N226	34.69	38.52	-0.01	0	0	0
29	N117A	37.03	42.45	0.00	0	0	0
29	N50A	18.66	20.96	0.35	0	0	0

Table B30

Reactions for 1.2 Dead Load + 0.2 Snow Load (UB)

LC	Joint	X [k]	Y [k]	Z [k]	MX [k-ft]	MY [k-ft]	MZ [k-ft]
30	N324	-17.69	21.28	-0.35	0	0	0
30	N372	-34.79	42.95	0.00	0	0	0
30	N440	-32.57	39.11	0.01	0	0	0
30	N549	-32.59	39.82	-0.01	0	0	0
30	N202	-32.59	39.82	0.01	0	0	0
30	N250	-32.57	39.11	-0.01	0	0	0
30	N141	-34.79	42.95	0.00	0	0	0
30	N75	-17.69	21.28	0.35	0	0	0
30	N300	17.65	19.40	-0.36	0	0	0
30	N348	34.78	39.02	0.00	0	0	0
30	N416	32.62	35.30	0.01	0	0	0
30	N525	32.59	36.06	-0.01	0	0	0
30	N178	32.59	36.06	0.01	0	0	0
30	N226	32.62	35.30	-0.01	0	0	0
30	N117A	34.78	39.02	0.00	0	0	0
30	N50A	17.65	19.40	0.36	0	0	0

Table B31

Reactions for 0.9 Dead Load + 1.6 Wind Load Case-1

LC	Joint	X [k]	Y [k]	Z [k]	MX [k-ft]	MY [k-ft]	MZ [k-ft]
31	N324	-9.02	8.01	-0.16	0	0	0
31	N372	-16.27	13.45	-0.03	0	0	0
31	N440	-15.15	12.02	0.01	0	0	0
31	N549	-15.43	12.63	0.00	0	0	0
31	N202	-15.43	12.63	0.00	0	0	0
31	N250	-15.15	12.02	-0.01	0	0	0
31	N141	-16.27	13.45	0.03	0	0	0
31	N75	-9.02	8.01	0.16	0	0	0
31	N300	0.84	12.58	-0.50	0	0	0
31	N348	-1.50	25.33	0.07	0	0	0
31	N416	-1.47	22.92	-0.01	0	0	0
31	N525	-1.33	23.36	0.00	0	0	0
31	N178	-1.33	23.36	0.00	0	0	0
31	N226	-1.47	22.92	0.01	0	0	0
31	N117A	-1.50	25.33	-0.07	0	0	0
31	N50A	0.84	12.58	0.50	0	0	0

Table B32

Reactions for 0.9 Dead Load + 1.6 Wind Load Case-2

LC	Joint	X [k]	Y [k]	Z [k]	MX [k-ft]	MY [k-ft]	MZ [k-ft]
32	N324	-5.16	6.42	-0.15	0	0	0
32	N372	-7.30	8.38	-0.02	0	0	0
32	N440	-6.93	8.36	0.01	0	0	0
32	N549	-7.16	8.51	0.00	0	0	0
32	N202	-7.16	8.51	0.00	0	0	0
32	N250	-6.93	8.36	-0.01	0	0	0
32	N141	-7.30	8.38	0.02	0	0	0
32	N75	-5.16	6.42	0.15	0	0	0
32	N300	-3.03	2.86	-0.52	0	0	0
32	N348	-10.82	2.48	0.08	0	0	0
32	N416	-9.31	2.41	-0.01	0	0	0
32	N525	-9.63	2.48	0.00	0	0	0
32	N178	-9.63	2.48	0.00	0	0	0
32	N226	-9.31	2.41	0.01	0	0	0
32	N117A	-10.82	2.48	-0.08	0	0	0
32	N50A	-3.03	2.86	0.52	0	0	0

Table B33

Deflections for Self Weight

Directions	Deflections [in]	Joints
X	± 0.094	N342, N347, N464, N469
Y	-0.15	N137, N162, N246, N247,
Z	± 0.037	N63, N88

Table B34

Deflections for Roof Load

Directions	Deflections [in]	Joints
X	± 0.263	N342, N347, N464, N469
Y	-0.327	N137, N162, N246, N368
Z	± 0.119	N63, N88

Table B35

Deflections for Snow Load (B)

Directions	Deflections [in]	Joints
X	± 0.314	N342, N347, N464, N469
Y	-0.487	N137, N162, N368, N393
Z	± 0.171	N63, N88

Table B36

Deflections for Snow Load (UB)

Directions	Deflections [in]	Joints
X	± 0.589	N150, N381
Y	-0.83	N213, N396
Z	± 0.342	N85, N334

Table B37

Deflections for Wind Load Case-1

Directions	Deflections [in]	Joints
X	± 0.617	N218, N347, N401, N469
Y	-0.56	N344, N466
Z	± 0.176	N60, N309

Table B38

Deflections for Wind Load Case-2

Directions	Deflections [in]	Joints
X	± 0.338	N218, N401
Y	-0.327	N162, N393
Z	± 0.116	N88, N337

Table B39

Deflections for Dead Load

Directions	Deflections [in]	Joints
X	± 0.358	N342, N347, N464, N469
Y	-0.478	N162, N368, N393,N396
Z	± 0.158	N63, N88, N312, N337

Table B40

Deflections for Dead Load + Snow Load (Balanced)

Directions	Deflections [in]	Joints
X	± 0.68	N342, N347, N464, N469
Y	-0.974	N137, N162, N368, N393
Z	± 0.342	N63, N88, N312, N337

Table B41

Deflections for Dead Load + Snow Load (Unbalanced)

Directions	Deflections [in]	Joints
X	± 0.788	N342, N347, N464, N469
Y	-1.208	N213, N396
Z	± 0.507	N88, N337

Table B42

Deflections for Dead Load + Wind Load Case-1

Directions	Deflections [in]	Joints
X	± 0.704	N342,N464
Y	-0.601	N217, N400
Z	± 0.308	N60, N309

Table B43

Deflections for Dead Load + Wind Load Case-2

Directions	Deflections [in]	Joints
X	± 0.495	N342,N464
Y	-0.486	N213, N396
Z	± 0.096	N52, N302

Table B44

Deflections for Dead Load + 0.75 Snow Load (Balanced) + 0.75 Wind Load Case-1

Directions	Deflections [in]	Joints
X	± 0.861	N342,N464
Y	-0.813	N345, N467
Z	± 0.379	N60, N309

Table B45

Deflections for Dead Load + 0.75 Snow Load (Balanced) + 0.75 Wind Load Case-2

Directions	Deflections [in]	Joints
X	± 0.70	N342,N464
Y	-0.666	N213, N396
Z	± 0.204	N63, N312

Table B46

Deflections for Dead Load + 0.75 Snow Load (Unbalanced) + 0.75 Wind Load Case-1

Directions	Deflections [in]	Joints
X	± 0.674	N342,N464
Y	-1.034	N213, N396
Z	± 0.283	N88, N337

Table B47

Deflections for Dead Load + 0.75 Snow Load (Unbalanced) + 0.75 Wind Load Case-2

Directions	Deflections [in]	Joints
X	± 0.518	N347, N464, N469, N573
Y	-1.081	N213, N396
Z	± 0.324	N88, N337

Table B48

Deflections for 0.6 Dead Load + Wind Load Case-1

Directions	Deflections [in]	Joints
X	± 0.559	N342, N347, N464, N469
Y	-0.528	N217, N400
Z	± 0.254	N60, N309

Table B49

Deflections for 0.6 Dead Load + Wind Load Case-2

Directions	Deflections [in]	Joints
X	± 0.37	N213, N396
Y	-0.341	N213, N396
Z	± 0.085	N52, N302

Table B50

Deflections for 1.4 Dead Load

Directions	Deflections [in]	Joints
X	± 0.504	N342, N347, N464, N469
Y	-0.672	N137, N162, N368, N393
Z	± 0.225	N63, N88, N312, N337

Table B51

Deflections for 1.2 Dead Load + 0.5 Snow Load (Balanced)

Directions	Deflections [in]	Joints
X	± 0.592	N342, N347, N464, N469
Y	-0.822	N137, N162, N368, N393
Z	± 0.283	N63, N88

Table B52

Deflections for 1.2 Dead Load + 0.5 Snow Load (Unbalanced)

Directions	Deflections [in]	Joints
X	± 0.645	N347, N469
Y	-0.861	N213, N396
Z	± 0.366	N88, N337

Table B53

Deflections for 1.2 Dead Load + 1.6 Snow Load (Balanced) + 0.8 Wind Load Case-1

Directions	Deflections [in]	Joints
X	± 0.48	N346, N468
Y	-1.21	N213, N396
Z	± 0.577	N63, N312

Table B54

Deflections for 1.2 Dead Load + 1.6 Snow Load (Balanced) + 0.8 Wind Load Case-2

Directions	Deflections [in]	Joints
X	± 0.683	N347, N469
Y	-1.12	N137, N368
Z	± 0.391	N63, N312

Table B55

Deflections for 1.2 Dead Load + 1.6 Snow Load (Unbalanced) + 0.8 Wind Load Case-1

Directions	Deflections [in]	Joints
X	± 0.855	N346, N468
Y	-1.16	N213, N396
Z	± 0.611	N88, N337

Table B56

Deflections for 1.2 Dead Load + 1.6 Snow Load (Unbalanced) + 0.8 Wind Load Case-2

Directions	Deflections [in]	Joints
X	± 0.66	N152, N383
Y	-1.08	N213, N396
Z	± 0.655	N88

Table B57

Deflections for 1.2 Dead Load + 1.6 Wind Load Case-1 + 0.5 Snow Load (Balanced)

Directions	Deflections [in]	Joints
X	± 0.260	N342, N464
Y	-0.983	N217, N400
Z	± 0.518	N60, N309

Table B58

Deflections for 1.2 Dead Load + 1.6 Wind Load Case-1 + 0.5 Snow Load (Unbalanced)

Directions	Deflections [in]	Joints
X	± 0.128	N342, N464
Y	-0.941	N213, N396
Z	± 0.392	N60, N309

Table B59

Deflections for 1.2 Dead Load + 1.6 Wind Load Case-2 + 0.5 Snow Load (Balanced)

Directions	Deflections [in]	Joints
X	± 0.808	N346, N468
Y	-0.769	N213, N396
Z	± 0.147	N52, N302

Table B60

Deflections for 1.2 Dead Load + 1.6 Wind Load Case-2 + 0.5 Snow Load (Unbalanced)

Directions	Deflections [in]	Joints
X	± 0.699	N213, N396
Y	-1.046	N213, N396
Z	± 0.167	N88, N337

Table B61

Deflections for 1.2 Dead Load + 0.2 Snow Load (Balanced)

Directions	Deflections [in]	Joints
X	± 0.495	N342, N347, N464, N469
Y	-0.674	N137, N162, N368, N393
Z	± 0.228	N63, N88, N312, N337

Table B62

Deflections for 1.2 Dead Load + 0.2 Snow Load (Unbalanced)

Directions	Deflections [in]	Joints
X	± 0.516	N347, N464, N469
Y	-0.664	N160, N391
Z	± 0.261	N88, N337

Table B63

Deflections for 0.9 Dead Load + 1.6 Wind Load Case-1

Directions	Deflections [in]	Joints
X	± 0.785	N342, N464
Y	-0.839	N217, N400
Z	± 0.401	N60, N309

Table B64

Deflections for 0.9 Dead Load + 1.6 Wind Load Case-2

Directions	Deflections [in]	Joints
X	± 0.575	N213, N396
Y	-0.524	N213, N396
Z	± 0.134	N52, N302

Table B65

Unity Check for Self Weight

Section Set	Shape	Unity Check	Members
Purlins	W8x15	0.08	M418, M441, M1135, M1158
Channels	C6x10.5	0.078	M936, M947, M1413, M1426
Double Angled	LL 4x4x4x0	0.144	M254, M296, M1060, M1102
WTs	Double angle with cover plate on top	0.136	M304, M460, M1110, M1184

Table B66

Unity Check for Roof Load

Section Set	Shape	Unity Check	Members
Purlins	W8x15	0.536	M418, M441, M1135, M1158
Channels	C6x10.5	0.212	M95
Double Angled	LL 4x4x4x0	0.332	M254, M296, M1060, M1102
WTs	Double angle with cover plate on top	0.24	M305, M459, M1111, M1185

Table B67

Unity Check for Snow Load-Balanced

Section Set	Shape	Unity Check	Members
Purlins	W8x15	0.278	M420, M439, M1137, M1156
Channels	C6x10.5	0.193	M936, M947, M1413, M1426
Double Angled	LL 4x4x4x0	0.463	M254, M296, M1060, M1102
WTs	Double angle with cover plate on top	0.401	M304, M460, M1110, M1184

Table B68

Unity Check for Snow Load-Unbalanced

Section Set	Shape	Unity Check	Members
Purlins	W8x15	0.613	M1735A, M1741A
Channels	C6x10.5	0.381	M1652, M1653
Double Angled	LL 4x4x4x0	0.633	M292, M1098
WTs	Double angle with cover plate on top	0.325	M297, M1103

Table B69

Unity Check for Wind Load Case-1

Section Set	Shape	Unity Check	Members
Purlins	W8x15	0.279	M441, M1158
Channels	C6x10.5	0.187	M1186, M470
Double Angled	LL 4x4x4x0	0.477	M243, M1649
WTs	Double angle with cover plate on top	0.285	M460, M1184

Table B70

Unity Check for Wind Load Case-2

Section Set	Shape	Unity Check	Members
Purlins	W8x15	0.301	M439, M1156
Channels	C6x10.5	0.201	M469, M1187
Double Angled	LL 4x4x4x0	0.249	M243, M1049
WTs	Double angle with cover plate on top	0.269	M262, M1068

Table B71

Unity Check for Dead Load

Section Set	Shape	Unity Check	Members
Purlins	W8x15	0.615	M418, M441, M1135, M1158
Channels	C6x10.5	0.256	M936, M947, M1413, M1426
Double Angled	LL 4x4x4x0	0.495	M254, M296, M1060, M1102
WTs	Double angle with cover plate on top	0.465	M304, M460, M1110, M1184

Table B72

Unity Check for Dead Load + Snow Load-Balanced

Section Set	Shape	Unity Check	Members
Purlins	W8x15	0.616	M418, M441, M1135, M1158
Channels	C6x10.5	0.452	M936, M947, M1413, M1426
Double Angled	LL 4x4x4x0	0.963	M254, M296, M1060, M1102
WTs	Double angle with cover plate on top	0.871	M304, M460, M1110, M1184

Table B73

Unity Check for Dead Load + Snow Load-Unbalanced

Section Set	Shape	Unity Check	Members
Purlins	W8x15	0.94	M1735A, M1741A
Channels	C6x10.5	0.634	M936, M1413
Double Angled	LL 4x4x4x0	0.999	M295, M1101
WTs	Double angle with cover plate on top	0.73	M460, M1184

Table B74

Unity Check for Dead Load + Wind Load Case-1

Section Set	Shape	Unity Check	Members
Purlins	W8x15	0.726	M418, M1135
Channels	C6x10.5	0.339	M457, M1175
Double Angled	LL 4x4x4x0	0.578	M246, M1052
WTs	Double angle with cover plate on top	0.435	M304, M1110

Table B75

Unity Check for Dead Load + Wind Load Case-2

Section Set	Shape	Unity Check	Members
Purlins	W8x15	0.726	M418, M1135
Channels	C6x10.5	0.333	M458, M1174
Double Angled	LL 4x4x4x0	0.379	M143, M1000
WTs	Double angle with cover plate on top	0.274	M304, M1110

Table B76

Unity Check for Dead Load + 0.75 Snow Load (Balanced) + 0.75 Wind Load Case-1

Section Set	Shape	Unity Check	Members
Purlins	W8x15	0.679	M418, M1135
Channels	C6x10.5	0.46	M458, M1174
Double Angled	LL 4x4x4x0	0.786	M254, M1060
WTs	Double angle with cover plate on top	0.747	M304, M1110

Table B77

Unity Check for Dead Load + 0.75 Snow Load (Balanced) + 0.75 Wind Load Case-2

Section Set	Shape	Unity Check	Members
Purlins	W8x15	0.68	M418, M1135
Channels	C6x10.5	0.45	M458, M1174
Double Angled	LL 4x4x4x0	0.646	M254, M1060
WTs	Double angle with cover plate on top	0.665	M304, M1110

Table B78

Unity Check for Dead Load + 0.75 Snow Load (Unbalanced) + 0.75 Wind Load Case-1

Section Set	Shape	Unity Check	Members
Purlins	W8x15	0.871	M1735A, M1741A
Channels	C6x10.5	0.599	M458, M1174
Double Angled	LL 4x4x4x0	0.647	M296, M1102
WTs	Double angle with cover plate on top	0.652	M297, M1103

Table B79

Unity Check for Dead Load + 0.75 Snow Load (Unbalanced) + 0.75 Wind Load Case-2

Section Set	Shape	Unity Check	Members
Purlins	W8x15	0.876	M1735A, M1741A
Channels	C6x10.5	0.589	M458, M1174
Double Angled	LL 4x4x4x0	0.659	M295, M1101
WTs	Double angle with cover plate on top	0.5	M297, M1103

Table B80

Unity Check for 0.6 Dead Load + Wind Load Case-1

Section Set	Shape	Unity Check	Members
Purlins	W8x15	0.508	M418, M1135
Channels	C6x10.5	0.247	M457, M1175
Double Angled	LL 4x4x4x0	0.522	M246, M1052
WTs	Double angle with cover plate on top	0.303	M255, M1061

Table B81

Unity Check for 0.6 Dead Load + Wind Load Case-2

Section Set	Shape	Unity Check	Members
Purlins	W8x15	0.508	M418, M1135
Channels	C6x10.5	0.245	M458, M1174
Double Angled	LL 4x4x4x0	0.257	M143, M1000
WTs	Double angle with cover plate on top	0.155	M251, M1058

Table B82

Unity Check for 1.4 Dead Load

Section Set	Shape	Unity Check	Members
Purlins	W8x15	0.758	M418, M441, M1135, M1158
Channels	C6x10.5	0.359	M936, M947, M1413, M1426
Double Angled	LL 4x4x4x0	0.695	M254, M296, M1060, M1102
WTs	Double angle with cover plate on top	0.652	M304, M460, M1110, M1184

Table B83

Unity Check for 1.2 Dead Load + 0.5 Snow Load (Balanced)

Section Set	Shape	Unity Check	Members
Purlins	W8x15	0.739	M418, M441, M1135, M1158
Channels	C6x10.5	0.405	M936, M947, M1413, M1426
Double Angled	LL 4x4x4x0	0.829	M254, M296, M1060, M1102
WTs	Double angle with cover plate on top	0.761	M304, M460, M1110, M1184

Table B84

Unity Check for 1.2 Dead Load + 0.5 Snow Load (Unbalanced)

Section Set	Shape	Unity Check	Members
Purlins	W8x15	0.739	M441, M1158
Channels	C6x10.5	0.497	M936, M1413
Double Angled	LL 4x4x4x0	0.817	M296, M1102
WTs	Double angle with cover plate on top	0.691	M460, M1184

Table B85

Unity Check for 1.2 Dead Load + 1.6 Snow Load (Balanced) + 0.5 Wind Load Case-1

Section Set	Shape	Unity Check	Members
Purlins	W8x15	0.784	M1735A, M1741A
Channels	C6x10.5	0.679	M458, M1174
Double Angled	LL 4x4x4x0	0.724	M254, M1060
WTs	Double angle with cover plate on top	0.69	M304, M1110

Table B86

Unity Check for 1.2 Dead Load + 1.6 Snow Load (Balanced) + 0.5 Wind Load Case-2

Section Set	Shape	Unity Check	Members
Purlins	W8x15	0.812	M1735A, M1741A
Channels	C6x10.5	0.668	M458, M1174
Double Angled	LL 4x4x4x0	0.79	M254, M1060
WTs	Double angle with cover plate on top	0.84	M304, M1110

Table B87

Unity Check for 1.2 Dead Load + 1.6 Snow Load (Unbalanced) + 0.5 Wind Load Case-1

Section Set	Shape	Unity Check	Members
Purlins	W8x15	0.823	M418, M1135, M1735A, M1741A
Channels	C6x10.5	0.876	M458, M1174
Double Angled	LL 4x4x4x0	0.722	M292, M1098
WTs	Double angle with cover plate on top	0.67	M297, M1103

Table B88

Unity Check for 1.2 Dead Load + 1.6 Snow Load (Unbalanced) + 0.5 Wind Load Case-2

Section Set	Shape	Unity Check	Members
Purlins	W8x15	0.768	M418, M1135, M1735A, M1741A
Channels	C6x10.5	0.864	M458, M1174
Double Angled	LL 4x4x4x0	0.72	M292, M1098
WTs	Double angle with cover plate on top	0.88	M297, M1103

Table B89

Unity Check for 1.2 Dead Load + + Wind Load Case-1 + 0.5 Snow Load (Balanced)

Section Set	Shape	Unity Check	Members
Purlins	W8x15	0.842	M418, M1135
Channels	C6x10.5	0.543	M457, M1175
Double Angled	LL 4x4x4x0	0.835	M246, M1052
WTs	Double angle with cover plate on top	0.718	M255, M1061

Table B90

Unity Check for 1.2 Dead Load + + Wind Load Case-1 + 0.5 Snow Load (Unbalanced)

Section Set	Shape	Unity Check	Members
Purlins	W8x15	0.843	M418, M1135
Channels	C6x10.5	0.635	M457, M1175
Double Angled	LL 4x4x4x0	0.759	M246, M1052
WTs	Double angle with cover plate on top	0.673	M255, M1061

Table B91

Unity Check for 1.2 Dead Load + + Wind Load Case-2 + 0.5 Snow Load (Balanced)

Section Set	Shape	Unity Check	Members
Purlins	W8x15	0.854	M418, M1135
Channels	C6x10.5	0.53	M458, M1174
Double Angled	LL 4x4x4x0	0.494	M143, M1000
WTs	Double angle with cover plate on top	0.541	M304,M1110

Table B92

Unity Check for 1.2 Dead Load + + Wind Load Case-2 + 0.5 Snow Load (Unbalanced)

Section Set	Shape	Unity Check	Members
Purlins	W8x15	0.796	M1735A, M1741A
Channels	C6x10.5	0.631	M458, M1174
Double Angled	LL 4x4x4x0	0.486	M143, M1000
WTs	Double angle with cover plate on top	0.428	M304, M1110, M1123

Table B93

Unity Check for 1.2 Dead Load + 0.2 Snow Load (Balanced)

Section Set	Shape	Unity Check	Members
Purlins	W8x15	0.738	M441, M1135
Channels	C6x10.5	0.346	M936, M947, M1413, M1426
Double Angled	LL 4x4x4x0	0.688	M254, M296, M1060, M1102
WTs	Double angle with cover plate on top	0.639	M304, M460, M1110, M1184

Table B94

Unity Check for 1.2 Dead Load + 0.2 Snow Load (Unbalanced)

Section Set	Shape	Unity Check	Members
Purlins	W8x15	0.684	M418, M1135
Channels	C6x10.5	0.383	M936, M1413
Double Angled	LL 4x4x4x0	0.697	M296, M1102
WTs	Double angle with cover plate on top	0.611	M460, M1184

Table B95

Unity Check for 0.9 Dead Load + + Wind Load Case-1

Section Set	Shape	Unity Check	Members
Purlins	W8x15	0.779	M418, M1135, M1735A, M1741A
Channels	C6x10.5	0.392	M457, M1175
Double Angled	LL 4x4x4x0	0.833	M246, M1052
WTs	Double angle with cover plate on top	0.472	M255, M1061

Table B96

Unity Check for 0.9 Dead Load + + Wind Load Case-2

Section Set	Shape	Unity Check	Members
Purlins	W8x15	0.78	M441, M1135
Channels	C6x10.5	0.409	M458, M1174
Double Angled	LL 4x4x4x0	0.464	M143, M1000
WTs	Double angle with cover plate on top	0.392	M304, M1123

Retrofitted Sections

In the analysis, it was decided to retrofit all overstressed steel sections (double angle sections) in top and bottom chords by adding cover plates to maintain the historic value of the truss. These overstressed double angle members were retrofitted by putting cover plates (0.5 inch thick) on top of them to control the limiting criteria (unity check < 1) (*Figure C43, Figure C4).* This was modeled in RISA using WT sections.

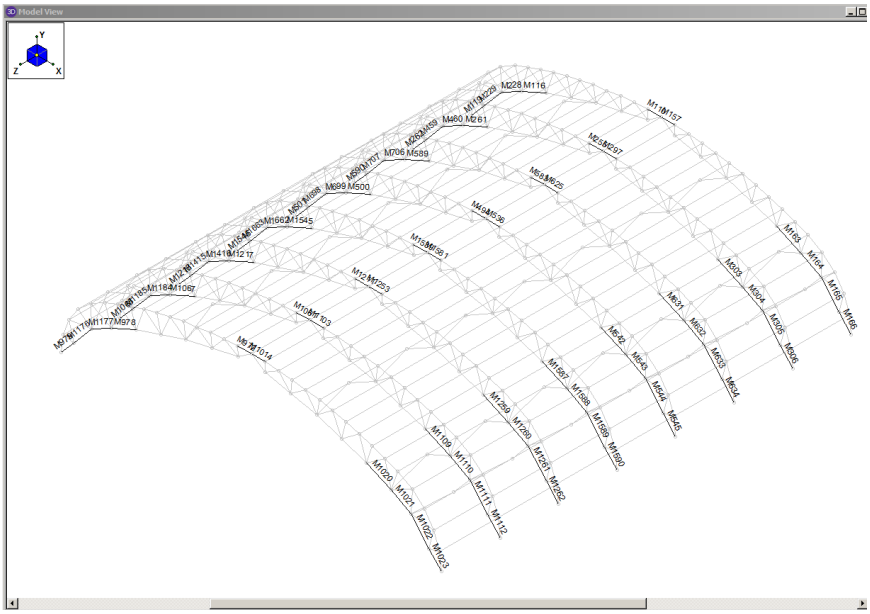

Figure C43. Members that need to be Retrofitted – Isometric

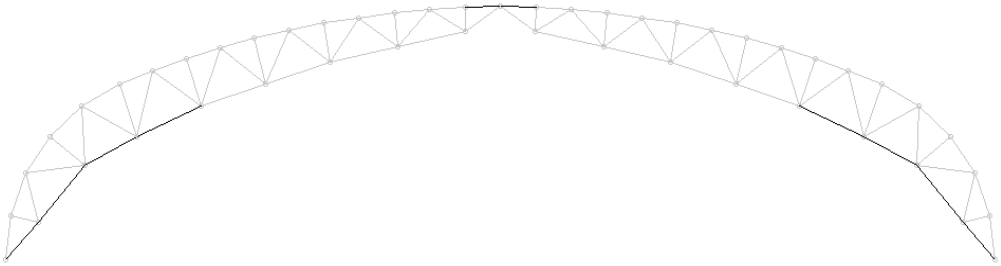

Figure C44. Members that need to be Retrofitted - Elevation

Table C1

List of Members that need to be Retrofitted

Retrofitted Sections	Location on Truss
M1020 to M1023	Bottom Chord Right
M1109 to M1112	
M1259 to M1262	
M1587 to M1590	
M542 to M545	
M631 to M634	
M303 to M306	
M163 to M166	
M978, M979, M1176, M1177	Bottom Chord Left
M1167, M1168, M1184, M118584,	
M1217, M1218, M1415, M1416,	
M1545, M1546, M1662, M1663	
M500, M501, M698, M699	
M589, M590, M706, M707	
M261, M262, M459, M460	
M116, M119, M228, M229	
M972, M1014, M1061, M1103	Top Chord Center
M1211, M1253, M1539, M1581	
M494, M536, M583, M625	
M255, M297, M110, M157	

Total 80 deficient members need to be retrofitted.

Appendix C

Detailed Analysis and Design of Concrete Elements

Appendix C includes the detailed calculations for stability analysis of the piers and the pier foundations considering eccentricity and soil pressure beneath the foundations, reinforcement design, and analysis of the foundations of the pier and three different approaches adopted to design the pier reinforcement. It also contains a brief analysis and design for the cross beams resting on the pier that run throughout the length of Hangar Q. Aforesaid computations are presented as follows.

Stability Analysis of Foundation

Maximum horizontal load and maximum vertical load

Total horizontal load should be taken equal to maximum reaction in X-direction from analysis of truss of Hangar Q.

Total horizontal load = Maximum reaction in X direction = 51.70 kips

Total vertical load should be calculated as summation of vertical load in Y-direction from analysis of truss and all vertical loads (Table C1, *Figure C1*).

Total vertical load = summation of all verticals loads

= vertical reaction in Y-direction + wt. of sec 1 + wt. of sec 2 + wt. of sec 3 + wt. of sec 4

=56 + 40.8 + 5.625+ 7.5 + 19.70 = 129.62 kips

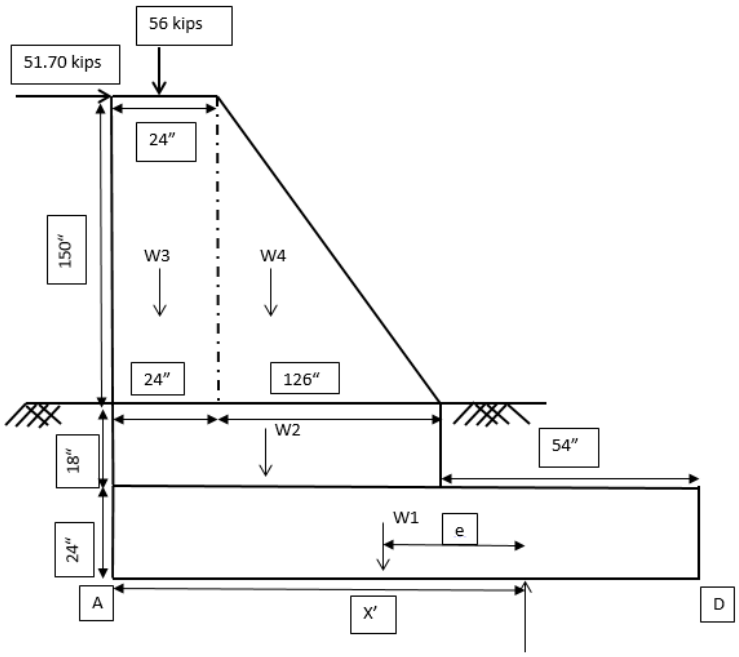

Figure C1. Elevation of Pier

Figure C2. Foundation of Pier (ASD) Plan View

Clockwise Moment = Negative, Counterclockwise Moment = Positive;

Considering *Figure C1*, Moment @ A:

(Total vertical load) X' = summation of moment due to all loads

= (total horizontal load) (lever arm from A) + (vertical reaction in Y-direction) (lever arm from A) + (wt. of section 1) (lever arm from A) + (wt. of section 2) (lever arm from A) + (wt. of section 3) (lever arm from A) + (wt. of section 4) (lever arm from A)

So, per formula: (129.62) X' = (51.70*192) + (56*12) + (40.8*102) + (5.625*75) + (7.5*12) + (19.70*66)

129.62 X’ = 9920.64 + 672 + 4161.60 + 421.875+ 90 + 1300.2

X’ = 127.80 inches < 204 inches from A;

e = X’ – (l/2) = 127.80 inch – 102 inch =25.80 inch < (b/6) =34 inch

Table C1

Weight of the Sections with Lever Arm from Heel (point A)

Weight of the sections	X from A (inch)
W1 = (204*24*96*150) / (12^3) * (1000) = 40.8 kips	X1 = 102
W2 = (150*24*150) / (12^3) * (1000) = 5.625 kips	X2 = 75
W3 = (150*24*24*150) / (12^3) * (1000) = 40.8 kips	X3 = 12
W4 = (126*150*24*150) / (2) *(12^3) * (1000) = 19.70 kips	X4 = 66

Calculate soil pressure area beneath foundation and building pressure on foundation: Length of foundation – distance of point of application of resultant vertical reaction = 204 inches – 127.80 inches = 76.20 inches = 1/3 X, so X = 228.60 inches > 204 inches, *Figure C3*. It would be a trapezoidal pressure distribution from soil beneath foundation as e < b/6.

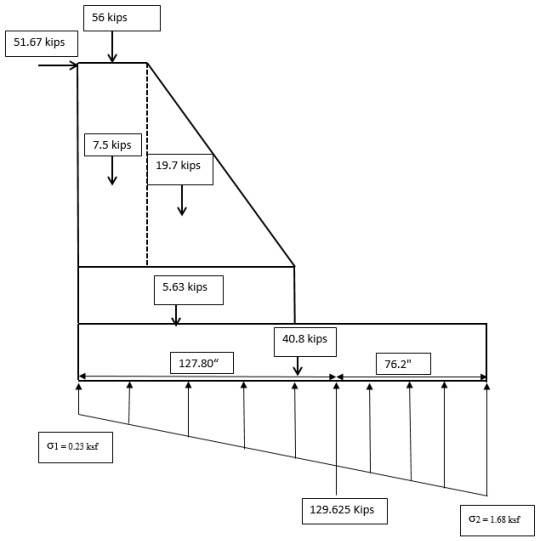

Figure C3. Soil Pressure Distribution Beneath Foundation

Total vertical load = 129.62 kips;

Acting on an area = (length of foundation) (width of foundation), *Figure C2*

Acting on an area = (204 inch) (96 inch) = 19584 $inch^2$ = 136 ft^2

Average building pressure = (129.625 Kips) / (136 ft^2) = 0.9531 ksf < 3 ksf

Maximum building pressure was calculated as:

(204 *96) σ_1 + (σ_2 - σ_1) (0.5*204*96) = 129.625 kips; considering forces

σ_1 (204*96*102) + (σ_2 - σ_1) (0.5*204*96*0.67*204) = (129.625*127.80); moments solving simultaneously the equation of forces and equation of moments;

σ_1 = 0.23 ksf , σ_2 = 1.68 ksf (*Figure 34*) which are less than 3 ksf, so foundation geometry (width, length) is stable under maximum ASD load combinations.

Design of Wall Footings

"The theory [1] used for designing beams is applicable to the design of footings with only a few modifications. The upward soil pressure under the wall footing of *Figure C19* tends to bend the footing into the deformed shape shown. The footings will be designed as shallow beams for the moments and shears involved. In beams where loads are usually only a few hundred pounds per foot and spans are fairly large, sizes are almost always proportioned for moment. In footings, loads from the supporting soils may run several thousand pounds per foot and spans are relatively short. As a result, shears will almost always control depths. It appears that the maximum moment in this footing occurs under the middle of the wall, but tests have shown that this is not correct because of the rigidity of such walls. If the walls are of reinforced concrete with their considerable rigidity, it is considered satisfactory to compute the moments at the faces of the walls (ACI Code 15.4.2). Should a footing be supporting a masonry wall with its greater flexibility, the code states that the moment should be taken at a section halfway from the face of the wall to its center (For a

column with a steel base plate, the critical section for moment is to be located halfway from the face of the column to the edge of the plate.)"

"To compute the bending moments and shears in a footing, it is necessary to compute only the net upward pressure, q_u, caused by the factored wall loads above. In other words, the weight of the footing and soil on top of the footing can be neglected. These items cause an upward pressure equal to their downward weights, and they cancel each other for purposes of computing shears and moments. In a similar manner, it is obvious that there are no moments or shears existing in a book lying flat on a table. Should a wall footing be loaded until it fails in shear, the failure will not occur on a vertical plane at the wall face but rather at an angle of approximately 45° with the wall, as shown in *Figure C19*. Apparently the diagonal tension, which one would expect to cause cracks in between the two diagonal lines, is opposed by the squeezing or compression caused by the downward wall load and the upward soil pressure."

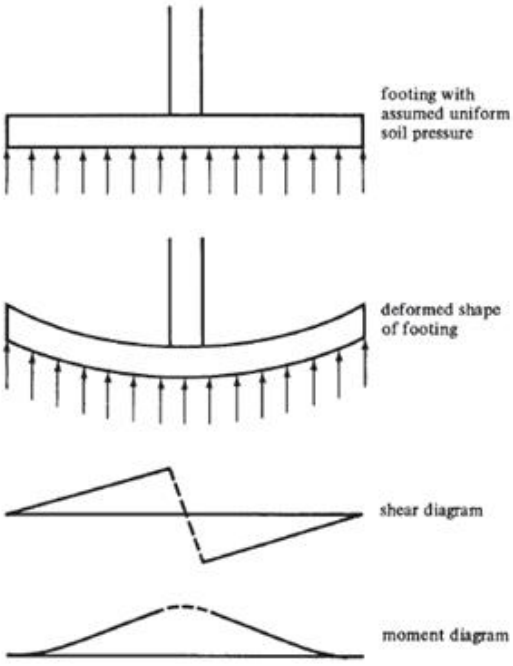

Figure C19. Shear and Moment diagram for wall footing with uniform soil pressure

"Outside this zone, the compression effect is negligible in its effect on diagonal tension. Therefore, for non-prestressed sections, shear may be calculated at a distance *d* from the face of the wall (ACI Code 11.1.3.1) because of the loads located outside the section. The use of stirrups in footings is usually considered impractical and uneconomical. For this reason, the effective depth of wall footings is selected so that V_u is limited to the design shear strength, ϕV_c , that the concrete can carry without web reinforcing, that is, $\phi 2\lambda\sqrt{f_c}\, b_w d$ (from ACI Section 11.3.1.1 and ACI Equation 11-3). Although the equation for V_c contains the term λ, it would be unusual to use lightweight concrete to construct a footing. The primary advantage for using lightweight concrete and its associated additional cost is to reduce the weight of the concrete superstructure. It would not be economical to use it in a footing."

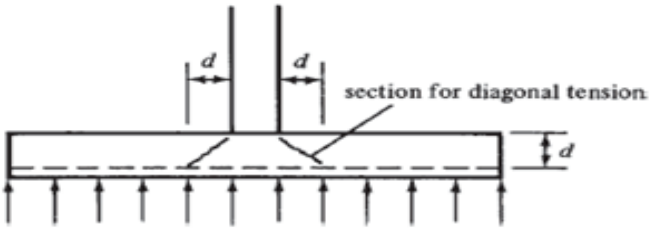

Figure C20. Critical Section for Shear in a Wall Footing

"The following expression is used to select the depths of wall footings:"

$$d = \frac{V_u}{(\phi)\left(2\lambda\sqrt{f'_c}\right)(b_w)}$$

"The design of wall footings is conveniently handled by using 12 inch widths of the wall, as shown in *Figure C20*. Such a practice is followed for the design of a wall footing. It should be noted that Section 15.7 of the code states that the depth of a footing above the bottom reinforcing bars may be no less than 6 inch for footings on soils and 12 inch for those on piles. Thus, total minimum practical depths are at least 10 inch for regular spread footings and 16 inch for pile caps. Various f_c' values, 3000 psi and 4000 psi concretes are commonly used for footings and are generally quite

economical. Occasionally, when it is very important to minimize footing depths and weights, stronger concrete may be used. For most cases, however, the extra cost of higher-strength concrete will appreciably exceed the money saved with the smaller concrete volume."

"The exposure category of the footing may control the concrete strength. ACI Section 4.2 requires that concrete exposed to sulfate have minimum f_c' values of 4000 psi or 4500 psi, depending on the sulfur concentration in the soil. The determination of a footing depth is a trial-and-error problem. The designer assumes an effective depth, *d*, computes the *d* required for shear, tries another *d*, computes the *d* required for shear, and so on, until the assumed value and the calculated value are within about 1 inch of each other."

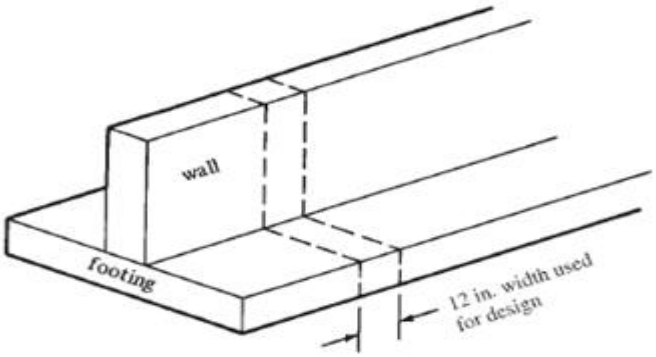

Figure C21. One Foot Design Strip Width for Wall Footing

"For two-way shear in slabs (& footings) V_c is smallest of

$$V_c = \left(2 + \frac{4}{\beta_c}\right)\sqrt{f_c}\, b_o d \qquad \text{ACI 11-35}$$

β_c = long side/short side of column concentrated load or reaction area < 2

b_o = length of critical perimeter;

$b_o = 4(c+d)$ – for square columns where one side = c

$b_o = 2(c_1+d) + 2(c_2+d)$ – for rectangular columns of sides c_1 and c_2

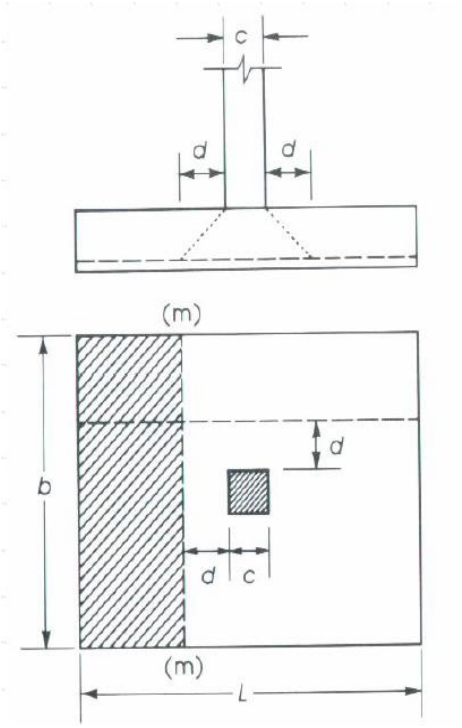

Figure C22. One Way Shear

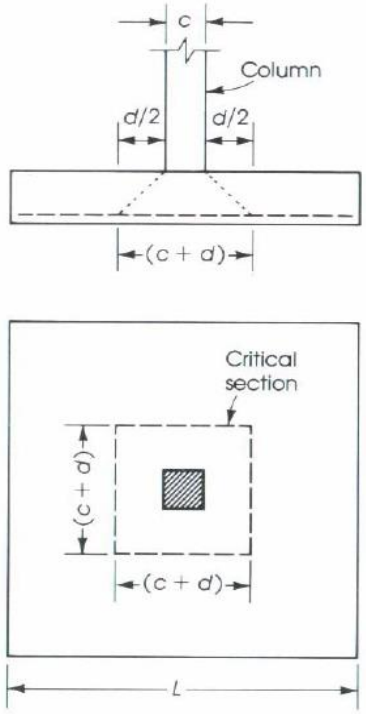

Figure C22A. Two Way Shear

The shear force V_u acts at a section that has a length

b_o = 4(c+d) or 2(c_1+d) +2(c_2+d) and a depth d; the section is subjected to a vertical downward load P_u and vertical upward pressure q_u.

$V_u = P_u - q_u (c+ d)^2$ for square columns

$V_u = P_u - q_u (c_1+d) (c_2+d)$ for rectangle columns

Allowable $\phi V_c = 4\phi \sqrt{f_c}\, b_o d$

$$d = \frac{V_u}{4\phi\sqrt{f_c}\, b_o}$$

Where $V_u = \phi Vc$

If *d* is not close to the assumed *d*, revise your assumptions. For footings with bending action in one direction the critical section is located a distance d from face of column;

$\phi V_c = 2\phi\sqrt{f_c}\, b_o d$

The ultimate shearing force at section m-m can be calculated

$V_u = q_u\, b\, (L/2 - C/2 - d)$. If no shear reinforcement is to be used, then d can be checked

If no shear reinforcement is to be used, then d can be checked, take $V_u = \phi\, V_c$

$$d = \frac{V_u}{2\phi\sqrt{f_c}\, b}$$

The bending moment in each direction of the footing must be checked and the appropriate reinforcement must be provided".

$$A_s = \frac{M_u}{\phi f_y \left(d - \frac{a}{2}\right)}$$

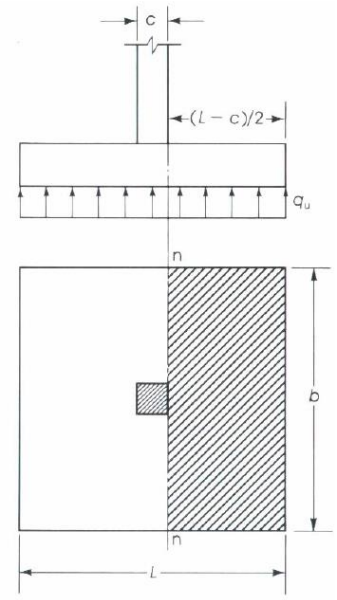

Figure C23. Moment Arm from Footing Edge

"Another approach is to calculated $R_u = M_u / bd^2$ and determine the steel percentage required ρ. Determine A_s then check if assumed a is close to calculated a as below:"

$$a = \frac{f_y A_s}{0.85 f_c\, b}$$

"The minimum steel percentage required in flexural members is $200/f_y$ with minimum area and maximum spacing of steel bars in the direction of bending shall be as required for shrinkage temperature reinforcement. The loads from the column act on the footing at the base of the column, on an area equal to area of the column cross-section. Compressive forces are transferred to the footing directly by bearing on the concrete. Tensile forces must be resisted by reinforcement, neglecting any contribution by concrete. Force acting on the concrete at the base of the column must not exceed the bearing strength of the concrete. $N_1 = \phi\ (0.85\ f_c\ A_1)$; where $\phi = 0.65$ and A_1 = bearing area of column."

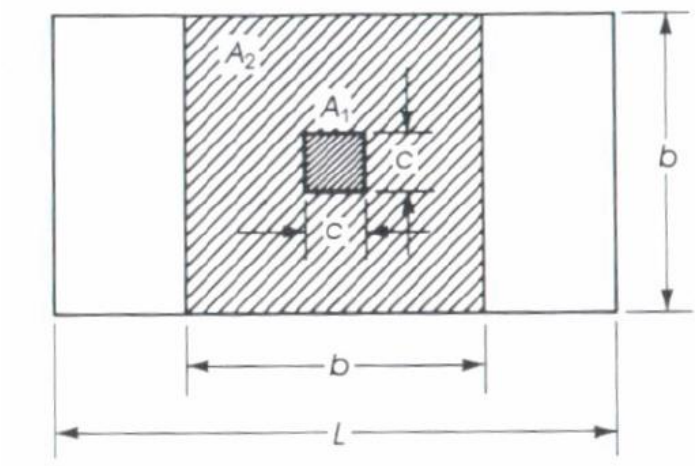

Figure C24. Bearing Strength Area Modification

"The value of the bearing strength may be multiplied by a factor $\sqrt{\frac{A_2}{A_1}} \leq 2$ for bearing on footing when the supporting surface is wider on all sides than the loaded area. The modified bearing strength $N_1 \leq \phi\ (0.85\ f_c\ A_1)\sqrt{\frac{A_2}{A_1}}$; $N_2 \leq 2\phi\ (0.85\ f_c\ A_1)$"

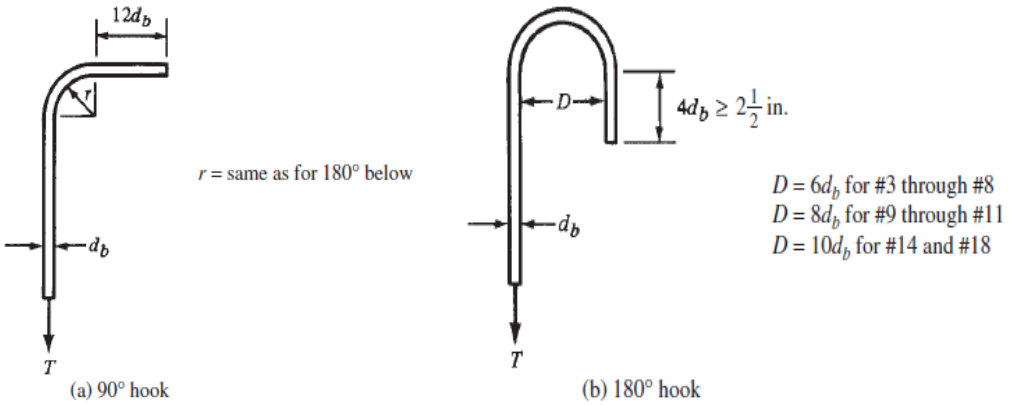

Figure C25. 90° Hook and 180° Hook Configuration

The development length for compression bars was given as:

$l_d = 0.02\ f_y\ d_b / \sqrt{f_c}$ but not less than $0.003\ f_y\ d_b \geq 8$ inch

The development length for tension bar bars was given as simplified equations:

$l_d = (f_y\ d_b\ \Psi_t\ \Psi_e) / (20\sqrt{f_c})$ – for #7 and larger bars

$l_d = (f_y\ d_b\ \Psi_t\ \Psi_e) / (25\sqrt{f_c})$ – for #6 and smaller bars and deformed wires

"Hooks: When sufficient space is not available to anchor tension bars by running them straight for their required development lengths, hooks may be used. (Hooks are considered ineffective for compression bars for development length purposes.) *Figure C25* shows details of the standard 90° and 180° hooks specified in 7.2 of the ACI Code. Either the 90° hook with an extension of 12 bar diameters ($12d_b$) at the free end or the 180° hook with an extension of 4 bar diameters ($4d_b$) but not less than 2.5 inch may be used at the free end. The radii and diameters shown are measured on the inside of the bends."

"The dimensions given for hooks were developed to protect members against splitting of the concrete or bar breakage, no matter what concrete strengths, bar sizes, or bar stresses are used. Actually, hooks do not provide an appreciable increase in

anchorage strength because the concrete in the plane of the hook is somewhat vulnerable to splitting. This means that adding more length (i.e., more than the specified $12d_b$ or $4d_b$ values) onto bars beyond the hooks doesn't really increase their anchorage strengths. The development length needed for a hook is directly proportional to the bar diameter. This is because the magnitude of compressive stresses in the concrete on the inside of the hook is governed by d_b. To determine the development lengths needed for standard hooks, the ACI (12.5.2) requires the calculation of; $l_{dh} = 0.02\ d_b\ \Psi_e\ f_y / \lambda \sqrt{f_c}$. The value of l_{dh}, according to ACI Section 12.5.1, may not be less than 6 in. or $8d_b$. For deformed bars, the ACI, Section 12.5.2, states that ψ_e in this expression can be taken as equal to 1.2 for epoxy-coated reinforcing and the λ used as equal to 0.75 for lightweight aggregate concrete. For all other cases, ψ_e and λ are to be set equal to 1.0. The development length, l_{dh}, is measured from the critical section of the bar to the outside end or edge of the hooks, as shown in *Figure C26."*

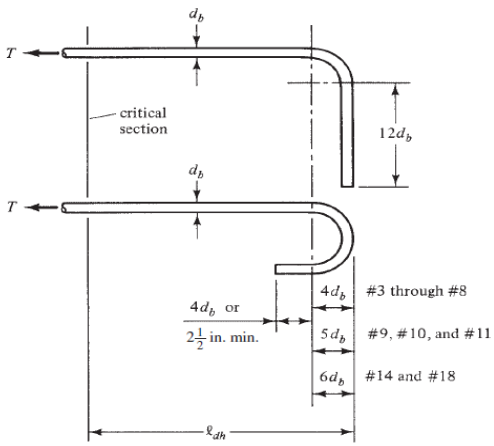

Figure C26. Hooked-Bar Details for Development of Standard Hooks.

Structural Analysis and Design of Pier Foundation

Based on pier and foundation geometry, *Figure C27* and *Figure C28*, it was decided to design the pier foundation as a wall footing. The upward soil pressure under the wall footing tended to bend the foundation upward as a fixed cantilever beam. The foundation was designed as shallow cantilever beams for the moments and shears involved. To start with, the depth of footing was assumed to be 24 inches considering the depth of frost line to be 33 inches [9] and from that adopted depth of excavation which was 42 inch. The weight of the concrete and the weight of the soil were calculated taking their densities into account, i.e. 150 pcf and 110 pcf, respectively. Effective soil pressure was derived subtracting the weight of concrete and the weight of soil from the allowable safe bearing pressure (3 ksf). Net upward pressure calculated considering maximum loading capacity of footing (k/ft) and respective minimum width of footing which were worked out from ASD and LRFD load combinations. Depth of reinforcement with crisscross layering was computed, subtracting cover and 1.5 diameter of the bar from assumed depth of footing (24 inches). Depth of reinforcement should be less than the depth of footing based on one way shear. It was necessary to compute the net upward pressure in order to work out the bending moments and shears in a footing caused by the factored wall loads. In other words, the weight of the footing and soil on top of the footing was neglected. These items caused an upward pressure equal to their downward weights, and they canceled each other for purposes of computing shears and moments. The percentage of steel (ρ) was calculated to come up with the area of steel. The area of steel was derived by multiplying the percentage of steel (ρ) by the area (bd) occupied by the pier. Among three major criterion that are used to calculate area of steel, which are flexure, shrinkage and bending moment, area of steel via flexure governed the design

of footing reinforcement. Number of bars was computed at bottom of footing per given geometry of foundation in both directions, i.e. longer and shorter directions per provided dimensions. For top portion of footing, we could adopt 50% of bending moment per suggested in 21.5.2.2 [11] for flexural longitudinal reinforcement: "Positive moment strength at joint face shall be not less than one-half (50%) the negative moment strength provided at that face of the joint." It meant that possible reversal of stresses could occur at both faces of the element, i.e. compression and tension. Area of steel and number of bars for top layer was computed similar to the bottom bars. Bearing stress at the base of the wall and top of the footing were checked to satisfy adequacy of bearing strength. Available development length was derived per provided geometry and cover. Required development length was derived per equations given in 12.2.2 [11]. Per calculations, sufficient development was not obtainable so we provided standard hooks in order to get the bond and anchorage of reinforcement with concrete. Lastly, according to these calculations, the total lengths of bars were computed as part of the detailing of the reinforcement.

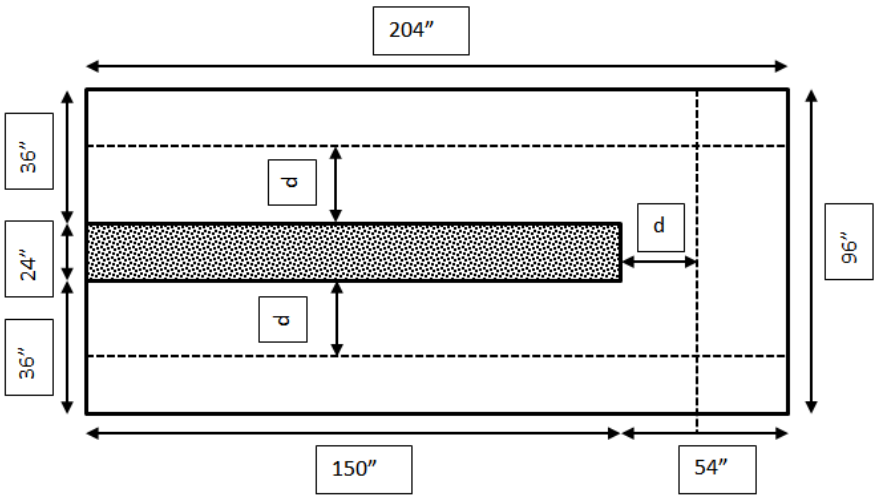

Figure C27. Plan of Foundation

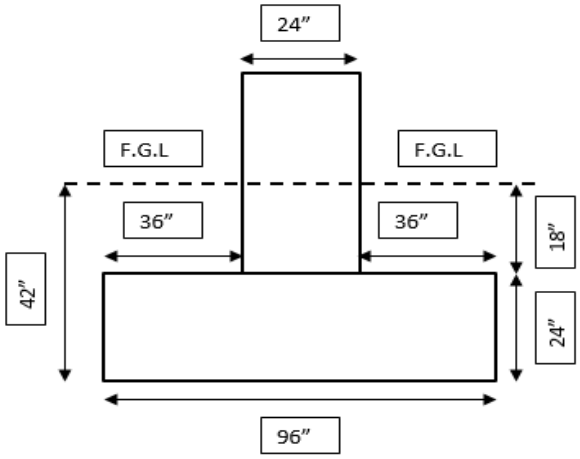

Figure C28. Section of Foundation

Assume depth of footing (2ft or 24 inches).

The weight of concrete (W_c) and the weight of soil (W_s) were as follows:

W_c = (unit weight of concrete) (depth of footing) = 150 pcf * 2 ft = 300 psf;

W_s = (unit weight of soil) (depth of excavation - depth of footing)

W_s = 110 pcf * (3 ft 6 inch– 2 ft) = 165 psf

The effective soil pressure was given as:

q_{eff} = allowable soil bearing pressure – weight of concrete – weight of soil

q_{eff} = 3000 – 300 – 165 = 1795 psf = 2.535 ksf

Net upward pressure $q_n = q_u$ = (1.6 *2.535) = 4.056 ksf

Depth of reinforcement by using #8 bars with crisscrossing layering:

d = depth of footing – cover – 1.5 d_b = 24 inches – 3 inches – 1.5 (1.0) = 19.50 inches

The depth of footing can also be calculated and confirmed by defining one way shear at section d as shown in *Figure C27*, plan of foundation; computing ultimate shear using equation where $\emptyset$ = resistance factor = 0.75; f_c = 3000 psi; b = width of footing:

$V_u = q_u\, b$ (overhang in longer or shorter direction – depth of reinforcement)

V_u = 4.056 * 1ft * ((54 – 19.5) / 12)) ft = 11.661 kips for shorter direction

V_u = 4.056 * 1ft * ((36 – 19.5) / 12)) ft = 5.577 kips for longer direction

$d = V_u / (\emptyset\ 2 \sqrt{f_c} b)$

d = (11.661 * 1000) / (0.75 * 2 * 54.77 * 12) = 11.828 inches < 19.5 inches

$d = V_u / (\emptyset\ 2 \sqrt{f_c} b)$

d = (5.577 * 1000) / (0.75 *2 * 54.77 * 12) = 5.656 inches < 19.5 inches

The bending moment of footing was calculated at the edge of the wall, *Figure C27*:

$M_u = q_n\ b$ (overhang in shorter direction)^2/ 2 = (4.056 * 1 * 4.5^2) / 2 = 41.07 k-ft

$M_u = q_n\ b$ (overhang in longer direction)^2 / 2 = (4.056 * 1 * 3^2) / 2 = 18.252 k-ft

R_u for the footing to find percentage of steel (ρ) of the footing:

$R_u = M_u / bd^2$ = 0.11 ksi for shorter direction

$R_u = M_u / bd^2$ = 0.048 ksi for longer direction; f_y = yield stress of steel = 60 ksi

$R_u = \omega\ f_c$ (1- 0.59 ω) = ω^2 – 1.7 ω + (1.7 R_u) / ($\emptyset f_c$) = 0

ω = 0.0417; ρ = ($\omega\ f_c / f_y$) = (0.0417 * 3) / 60 = 0.002085 for shorter direction

ω = 0.01796; ρ = ($\omega\ f_c / f_y$) = (0.01796 * 3) / 60 = 0.000898 for longer direction

$A_s = \rho bd$ = (0.002085 * 12 inches * 19.5 inches) = 0.49 inch^2; amount of steel required; A_s = 0.0018bh = (0.0018 * 12 inches * 24 inches) = 0.52 inch^2; minimum for shrinkage, Where h = depth of footing, d = depth of reinforcement

A_s = (200bd) / f_y = (200 * 12 inch * 19.5 inch) / (60000) = 0.78 inch^2; minimum for flexure considering maximum area from above three equations and using #8 bar (0.79 inch^2 each bar) computed the number of bars (n) required:

n = A_s for flexure / area of #8 bars = 0.78 / 0.79 = 0.987 ≈ 1 bar

put 1 bar/ ft, i.e. #8 bar @ 1 ft c/c in both directions, i.e. longer and shorter direction

so we can have, n - 1 = (length of footing – 2 (cover)) /12

n - 1 = (204 – 2 (3)) / 12 =16.5; n = 17.5 ≈ 18 – in shorter direction

and we can have, n - 1 = (width of footing - 2 (cover)) /12

n - 1= (96 – 2(3)) / 12 = 7.5; n= 8.5 ≈ 9 inches longer direction

so bottom slab bars #8 @ 12 inches c/c-both directions , *Figure* C29 and *Figure C30*

For top slab bars, we can adopt 50% of area provided in bottom slab due to possible reversal of stresses of compression and tension at top and bottom face of footing [11]:

A_s provided for top slab = 0.5 (A_s provided for bottom slab)

= 0.50 *0.78 = 0.39 inch^2; *Figure C30* and *Figure C31*

so top slab bars; n = A_s provided for top slab/ area of #6 bars = 0.39/0.44 =0.886 ≈ 1.

Put 1 bar/ft c/c, i.e. #6 @ 12 inches c/c in both directions, i.e. longer and shorter directions.

Check the bearing stress:

The bearing strength N_1, at the base of the wall:

Area A_1 = (thickness of wall) (width of wall) = 24 inches*12 inches = 288 inch^2

$N_1 = Ø\ (0.85\ f_c\ A_1)$ = 0.65*(0.85*3*24*12) = 477.36 kips

The bearing strength, N_2 at the top of the footing is:

$N_2 = N_1 \sqrt{\frac{A_2}{A_1}} \leq 2N_1$; A_2 = (length of footing) (width of wall) = 17 ft * 1 ft = 17 ft^2;

A_1 = (thickness of wall) (width of wall) = 2 ft * 1 ft in^2 = 2 ft^2

N_2 = 477.36 * 2.915 = 1391.73 kips > 2 (477.36)

so we might take $N_2 = 2N_1$ = 954.7 kips > 46.03 kips,

It was adequate in bearing stress.

Minimum dowel steel bars were superseded due to practical aspect of design, constructability and in lieu of that, the main pier reinforcement was extended to the bottom slab reinforcement of the footing and tied up into them. Minimum temperature and shrinkage reinforcement was also superseded by providing reinforcement with full length in both directions for the bottom and top of the slab in the footing.

Available development length was derived based on the provided geometry and the cover. The required development length was derived per equations given in 12.2.2 [11]. Sufficient development length was not available according to calculations so we provided a standard hook to get the required bond and anchorage of reinforcement with concrete. The available development length was derived taking the length of the footing into account, the depth of the footing, and the cover:

Available development length = width of footing – cover – (depth of footing / 2)

Available development length = 33 inches (shorter direction)

Available development length = 51 inches (longer direction)

$l_d = (f_y d_b) / (20\sqrt{f_c}\,)$ [11] = (60000 * 1) / (20 * 54.77)

l_d = 54. 77 inches > 51 inches for #8 bars, it is NOT OK.

$l_d = (f_y d_b) / (25\sqrt{f_c}\,)$ [11] = (60000 * 0.750) / (25 * 54.77)

l_d = 32.86 inches < 33 inches for #6 bars, it is OK.

So, adequate development length was not available for #8 bars. It was needed to provide hooks to introduce the necessary tension development length. Per 12.5.2 [11] development of standard hooks in tension given by: $l_{dh} = 0.02\, d_b\, \Psi_e\, f_y / \lambda \sqrt{f_c}$ where Ψ_e and λ were be taken as 1.0 for bars not coated epoxy and normal weight of concrete considered.

Ψ_e = coating factor; λ = lightweight aggregate concrete factor

$l_{dh} = (0.02\, d_b\, f_y) / \sqrt{f_c}$ = (0.02 * 1.0 * 60000) / 54.77 = 21.90 inches < 51 inches for #8 bars

"The dimensions given for the hooks were developed to protect members against splitting of the concrete or bar breakage, no matter what concrete strengths, bar sizes, or bar stresses were used. Actually, hooks do not provide an appreciable increase in anchorage strength because the concrete in the plane of the hook was

somewhat vulnerable to splitting. This meant that adding more length (i.e., more than the specified $12d_b$ or $4d_b$ values) onto bars beyond the hooks didn't really increase their anchorage strengths. Either the 90° hook with an extension of 12 bar diameters ($12d_b$) at the free end or the 180° hook with an extension of 4 bar diameters ($4d_b$) but not less than 2.5 inch could be used at the free end. The radii and diameters shown were measured on the inside of the bends. We adopted 90° hook for #8 and #7 bars for footing.

$12d_b$ = 12 *1 = 12 inches and $D = 6d_b$ = 6 * 1 = 6 inches; $r = D/2$ = 3 inches

Total length for #8 bar = (thickness of wall) + 2(l_{dh}) + $12d_b$ + r

Total length for #8 bar =24 inches + 2 (21.90 inches) + 12 inch + 3 inches = 82.8 inches

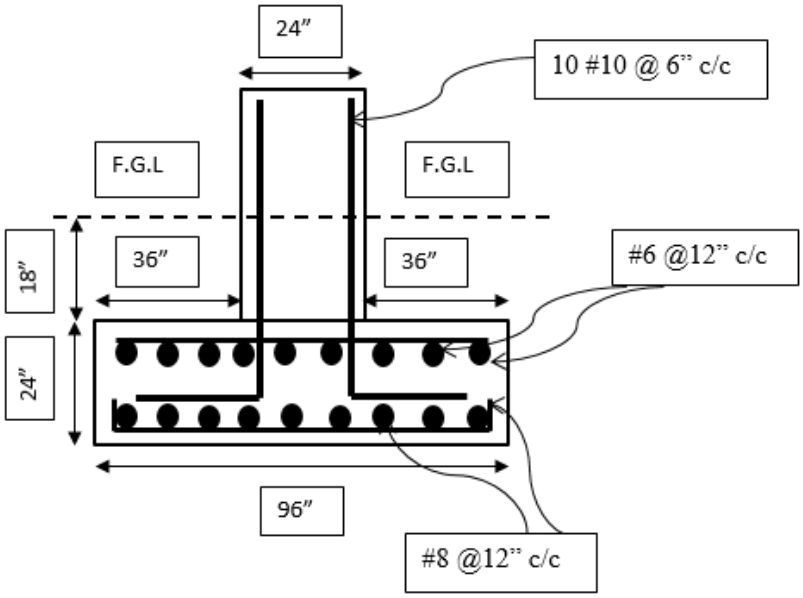

Figure C29. Reinforcement Detail for Footing

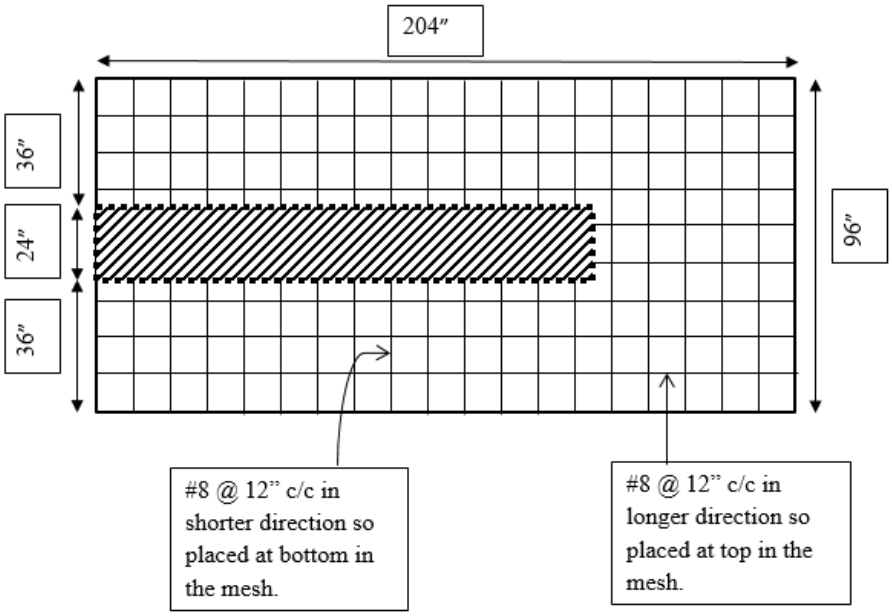

Figure C30. Reinforcement Detail for Footing – Bottom Slab

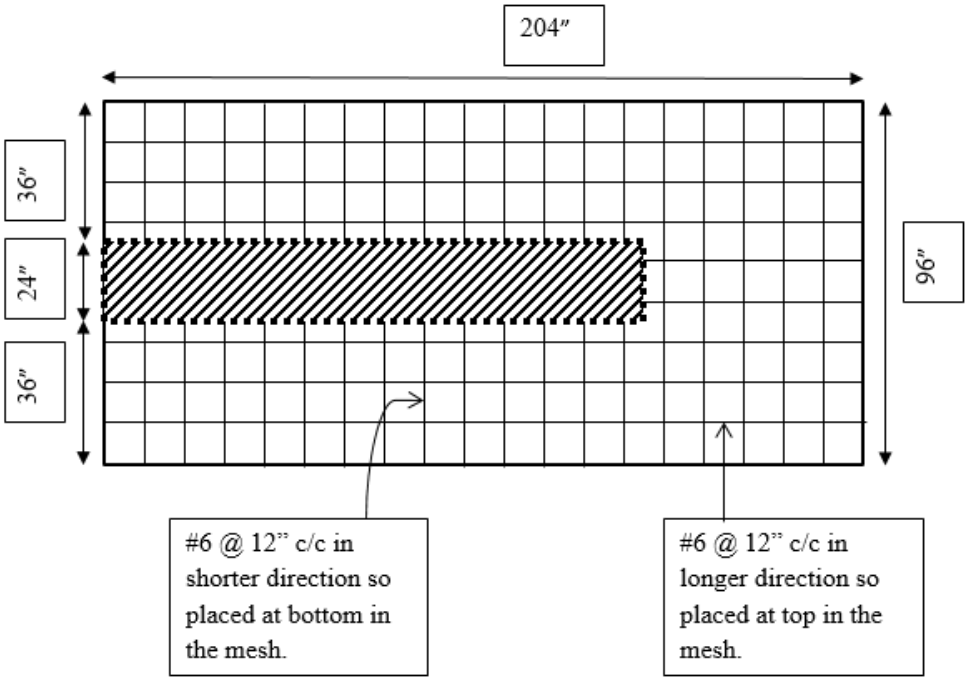

Figure C31. Reinforcement Detail for Footing- Top Slab

Analysis and Design of Pier

Reinforcement details for the pier were derived by adopting three different approaches as listed below:

1. Cantilever beam method
2. Non-linear strain distribution method (deep beam concept)
3. Shear wall method

Cantilever beam method. In this approach, the pier was considered as a reinforced concrete cantilever beam to analyze and design the reinforcement details. Here, to design pier reinforcement, maximum load values from the LRFD load combinations were adopted. Four different sections were incorporated to consider precisely the behavior of the cantilever beam with varying depth, two of them were at the two ends (1-1 and 4-4) and the remaining two of them were at distance of 50 mm (2-2 and 3-3) apart as shown in *Figure C33*. Each section was analyzed and designed separately and then the reinforcement details were worked out.

In these calculations, yield stress of steel f_y = 60 ksi, compressive strength of concrete f_c' = 3000 psi, and resistance factors ($Ø$) for flexure = 0.9 and for shear = 0.75 were taken

Nominal moment $M_n = M_u / Ø$

Section strength ; $M_n = A_s f_y (d - a/2)$ and $a = (A_s f_y) / (0.85 f_c' b)$

Solve for $A_s \geq (0.85 f_c' b \text{ d}) / f_y [1 - \sqrt{1 - (2 M_n)} / (0.85 f_c' b d^2)]$

Minimum area 1; $A_s \geq (3\sqrt{f'_c} bd) / f_y$; minimum area 2 ; $A_s \geq (200bd) / f_y$

Nominal strength $M_n = Ø A_s f_y (d - a/2)$

Factored force $V_u = 1.6 P_L$; factored moment $M_n = 1.6 P_L L$

$A_{vmin} = (0.75 \sqrt{f'_c} b_w s) / f_{yt}$ but shall not be less than $(50 b_w s) / f_{yt}$;

If $V_n < V_c/2$, then no shear reinforcement is required.

If $V_n > V_c/2$ than design shear reinforcement is required.

Assume ACI section 11.4.6 for Minimum Shear Reinforcement:

Nominal load $V_n = V_u / Ø$; concrete support $V_c = 2 \lambda \sqrt{f'_c} bd$;

Required support $V_s = V_n - V_c$; required area $A_v/s = V_s/ f_{yt} d$

The spacing of reinforcement closet to the tension face, s , shall not exceed that given by $s = 15 (40{,}000/f_s) - 2.5c_c$ (Eq 10-4) but not greater than $12 (40{,}000/f_s)$, where c_c is the least distance from the surface of reinforcement or prestressing steel to the tension face. Calculated stress f_s in reinforcement closest to the tension face at service load shall be computed based on the unfactored moment. It shall be permitted to take f_s as 2/3 f_y. Note that the calculations for sections 1-1 and 3-3 are presented in Chapter 6, thus only the calculations for sections 2-2 and 4-4 are presented below.

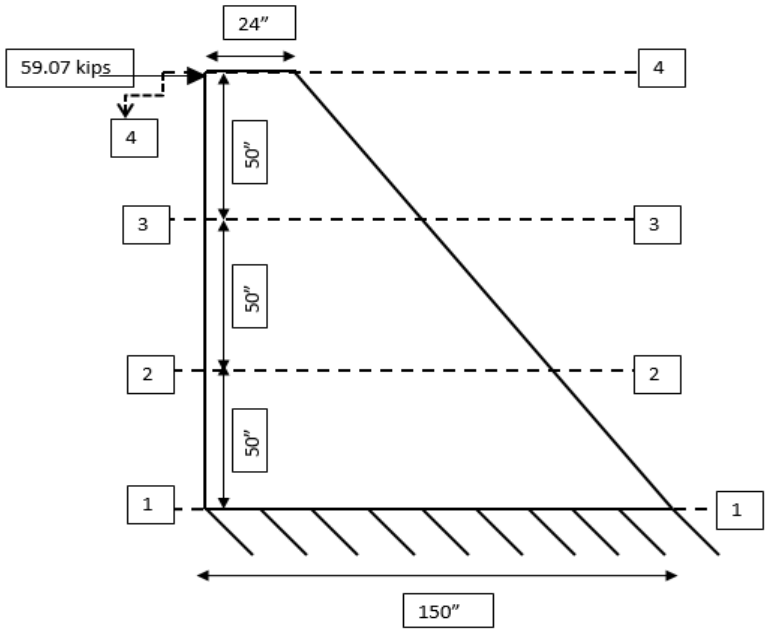

Figure C32. Pier as Cantilever Beam

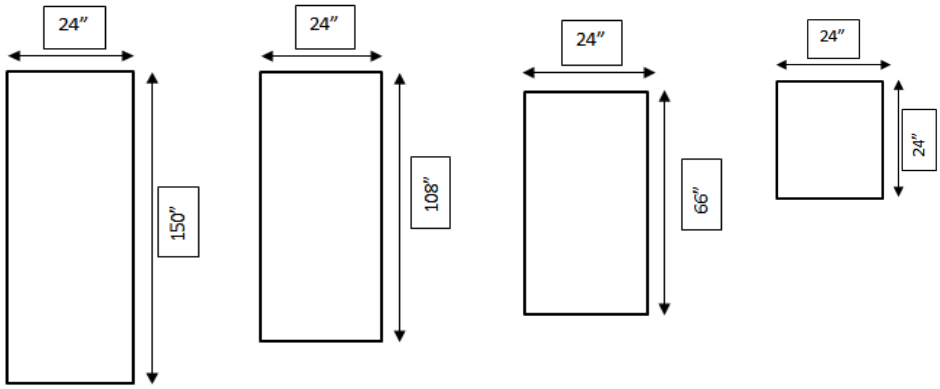

Figure C33. Sections of Pier as Cantilever Beam

Design of the beam for flexure (sec 2-2). To analyze and design the cantilever beam in flexure at sec 2-2 the basic dimensions were used as shown in *Figure C32* and *33.* The nominal moment of section (M_n) was calculated taking into account the point load (*Figure C32*) and moment arm from sec 2-2 to the point load with M_n = 8406.67 kip-inches.

The area of steel was calculated using three discrete equations:

$A_s \geq (0.85\, f_c'\, b\, d) / f_y\, [1- \sqrt{1} - (2\, M_n) / (0.85\, f_c'\, b\, d^2)]$; $A_s \geq 1.614$ inch^2

Minimum area 1; $A_s \geq (3\sqrt{f'_c}\, bd) / f_y$; $A_s \geq 6.835$ in^2

Minimum area 2 ; $A_s \geq (200bd) / f_y$; $A_s \geq 8.32$ inch^2

The area of steel was derived using the minimum area 2 equation which governed.

8 #10 were adopted, A_s = 10.16 inch^2 > required A_s = 8.32 inch^2 so it is OK.

To calculate the lever arm between tension and compression forces, first it was required to compute the depth of compression (a):

$a = (A_s\, f_y) / (0.85\, f_c'\, b)$ a = 9.960 inches.

Lever arm = $(d - a/2)$

The normal bending strength was found in order to verify that the section is sufficient to resist moment:

$M_n = Ø\, A_s\, f_y\, (d - a/2)$ = 54,326.12 kip-inches > 9,000 kip-inches.

Thus, the section is sufficient and adequate.

Design of the beam for shear (sec 2-2). To analyze and design the cantilever beam in shear at sec 2-2 the basic dimensions were used as shown in *Figure C32* and *C33*. The factored shear force was calculated considering the maximum load on pier from LRFD:

Factored shear force, V_u =144 kips. The factored moment was computed taking distance of load from support as a moment arm:

Factored moment M_n = 14,400 kip-inches

The nominal shear load was calculated incorporating $Ø$ = 0.75

Nominal load V_n = 192 kips

The shear force carried by the concrete, V_c = 273.42 kips

$V_n > (V_c/2)$ thus, shear reinforcement is required

The shear force carried by the steel was computed by subtracting the shear carried by the concrete from the nominal shear load; V_s = -81.42 kips

The negative sign indicated that theoretically it was not required to have shear reinforcement so minimum shear reinforcement was provided as if $V_n < (V_c/2)$.

For minimum spacing of stirrups should be considered from either half of section (d/2) depth or 24 inches, i.e. s_{max} = 24 inches.

Minimum area of shear reinforcement was given as:

$A_{vmin/s} = (0.75 \sqrt{f'_c}\, b_w\, s) / f_{yt}$ or $(50 b_w s) / f_{yt}$: greater value should be adopted.

$A_{vmin/s}$ = 0.016 inch^2/ inch or 0.020 inch^2 /inch,

So $A_{vmin/s}$ = 0.020 inch^2 /inch;

Design of the beam for flexure (sec 4-4). To analyze and design the cantilever beam in flexure at sec 4-4 the basic dimensions were used as shown in *Figure C32* and *C33*. The nominal moment of section (M_n) was calculated taking into account the point load and the moment arm from sec 4-4 to the point load:

M_n = 0 kip-inches

The area of steel was calculated using three discrete equations:

$A_s \geq (0.85 f_c' b d) / f_y [1- \sqrt{1 - (2 M_n)} / (0.85 f_c' b d^2)]$: $A_s \geq 0$ inch^2

Minimum area 1; $A_s \geq (3\sqrt{f'_c} bd) / f_y$; $A_s \geq 1.314$ inch^2

Minimum area 2; $A_s \geq (200bd) / f_y$; $A_s \geq 1.6$ inch^2 controls

The area of steel was derived using the minimum area 2 equation, which governed.

2 #10 were adopted, A_s = 2.54 inch^2 > governed A_s = 1.6 inch^2 so it is OK;

To calculate the lever arm between the tension and compression forces, first it was required to compute the depth of compression (a):

$a = (A_s f_y) / (0.85 f_c' b)$; a = 2.50 inches;

Lever arm = $(d - a/2)$

The nominal strength was calculated to verify the section is sufficient to resist moment:

$M_n = Ø A_s f_y (d - a/2)$ = 2,572.42 kip-inches > 0 kip-inches

Therefore, the section is sufficient.

Design of the beam for shear (sec 4-4). To analyze and design the cantilever beam in shear at sec 4-4 the basic dimensions were used as shown in *Figure C32* and *C33*. The factored shear force was calculated considering the maximum load on the pier from LRFD factored force V_u = 144 kips**.** The factored moment was computed taking the distance of the load from the support as a moment arm:

Factored moment M_n = 0 kip-inches

The nominal shear load was worked out incorporating Ø = 0.75:

Nominal shear load V_n = 192 kips

Shear force carried out by concrete, V_c = 52.58 kips

$V_n > V_c/2$, so shear reinforcement is required.

The shear force carried by the steel was computed subtracting shear carried by the concrete from the nominal shear load; V_s = 139.72 kips. As shear reinforcement is required, it is necessary to check if required area is more than minimum area.

Required area $A_v/s = V_s/ f_{yt}\, d$ = 0.116 inch^2/inch;

$A_{vmin/s} = (0.75 \sqrt{f'_c}\, b_w\, s) / f_{yt}$ or $(50 b_w s) / f_{yt}$: = 0.020 inch^2/inch < 0.116 inch^2/inch

#4 stirrups @ 20inches c/c

Deep Beams - A Non-Linear Strain Distribution Method:

"Deep beams [2] are structural elements loaded as beams but having a large depth/thickness ratio and a shear span/depth ratio not exceeding 2 for concentrated load and 4 for distributed load, where the shear span is the clear span of the beam for distributed load. Floor slabs under horizontal loads, wall slabs under vertical loads, short-span beams carrying heavy loads, and some shear walls are examples of this type of structural element. Because of the geometry of deep beams, they behave in a non-linear analysis as two dimensional rather than one-dimensional members and are subjected to a two-dimensional state of stress. As a result, plane sections before bending do not necessary remain plane after bending. The resulting strain distribution is no longer considered linear, and shear deformations that are neglected in normal beams become significant compared to pure flexure. Consequently, the stress block becomes nonlinear even at the elastic stage. At the limit state of ultimate load, the compressive stress distribution in the concrete would no longer follow the same shape or intensity."

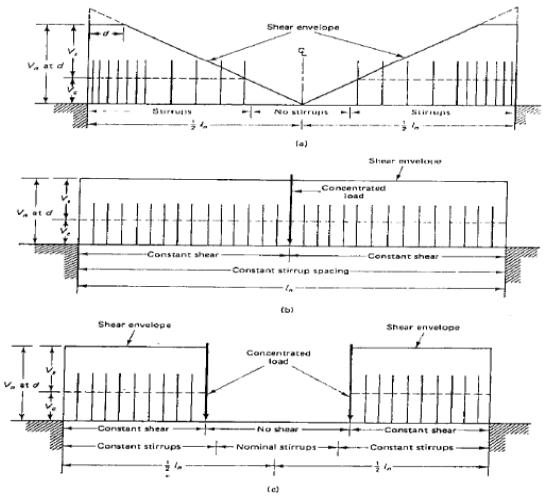

Figure C34. Schematic Stirrups Distribution

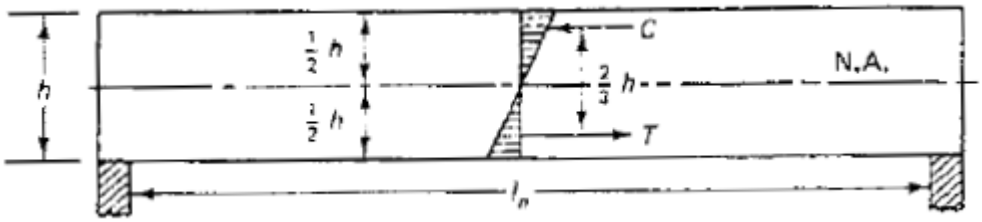

Figure C35. Elastic Distribution in Normal Beams (l_n/h = 3.5 to 5)

"Various stirrup arrangements have been presented in *Figure C34* which include: (a) stirrups spacing for uniformly distributed load on beam; (b) stirrups spacing for centrally loaded beam; (c) stirrups spacing for third point loaded beam. Self weight is not included in the shear envelope. *Figure C35* illustrates the linearity of the stress distribution at midspan prior to checking in a normal beam where the effective span/depth ratio exceeds a value of 3.5 to 5. In contrast, *Figure C36* shows the nonlinearity of stress at midspan corresponding to the non-linear strain under discussion. Recognize also that the magnitude of the maximum tensile stresses at the bottom fiber far exceeds the magnitude of the maximum compressive stress. The stress trajectories in *Figure C36 (c)* confirm this observation. Note the steepness and concentration of the principal tensile stress trajectories at midspan and the

concentration of the compressive stress trajectories at the support for both cases of loading of the beam at top or bottom. The concrete cracks in a direction perpendicular to the tensile principal stress trajectories. As the load increases, the cracks widen and propagate and more cracks open."

"Hence, less and less concrete remains to resist the indeterminate state of stress. Because the shear span is small, the compressive stresses in the support region affect the magnitude and direction of the principal tensile stresses such that they become less inclined and lower in value. In many cases, the cracks would almost be vertical or follow the direction of the compression trajectories, with the beam almost shearing off from the support in a total shear failure. Hence, in the case of deep beams, horizontal reinforcement is needed throughout the height of the beams, in addition to the vertical shear reinforcement along the span. From *Figure C36* the steep gradient of the tensile stress trajectories at lower fibers, a concentration of horizontal reinforcing bars is required to resist the high tensile stresses at the lower regions of the deep beam. Additionally, the high depth/span ratio of the beam should provide an increased resistance to the external shear load due to a higher compressive arch action. Consequently, it should be expected that the nominal resisting shear strength V_c for the plain concrete in deep beams will considerably exceed the V_c value for normal beams. In summary, shear in deep beams is a major consideration in their design. The magnitude and spacing of both the vertical and horizontal shear reinforcement differ considerably from those used in normal beams, as well as the expressions that have to be used for their design."

"From the above discussion , it can be inferred that deep beams ($a/d < 2.0$ and $l_n/d < 4.0$) have a higher nominal shear resistance V_c than do normal beams, where a = shear span to support face for concentrated load and, l_n = shear span for distributed

load (*Figure C36*). While the critical section for calculating the factored shear force V_u is taken at distance d from the face of the support in nominal beams, the shear plane in the deep beam is considerably steeper in inclination and closer to the support. If x is the distance of the failure plane from the face of the support, l_n the clear span for uniformly distributed load, and a the shear arm or span for concentrated loads, the expression for distance is Uniform Load: x = 0.15 l_n; Concentrated Load: x = 0.50a. In either case, the distance x should not exceed the effective depth d. The factored shear force V_u has to satisfy the condition: $V_u \leq \emptyset 10\ (\sqrt{f_c'})b_w d$ or $V_n = 10\ (\sqrt{f_c'})b_w d$. If not, the section has to be enlarged. The strength reduction factor $\emptyset = 0.75$. The present ACI code [11] does not give guidance on determining the shear value V_c of the plain concrete or the maximum permissible value, although the shear capacity of the plain concrete in the deep beams has to be considerably higher than in normal beams as shown in equation below. The limiting value of $V_c \leq 3.5\ (\sqrt{f_c'})b_w d$ in normal beams."

"The nominal shear resisting force V_c of the plain concrete can be taken as:

$V_c = (3.5 - 2.5\ (M_u / V_u d)\ (1.9\ (\sqrt{f_c'} + 2500\ \rho_w\ (V_u d / M_u)\ b_w d \leq 6\ \sqrt{f_c'}\ b_w d$

Where $1.0 < (3.5 - 2.5\ (M_u / V_u d) \leq 2.5$. This factor is a multiplier of the basic equation for V_c in normal beams to account for the higher resisting capacity of the deep beams. If some minor unsightly cracking is not tolerated, the designer can use $V_c = 2\ \sqrt{f_c'}\ b_w d$ when the factored shear V_u exceeds $\emptyset V_c$, shear reinforcement has to be provided such that $V_u \leq \emptyset\ (V_c + V_s)$, where V_s is the force resisted by the shear reinforcement."

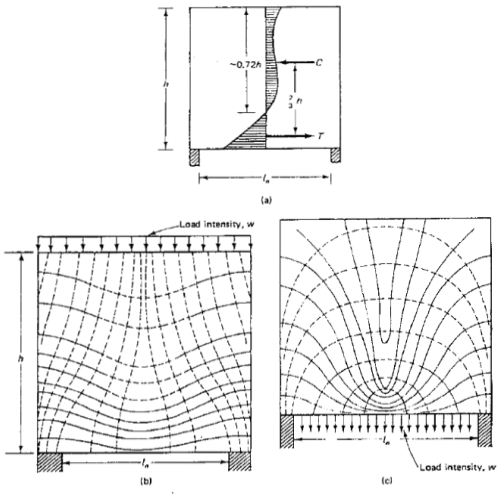

Figure C36. Elastic Stress Distribution in Deep Beams

"As shown in *Figure C36*; (a) deep beam ($l_n/h \leq 1.0$); (b) principal stress trajectories in deep beams loaded on top; (c) principal stress trajectories in deep beams loaded at bottom. Maximum vertical spacing and horizontal spacing could be find out as:

Maximum $s_v \leq d/5$ or 12 inch; Maximum $s_h \leq d/5$ or 12 inches. Whichever is smaller

Minimum $A_{vh} = 0.0015b\ s_h$; Minimum $A_v = 0.0025b\ s_v$.

A_v = total area of vertical reinforcement spaced at s_v in the horizontal direction at both faces of the beam

A_{vh} = total area of horizontal reinforcement spaced at s_h in the vertical direction at both faces of the beam."

"The shear reinforcement required at the critical section must be provided throughout the deep beams. In the case of continuous deep beams, because of the large stiffness and negligible rotation of the beam section at the supports, the continuity factor at the first interior support has a value close to 1.0. Consequently, the same reinforcement for shear can be used in all spans for all practical purposes if all the spans are equal and similarly loaded."

"The ACI code [11] does not specify a design procedure but requires a rigorous nonlinear analysis for the flexural analysis and design of deep beams. The simplified provisions presented [11] are based on the recommendations of the Euro-International concrete committee [3] (CEB Ref.6.8). *Figure C35* shows a schematic stress distribution in a homogeneous deep beam having a span/depth ratio l_n/h =1.0. It was experimentally observed that the moment lever arm does not change significantly even after initial cracking."

"$A_s = M_u/ \emptyset f_y jd \geq 3\sqrt{f_c'}bd / f_y \geq 200\ bd / f_y$. The lever arm as recommended by CEB is $jd = 0.2\ (l + 2h)$ for $1 \leq l/h < 2$; $jd = 0.6l$ for $l/h < 1$ where l is the effective span measured center to center of supports or 1.15 clear span l_n , whichever is smaller. The tension reinforcement has to be placed in the lower segment of beam height such that the segment height is $y = 0.25h – 0.05l < 0.20h$. It should consist of closely spaced small diameter bars well anchored into the supports."

"7.12.2.1 [11] Area of shrinkage and temperature reinforcement shall provide at least the following ratios of reinforcement area to gross concrete area, but not less than 0.0014: (a) Slabs where Grade 40 or 50 deformed bars are used, the ratio should be 0.0020. (b) Slabs where Grade 60 deformed bars or welded wire reinforcement are used, the ratio should be 0.0018 7.12.2.2 [11]. Shrinkage and temperature reinforcement shall be spaced not farther apart than five times the slab thickness, nor farther apart than 18 inch."

In this approach, the pier was analyzed and designed as a deep beam using non-linear strain distribution methodology. Here also we consider LRFD load combination for this approach. In non-linear distribution, it is require to identify the critical section to see whether maximum moment occurs there or at base / support to detail reinforcement.

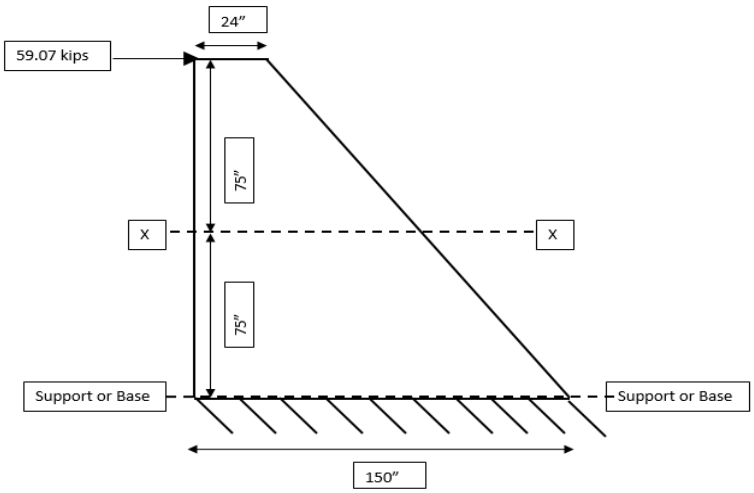

Figure C37. Pier as a Deep Beam for Section at Support/Base

Non-Linear strain distribution approach for pier as a deep beam at base/support.

For Flexure Design:

Taking width of Beam b_w = 24 inches = 2 ft, Ht. of beam h = 150 inches = 12.5 ft

Shear span to face of support, a =150 inches = 12.5 ft. = distance from point load to support/base.

Assuming depth $d = 0.9h$ = 0.9*150 inches = 135 inches =11.25 ft

Check for Deep Beam: a/d = 150 / 135= 1.11 < 2, OK for concentrated load

Distance of critical section, x = 0.50a = 0.50*150 inches = 75 inches = 6.25 ft from face of support Shear force at critical section (x-x),

i.e. defined as algebraic sum of all the forces acting on one side of section.

V_u(x-x) = 59070 lb = 59.07 kips at critical section from face of support.

M_u(x-x) = V_u(x-x) (lever arm) = 59070 lb * 75 = 4430250 lb-in = 369.19 k-ft

M_u at Support = V_u(x-x) (lever arm) = 59070 lb * 150 inches

= 8860500 lb-in = 738.375 k-ft .

Check for V_u(x-x) = 59.07 Kips $\leq$ *Ø 10* ($\sqrt{f_c'}$) $b_w d$

Ø 10 ($\sqrt{f_c'}$)$b_w d$ = 0.75*10*$\sqrt{3000}$ *24*135 = 1330.96 kips

V_u(x-x) = 59.07 kips $\leq$ 1330.96 kips, hence , section is OK.

To find V_c = *(3.5 – 2.5 (M_u / V_u d) (1.9* ($\sqrt{f_c'}$ *+ 2500* ρ_w *(V_u d / M_u)* $b_w d \leq 6$ ($\sqrt{f_c'}$ $b_w d$

K = (3.5 – 2.5 (M_u / V_u d) = 2.11 for M_u(x-x) = 369.19 k-ft

K = (3.5 – 2.5 (M_u / V_u d) = 0.72 <1, so *K* =1 for M_u at Support = 738.375 k-ft

First it is required to find the steel percentage to be used in flexure design as tension reinforcement. Flexural design of pier as a deep beam, check *a/h* and final lever arm: *jd*

a/h = (150 /150) = 1, it falls 1 $\leq$ 1 < 2, so ok for concentrated load

jd = 0.2(a+ 2h) = 0.2 (150 inches + 2*150 inches) = 90 inch = 7.5 ft.

Horizontal Reinforcement:

$A_s = M_u / Ø\ f_y jd$ = 0.92 inch^2 for M_u(x-x) = 369.19 k-ft

$A_s = M_u / Ø\ f_y jd$ = 1.82 inch^2 for M_u at Support = 738.375 k-ft

(3$\sqrt{f'_c}$*bd) / f_y* = 8.873 inch^2, *200b_wd/f_y* = 10.80 inch^2 controls.

Choosing bars: A_s = 10.80 inch^2:

Use 10 #10, A_s (Provided) = 12.70 inch^2, as a tension reinforcement.

The point up to which A_s is to be distributed in the tension zone (segment) of the beam is; *Y= 0.25h-0.05a < 0.20h*; putting *h* = 150 inches and *a* = 150 inches

Y= 30 inches $\leq$ 30 inches. It indicated that the first 30-inch distance along the support of the pier was in the tension zone and the remaining 120-inch distance was in the compression zone (*Figure 42A*). The spacing for the tension steel was calculated to be 6 inches c/c, so 5 bars on each face of the pier were placed. The percentage of vertical tension steel was calculated, $\rho_w = A_s / (b_w d)$ = 0.40 % = 0.0040

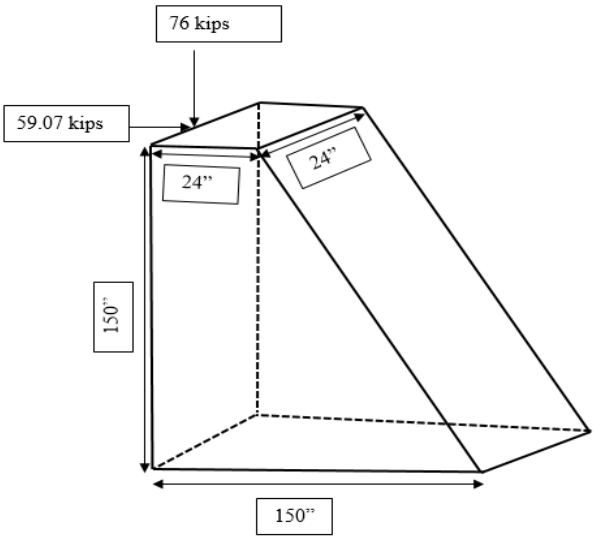

Figure C38. Tension and Compression Zone in Deep Beam

Vertical reinforcement for the compression zone (Figure *C38*) may be adopted arbitrarily as the same as of the tension reinforcement from stress block diagram (tension = compression) and constructability point of view. Thus, the area of steel for compression reinforcement was adopted as = 12.70 inch^2. As vertical compression reinforcement, 16 - #7 bars (8 bars on each face) were placed at 15 inches c/c spacing for the remaining 120 inches.

The shear carried by the concrete was calculated using the equation below:

$V_c = K(1.9 (\sqrt{f_c}' + 2500 \rho_w (V_u d / M_u) b_w d \leq 6 (\sqrt{f_c}' b_w d)$

Where $K = (3.5 – 2.5 (M_u / V_u d)$ = 2.11 for M_u(x-x) = 369.19 kip-ft

and $K = (3.5 – 2.5 (M_u / V_u d)$ = 0.72 < 1, for M_u at support = 738.375 kip-ft

for K=2.11 , V_c = 904.37 kips ≤ 1064.77 kips

for K=1, V_c = 382.90 kips ≤ 1064.77 kips

Ø V_c /2 = (678.27) / 2 = 339.14 kips for K = 2.11

Ø V_c /2 = (287.17) / 2 = 143.58 kips for K =1

V_u = 59.07 kips < 339.14 kips and 143.58 kips

As per these calculations, V_c was adequate in both cases. The applied load (shear) on the deep beam was less than shear carried by concrete. Hence, no design shear reinforcement was required, but as per the requirement of deep beam, this should have minimum shear reinforcement for the present case.

The minimum horizontal shear reinforcement was calculated as, $A_{vh} = 0.0015 b_w s_v = 0.43$ inch^2. The maximum vertical spacing (s_v) for horizontal shear reinforcement was as: s_v = min (d/5 inches or 12 inches) = 12 inches. #5 horizontal bars were placed at a vertical spacing of 12 inches c/c at both faces of the deep beam, so the area provided for horizontal reinforcement, A_{vh} (provided) = 0.62 inch^2. The minimum vertical shear reinforcement was computed as: $A_v = 0.0025 b_w s_v = 0.72$ inch^2. The maximum horizontal spacing s_h = min (d/5 inches or 12 inches) = 12 inches. #4 vertical bars were placed at horizontal spacing of 12 inches c/c at both faces of the pier so the area provided for vertical reinforcement; A_v (provided) = 0.80 inch^2. Temperature and shrinkage reinforcement was also derived for the pier using three different equations given in ACI 318-11 [11] as follow: $A_s = 0.0020bh = 0.58$ inch^2; $A_s = 0.0018bh = 0.52$ inch^2; $A_s = 0.0014bh = 0.40$ inch^2.

The area provided for minimum shear reinforcement (horizontal or vertical) was greater than the area required for temperature and shrinkage reinforcement, so there was no need to have temperature and shrinkage reinforcement as minimum shear reinforcement superseded temperature and shrinkage reinforcement. Based on constructability, it was preferable to have reinforcement in the compression zone (on both faces) which would replace the vertical compression reinforcement (16 - #7 @ 15 inches c/c) and vertical shear reinforcement (#4 @ 12 inches c/c). Finally, through optimal design consideration, #7 @ 12 inches c/c was adopted in lieu of vertical compression reinforcement and vertical shear reinforcement.

Shear Wall Method

"In shear walls for tall buildings, it is necessary to provide adequate stiffness to resist the lateral forces caused by wind and earthquake. When such buildings are not properly designed for these forces, there may be very high stresses, vibrations, when the forces occur. The results may include not only severe damage to the buildings but also considerable discomfort for their occupants. When reinforced concrete walls with their very large in-plane stiffnesses are placed at certain convenient and strategic locations, often they can be economically used to provide the needed resistance to horizontal loads. Such walls, called shear walls, are in effect deep vertical cantilever beams that provide lateral stability to structures by resisting the in-plane shears and bending moments caused by the lateral forces. As the strength of shear walls is almost always controlled by their flexural resistance, their name is something of a misnomer. It is true, however, that on some occasions they may require some shear reinforcing to prevent diagonal tension failures."

"Indeed, one of the basic requirements of shear walls designed for high seismic forces is to ensure flexure rather than shear-controlled design. *Figure C39* shows a shear wall subjected to a lateral force, V_u. The wall is in actuality a cantilever beam of width *h* and overall depth l_w. In part (a) of the figure, the wall is being bent from left to right by *Vu*, with the result that tensile bars are needed on the left or tensile side. If *Vu* is applied from the right side as shown in part (b) of the figure, tensile bars will be needed on the right-hand end of the wall. Thus, it can be seen that a shear wall needs tensile reinforcing on both sides because *Vu* can come from either direction."

"For horizontal shear calculations, the depth of the beam from the compression end of the wall to the center of gravity of the tensile bars is estimated to

be about 0.8 times the wall length, l_w, as per Section 11.10.4 [11]. (If a larger value of *d* is obtained by a proper strain compatibility analysis, it may be used.) The shear wall acts as a vertical cantilever beam. In providing lateral support, it is subjected to both bending and shear forces. For such a wall, the maximum shear, *Vu*, and the maximum moment, *Mu*, can be calculated at the base. If flexural stresses are calculated, their magnitude will be affected by the design axial load, *Nu*, and thus its effect should be included in the analysis. Shear is more important in walls with small height-to-length ratios. Moments will be more important for higher walls, particularly those with uniformly distributed reinforcing. It is necessary to provide both horizontal and vertical shear reinforcing for shear walls. The commentary (R11.9.9) [11] says that in low walls, the horizontal shear reinforcing is less effective, and the vertical shear reinforcing is more effective because the vertical shear reinforcing contributes to the shear strength of a wall by shear friction."

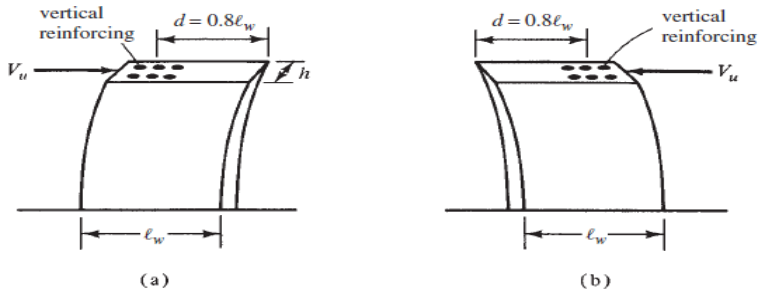

Figure C39. Shear Wall Loaded in Opposite Directions

"Reinforcing bars are placed around all openings, whether or not structural analysis indicates a need for them. Such a practice is deemed necessary to prevent diagonal tension cracks, which tend to develop radiating from the corners of openings. The factored beam shear must be equal to or less than the design shear strength of the wall: $V_u \leq \emptyset V_n$.

The design shear strength of a wall is equal to the design shear strength of the concrete plus that of the shear reinforcing: $V_u \leq \emptyset V_c + \emptyset V_s$."

"The nominal shear strength, V_n, at any horizontal section in the plane of the wall may not be taken greater than 10 $(\sqrt{f_c'})\ hd$ (11.9.3) [11]. In designing for the horizontal shear forces in the plane of a wall, d is to be taken as equal to 0.8 l_w, where l_w is the horizontal wall length between faces of the supports, unless it can be proved to be larger by a strain compatibility analysis (11.9.4) [11]. Section 11.10.5 [11] states that unless a more detailed calculation is made, the value of the nominal shear strength, V_c, used may not be larger than $2\lambda(\sqrt{f_c'})hd$ for walls subject to a factored axial compressive load, N_u. Should a wall be subject to a tensile load, N_u, the value of V_c may not be larger than the value obtained with the following equation: $V_c = 2\ (1 + N_u / 500\ A_g)\ 2\lambda\ (\sqrt{f_c'})\ b_w\ d \geq 0$. Using a more detailed analysis, the value of V_c is to be taken as the smaller value obtained by substituting into the two equations that follow, in which N_u is the factored axial load normal to the cross section occurring simultaneously with V_u. N_u is to be considered positive for compression and negative for tension (11.10.6) [11]:

$V_c = 3.3\lambda\ (\sqrt{f_c'})\ hd + (N_u d/4\ l_w)$ or

$V_c = [0.6\ \lambda\ \sqrt{f_c'} + l_w\ (\ 1.25\ \lambda\ \sqrt{f_c'} + 0.2\ N_u/\ l_w h) / (M_u/V_u) - (l_w/2)]hd$

The first of these equations was developed to predict the inclined cracking strength at any section through a shear wall corresponding to a principal tensile stress of about $4\ \lambda\ \sqrt{f_c'}$ at the centroid of the wall cross section. The second equation was developed to correspond to an occurrence of a flexural tensile stress of $6\ \lambda\ \sqrt{f_c'}$ at a section $l_w/2$ above the section being investigated. Should $Mu/Vu - l_w/2$ be negative, the second equation will have no significance and will not be used."

"The values of V_c computed by the two preceding equations at a distance from the base equal to $l_w/2$ or $h_w/2$ (whichever is less) are applicable for all sections between this section and one at the wall base (11.9.7) [11]. Should the factored shear, V_u, be less than $\emptyset\, V_c/2$ computed as described in the preceding two paragraphs, it will not be necessary to provide a minimum amount of both horizontal and vertical reinforcing. Should V_u be greater than $\emptyset\, V_c$, shear wall reinforcing must be designed as described in Section 11.9.9 [11]. If the factored shear force, V_u, exceeds the shear strength, $\emptyset\, V_c$, the value of V_s is to be determined from the following expression, in which A_v is the area of the horizontal shear reinforcement and s is the spacing of the shear or torsional reinforcing in a direction perpendicular to the horizontal reinforcing (11.9.9.1) [11]: $V_s = A_v\, f_y\, d / s$. The amount of horizontal shear reinforcing, ρ_t (as a percentage of the gross vertical concrete area) shall not be less than 0.0025 (11.9.9.2) [11].The maximum spacing of horizontal shear reinforcing, s_2, shall not be greater than $l_w/5$, $3h$, or 18 inches (11.9.9.3) [11].The amount of vertical shear reinforcing, ρ_n (as a percentage of the gross horizontal concrete area) shall not be less than the value given by the following equation, in which h_w is the total height of the wall (11.9.9.4) [11].$\rho_l = 0.0025 + 0.5\,(2.5 - h_w / l_w)\,(\rho_h - 0.0025)$."

"It shall not be less than 0.0025 but need not be greater than the required horizontal shear reinforcing, ρ_t. For high walls, the vertical reinforcing is much less effective than it is in low walls. This fact is reflected in the preceding equation, where for walls with a height/length ratio less than half, the amount of vertical reinforcing required equals the horizontal reinforcing required. If the ratio is larger than 2.5, only a minimum amount of vertical reinforcing is required (i.e., $0.0025sh$). The maximum spacing of vertical shear reinforcing shall not be greater than $l_w/3$, $3h$, or 18 inch (11.9.9.5) [11]."

In this method, the pier is considered to be a shear wall and designed accordingly:

f_c' = 3000 psi, f_y = 60000 psi = 60 ksi

h = thickness of wall = 24 inches, l_w = length of wall = 150 inches,

h_w = ht. of wall = 150 inches, V_u = 90 kips

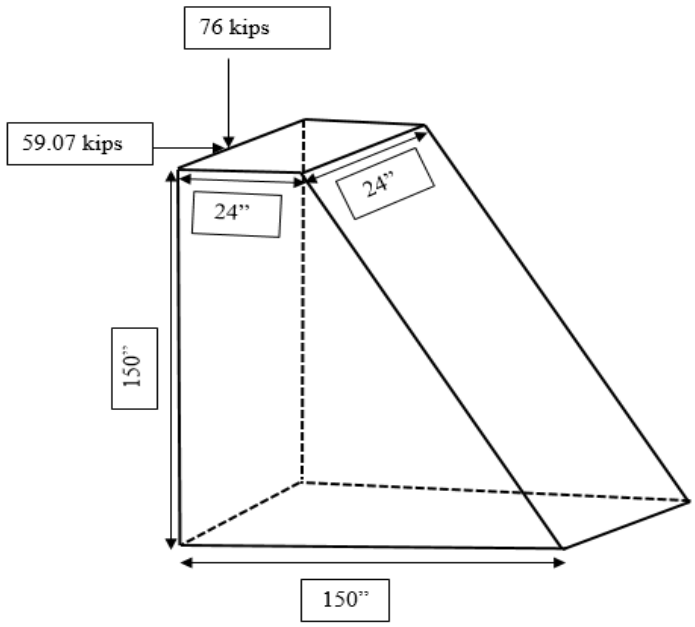

Figure C40. Pier as Shear Wall

Step 1: Is the wall thickness satisfactory? (ACI Section 11.9.4)

$V_u = Ø10\ (\sqrt{f_c'})hd$ (ACI Section 11.9.3) where $d = 0.8\ l_w = 0.8 * 150$ inches = 120 inches

V_u = 0.75*10*($\sqrt{3000}$) 24*120 = 1183.08 kips > 59.07 kips, hence thickness is OK.

Step 2: Compute *Vc* for wall (lesser of two values)

(a) $V_c = 3.3\lambda(\sqrt{f_c'})hd + (N_u d/4l_w) = 3.3*1.0*(3000)^{(1/2)}24*120 + 15200$

V_c = 535.75 kips (ACI Eq.11-27)

(b) $V_c = [0.6\ \lambda\ \sqrt{f_c'} + l_w\ (\ 1.25\ \lambda\ \sqrt{f_c'} + 0.2\ N_u/\ l_w h)\ /\ (M_u/V_u) - (l_w/2)]$ hd (ACI Eq. 11-

28) Computing V_u and M_u at the lesser of $l_w/2$ =150/2 = 75 inches, $h_w/2$ = 150/2 = 75 inches from base (ACI sec 11.9.7).

From ACI 11.9.7, sections located closer to wall base than a distance l_w /2 or one-half the wall height, whichever is less, shall be permitted to be designed for the same V_c as that computed at a distance l_w /2 or one-half the height.

V_u = 59.07 kips,

M_u = 59.07 kips (150 inches – 75 inches) = 4430.25 kip-in = 369.19 kip-ft

V_c = [(0.6*1.0*(54.77)) + (150(1.25*1.0*(54.77) + 0) 24*120) / (4430.25 /59.07) – 75)] (24*120)

V_c = 94.64 kips + infinity = infinity; because second term of equation (b) gives denominator zero so it would be infinity solution.

So option (a) was the governing value of V_c for wall.

Step 3: Is shear reinforcing needed?

ØV_c/2 = (0.75*1.0*520.55)/2 = 195.21 kips > 59.07 kips. It is OK in shear.

Hence, no shear reinforcement is required.

Step 4: Design of vertical (longitudinal) reinforcement

Per ACI 14.3.2; $\rho_l = A_{v,\,vert}/hs_1$ = 0.0015

From ACI 14.3.2, minimum ratio of vertical reinforcement area to gross concrete area ρ_l shall be: (a) 0.0012 for deformed bars not larger than No.5 with f_y not less than 60,000psi, or (b) 0.0015 for other deformed bars, or

(c) 0.0012 for welded wire reinforcement not larger than W31 or D31.

For spacing s_1, smaller of 3h = 3*24 = 72 inches or 18 inches or d/5 = 120/5 = 24 inches,

So s_{1max} = 18 inches, therefore we may go with typical 12 inches spacing c/c, s_1 =12 inches

$A_{v,\,vert}$ = 0.0015*24*12 = 0.43 inch^2

Provide #5 horizontal bars at 12 inch c/c spacing = 0.62 inch^2

Step 5: Design of horizontal (transverse) reinforcement

Per ACI 14.3.3, $\rho_t = A_{v,\,horiz}/hs_2$ = 0.0025

Sec 14.3.3 Minimum ratio of horizontal reinforcement area to gross concrete area ρ_t shall be: (a) 0.0020 for deformed bars not larger than No.5 with f_y not less than 60,000 psi, or (b) 0.0025 for other deformed bars, or

(c) 0.0020 for welded wire reinforcement not larger than W31 or D31.

For spacing s_2; smaller of 3h = 3*24 = 72 inch or 18 inches or d/5 = 120/5 = 24 inches, so:

s_{2max} = 18 inches, therefore we may go with typical 12 inches spacing c/c, s_2 =12 inches

$A_{v,\,horiz}$ = 0.0025*24*12 = 0.72 inch^2

Provide #4 vertical bars at 12 inches c/c spacing = 0.8 inch^2

Step 6: Design of vertical flexural reinforcement

M_u = 59.07 kips * 150 inch = 8860.5 kip-in = 738.37 kip-ft at base of wall.

$M_u/\emptyset bd^2$ = (8860.5 *1000) lb-in/ (0.90*24*120^2) = 28.49 lb/inch^2

$\rho = \rho_{min}$ for flexure = 0.0033 (from Appendix A, Table A.12)

$A_s = \rho bd$ = 0.0033*24*120 = 9.504 inch^2

b = wall thickness = 24 inches, $d=0.8l_w$ =120 inches

Use 8 #10 bars each end (assuming V_u could come from either direction)

Referring to all of the above calculations, we must compare (Table C7) for all three design approaches to use the most structurally sound and stable reinforcement detail which can sustain the anticipated worst loading combinations as determined by the structural analyses. Therefore, we adopted design of reinforcement derived via the

deep beam concept following the non-linear approach [3]. In future, one may incorporate strut and tie model methodology to design more precise and economical reinforcement details of pier as a deep beam in lieu of non-linear approach.

Table C7

Summary of Reinforcement Detail from Three Different Approaches

Linear Approach (Cantilever Beam Concept)			
Sec 1-1	Sec 2-2	Sec 3-3	Sec 4-4
10 #10	8 #10	4 #10	2 #10
Flexure Reinforcement for all four sections			
#4 @ 20 inches c/c or lesser spacing- Shear Reinforcement			

Non-Linear Approach (Deep Beam Concept)
#10 @ 6 inches c/c- Vertical Tension Reinforcement
#7@12 inch c/c- Vertical Compression and Shear Reinforcement
#5 @12 inches c/c - Horizontal Shear Reinforcement

RCC Shear Wall (Wall Concept)
8 #10- Flexure Reinforcement
#4 @12 inches c/c -Vertical Shear Reinforcement
#5 @12 inches c/c - Horizontal Shear Reinforcement

Cross Beam Analysis and Design

The cross beams connect the tops of the piers. The purpose of the cross beams is to maintain the correct spacing of the truss bases. Thus, the cross beams serve to stabilize the tops of the piers relative to each other in the longitudinal direction.

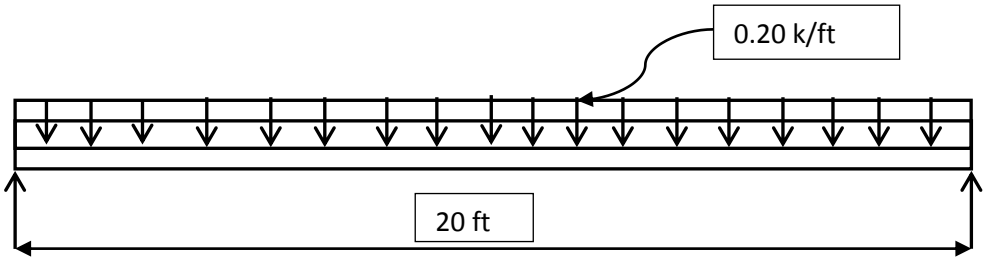

Figure C41. Design of Cross Beam on Top of Buttress

Using LRFD and an assumed live load of five 200 lb men on top of the beam at one time, a model was designed for a worst case scenario. The beam does not appear to be taking any vertical load from the hangar and is considered to be a continuous beam running from pier to pier.

b = 12 inches, *h* = 8 inches, span = 240 inches = 20 ft on center to center spacing,

Diameter of bar = 0.50 inches for #4 bar

d = 8 – 1.5 – (0.50/2) – 0.375 = 5.75 inches

Self Weight (Dead Load of Beam) = 150 lb/ft^3 * (8/12 ft)*(12/12 ft)*(20 ft)

= 2000 lb = 2 kips

= (2 kips/ 20 ft) = 0.1 kips/ft *1.2 = 0.12 k/ft

Self Weight (Dead Load of Beam) = 0.12 k/ft

Live Load on Beam = 5*200*1.6 = 1600 lb = 1.6 kips

So, uniformly distributed live load = 1.6 kips / 20ft = 0.080 k/ft,

This load was applied as a uniformly distributed load.

Total Load on Beam, w = DL + LL = 0.12 k/ft + 0.080 k/ft = 0.20 k/ft

Maximum Moment in the Beam = $wl^2/8$ = (0.20 *(20)^2) /8 = 10 kips-ft

As per assumption, the bottom is in tension and the top is in compression.

Max. Shear = V = (wl) /2 = 2 kips as a reaction on each support (*Figure C42*).

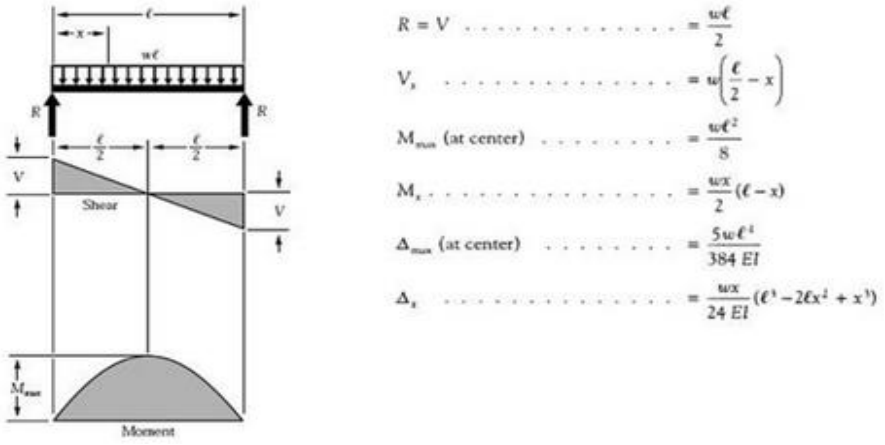

Figure C42. Simply Supported Beam Shear Force and Bending Moment

The design of the reinforcement for the concrete beam will be as follows:

Nominal moment $M_n = M_u / Ø$

$M_n = (10 * 12) / 0.90 = 133.34$ kip-inches

$M_n = A_s f_y (d - a/2)$ and $a = (A_s f_y) / (0.85 f_c' b)$

133.34 kip-inches = $A_s * 60 (5.75 – 1.22 A_s)$

$A_s^2 – 4.713 A_s + 1.821 = 0$

By solving the quadratic equations:

$A_s = 8.523$ inch^2 or 0.23 inch^2; two solutions from the quadratic equations. Most feasible value should be considered to get sound structural reinforcement**,**

so $A_s = 0.23$ inch^2 was adopted.

Check for A_s min:

1) A_s min 1 = $(3\sqrt{f_c'}\, bd) / f_y$ or 2) A_s min 2 = $(200bd) / f_y$

1) $A_s$min 1 = 0.217 inch^2 or 2) A_s min 2 = 0.265 inch^2

Among these three values, A_s =0.265 inch^2 was considered as the required

reinforcement area to be detailed. The number of bars, n = 2 - #4 bars as bottom tension bar.

Check for Cover:

[8- (0.50*2) – (1.5*2)] / 2 = 2 inches > minimum =1 inches so it is OK.

As the cross beam follows regular beam criteria (width to depth ratio < 1) and it only holds the pier and truss but does not transfer any kind of load, there was no requirement of minimum shear reinforcement.

Now, the calculations for development length are as follows. First and foremost, it is required to calculate available development length to compare with actual development length.

$l_d = f_y\, d_b\, \Psi_t\, \Psi_e \;/\; 25\sqrt{f_c'}$

l_d = (60000*0.50*1.0*1.0) / (25*54.77) = 21.91 inches,

Where:

Ψ_t = bar-location factor = 1.0; for bottom bars per ACI 12.2.4 [11].

Ψ_e = coating factor = 1.0; for uncoated and galvanized reinforcement per ACI 12.2.4 [11].

As it was designed as a simply supported beam so development l_d is OK.

The reinforcement of the cross beam could experience drastic temperature differences. Therefore, it was necessary to carry out the thermal expansion check for the beam which could affect the load bearing capacity of the steel bars. These calculations are as follows:

$\alpha\,(\Delta T) = (P) / (AE)$;

α = Thermal expansion coefficient = (4.1 to 7.3) * $10^{(-6)}$/ °F; [11]

ΔT = Maximum seasonal temperature difference = 120 - 0 = 120 °F [11]

P = Load (kips)

A = area of provided reinforcement (inch^2)

E = Concrete Modulus = 29000 psi [11]

So, P = (α) * (ΔT) * (AE):

P = (7.3 * $10^{(-6)}$ * 120) *(0.1963*2*29000) = 9.97 kips

The yield load of steel = (yield stress of steel) * (area of steel bars provided)

The yield load of steel = (60) * (0.1963*2) = 23.56 kips > 9.97 kips so it is OK.

Cross beam is OK in thermal expansion.